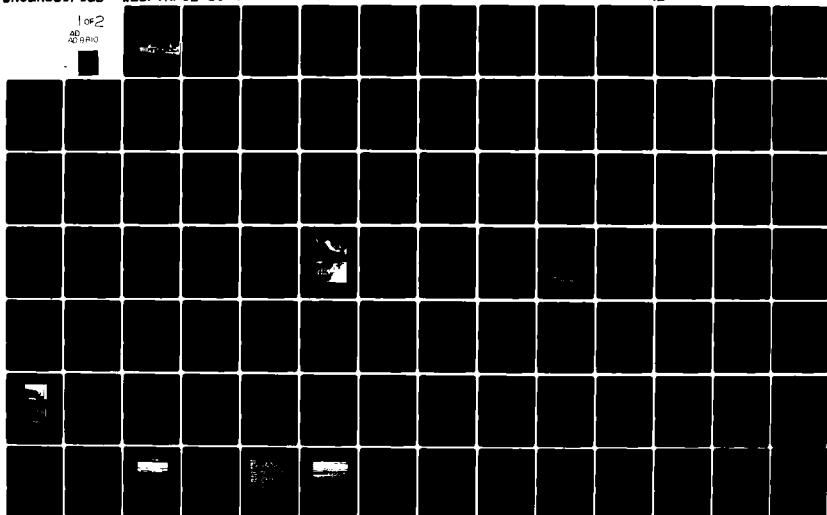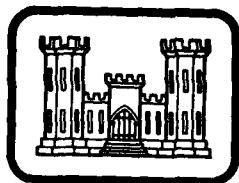ARMY ENGINEER WATERWAYS EXPERIMENT STATION VICKSBURG--ETC F/G 8/11
EVALUATION OF GEOPHYSICAL METHODS FOR CAVITY DETECTION AT THE W--ETC(U)
JUN 80   D K BUTLER, W L MURPHY

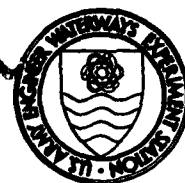UNCLASSIFIED WES/TR/GL-80-4   NL

1 OF 2
AD
A088 101

LEVEL (12)

TECHNICAL REPORT GL-80-4

EVALUATION OF GEOPHYSICAL METHODS FOR CAVITY DETECTION AT THE WES CAVITY TEST FACILITY

by

Dwain K. Butler, William L. Murphy

Geotechnical Laboratory
U. S. Army Engineer Waterways Experiment Station
P. O. Box 631, Vicksburg, Miss. 39180

June 1980
Final Report

Approved For Public Release; Distribution Unlimited

DTIC
ELECTE
AUG 2 2 1980
S
A

Prepared for Office, Chief of Engineers, U. S. Army
Washington, D. C. 20314

Under CWIS Work Unit 31150

80 8 22 014

Destroy this report when no longer needed. Do not return
it to the originator.

The findings in this report are not to be construed as an official
Department of the Army position unless so designated.
by other authorized documents.

The contents of this report are not to be used for
advertising, publication, or promotional purposes.
Citation of trade names does not constitute an
official endorsement or approval of the use of
such commercial products.

REPORT DOCUMENTATION PAGE		READ INSTRUCTIONS BEFORE COMPLETING FORM
1. REPORT NUMBER Technical Report GL-80-4	2. GOVT ACCESSION NO. AD-A088 101	3. RECIPIENT'S CATALOG NUMBER
4. TITLE (and Subtitle) EVALUATION OF GEOPHYSICAL METHODS FOR CAVITY DETECTION AT THE WES CAVITY TEST FACILITY		5. TYPE OF REPORT & PERIOD COVERED Final report
		6. PERFORMING ORG. REPORT NUMBER
7. AUTHOR(s) Dwain K. Butler William L. Murphy		8. CONTRACT OR GRANT NUMBER(s)
9. PERFORMING ORGANIZATION NAME AND ADDRESS U. S. Army Engineer Waterways Experiment Station Geotechnical Laboratory P. O. Box 631, Vicksburg, Miss. 39180		10. PROGRAM ELEMENT, PROJECT, TASK AREA & WORK UNIT NUMBERS CWIS Work Unit 31150
11. CONTROLLING OFFICE NAME AND ADDRESS Office, Chief of Engineers, U. S. Army Washington, D. C. 20314		12. REPORT DATE June 1980
		13. NUMBER OF PAGES 134
14. MONITORING AGENCY NAME & ADDRESS(if different from Controlling Office)		15. SECURITY CLASS. (of this report) Unclassified
		15a. DECLASSIFICATION/DOWNGRADING SCHEDULE

16. DISTRIBUTION STATEMENT (of this Report)

Approved for public release; distribution unlimited.

17. DISTRIBUTION STATEMENT (of the abstract entered in Block 20, if different from Report)

18. SUPPLEMENTARY NOTES

19. KEY WORDS (Continue on reverse side if necessary and identify by block number)
Cavities (Underground)
Cavity detection
Geophysical exploration
Resistivity surveys
Seismic surveys
Subsurface exploration

20. ABSTRACT (Continue on reverse side if necessary and identify by block number)

The study reported herein was undertaken to plan and construct a controlled Cavity Test Facility for use in preliminary evaluation of geophysical methods as cavity location or delineation tools and to evaluate several geophysical techniques to determine whether signatures could be obtained that would help to either locate a cavity or, once located, to determine its size, depth, or shape in plan view. → next page

(Continued)

DD ₁ FORM 73 1473 EDITION OF 1 NOV 65 IS OBSOLETE

20. ABSTRACT (Concluded).

$\Rightarrow$ Seismic studies conducted at the Cavity Test Site consisted of surface compression-(P-) wave refraction surveys, crosshole shear-(S-) wave surveys, shallow seismic reflection surveys, "Meissner wave-front" surveys, and a sonar investigation. Results for each of these studies are given.

Surface resistivity surveys were also made, including the following methods: Modified Bristow or Bristow-Bates, Wenner profiling, Schlumberger sounding, and dipole-dipole. Subsurface resistivity tests were also accomplished.

Radar tests using three different radar systems--a 4.2-GHz continuous wave-frequency modulated (CW-FM) system, a 100-Hz pulse radar system, and a 300-MHz pulse radar system--were also performed at the Cavity Test Facility.

Results of the attempt to detect cavities at the WES Cavity Test Facility were mostly negative. It is recommended that an alternate test site be found where conditions are not as extreme, that cavity detection research continue, and that the following geophysical methods be investigated: (a) microgravimetric techniques including gravity-gradient measurements, (b) high-resolution seismic profiling, (c) expanding spread seismic fan shooting, (d) cavity diffraction signatures with crosshole geometry, and (e) continued study of subsurface probing radar to determine the lithology dependence of its applicability.

Appendix A presents seismic reflection records, and Appendix B contains data sheets for Bristow-Bates surveys.

PREFACE

This investigation was conducted by the U. S. Army Engineer Waterways Experiment Station (WES) for the Office, Chief of Engineers, as part of CWIS Work Unit 31150, "Remote Delineation of Cavities and Discontinuities in Rock."

Many individuals contributed to this investigation, including Messrs. J. R. Curro, Jr., D. M. Kronig, E. S. Stewart, D. H. Douglas, and D. K. Butler, and Dr. A. G. Franklin of the Earthquake Engineering and Geophysics Division (EE&GD), Geotechnical Laboratory (GL); Messrs. W. L. Murphy, J. B. Warriner, R. F. Anderson, and D. Taylor of the Engineering Geology and Rock Mechanics Division, GL, WES; Mr. P. J. Tarantolo and Dr. R. R. Unterberger, Department of Geophysics, Texas A&M University; and Mr. R. C. Benson, Technos, Inc. The work was performed intermittently during the period June 1975 to October 1978. This report was written by Messrs. Butler and Murphy and documents the initial efforts conducted under Work Unit 31150.

The work was performed under the general supervision of Mr. R. F. Ballard, Jr., Chief, Field Investigations Group, EE&GD; Drs. F. G. McLean and P. F. Hadala, former Chief and Chief, respectively, EE&GD; and Mr. James P. Sale, Chief, GL.

COL John L. Cannon, CE, and COL Nelson P. Conover, CE, were Commanders and Directors of the WES during the conduct of this investigation. Mr. Fred R. Brown was Technical Director.

1

CONTENTS

CONVERSION FACTORS, U. S. CUSTOMARY TO METRIC (SI)
UNITS AND METRIC (SI) TO U. S. CUSTOMARY
UNITS OF MEASUREMENT

Units of measurement used in this report can be converted as follows:

Multiply	By	To Obtain
	U. S. Customary to Metric (SI)	
degrees (angle)	0.01745329	radians
feet	0.3048	metres
feet per second	0.3048	metres per second
inches	2.54	centimetres
miles per hour (U. S. statute)	1.609344	kilometres per hour
ohm-feet	0.003048	ohm-centimetres
	Metric (SI) to U. S. Customary	
centimetres	0.3937007	inches
metres	3.280839	feet
metres per second	3.280839	feet per second
ohm-centimetres	328.0839	ohm-feet

EVALUATION OF GEOPHYSICAL METHODS FOR CAVITY
DETECTION AT THE WES CAVITY TEST FACILITY

PART I: INTRODUCTION

Background

1. Subsurface cavities are a problem frequently encountered prior
to, during, and after construction in many areas of the country with
solution-susceptible bedrock (limestones, dolomites, and evaporites
primarily). Such cavities can threaten the safety of structures of all
types by impairing the bearing capacity of the foundation, and in the
case of water-retention structures such as earth dams, the cavities
can lead to piping failure of the dam if not properly treated. Of
lesser, but still serious, importance is the fact that such cavities
can lead to economically intolerable water losses from reservoirs. If
detected during the site investigation phase, either the site can be
relocated or the construction plan altered to deal with the problem.
However, if cavities are detected during construction, the option to
relocate the site is frequently not viable, and the increase in cost
required by changing the construction plan at this stage can be very
large. For cavities that are discovered after construction, the reme-
dial options may be few, and the consequences of undiscovered or
untreated cavities at a water-retention project can range from unac-
ceptable water loss to a life-endangering failure caused by loss of
bearing capacity or piping of earth materials covering cavity exits
or entrances. Thus, it is preferable to detect and delineate cavities
early in the site investigation phase. Though it will almost cer-
tainly be impossible to detect every cavity in the site investigation
phase, it is desirable to gain enough information to make reasonable
evaluations of the extent of the problem at a given site and make
reasonable estimates of the cost of dealing with it.

2. Although there frequently are surface indicators of subsurface

cavities, such as depressions, lineations, anomalous vegetative stress, etc., detection and delineation of cavity systems (if found at all prior to construction) require geophysical surveying and drilling. Of course, drilling is required in any event to verify geophysical indications, although to achieve the same degree of site definition, the combined program is far less costly than drilling alone (Headquarters, Department of the Army 1978). Even if one anticipates reasonable advances in technology, geophysical methods, and for that matter drilling, do not hold the possibility of discovering every cavity that might hold the potential for causing piping. This situation must be dealt with through the use of defensive design measures. However, even in this area, the partial information obtained can be used to guide decisions regarding the type and degree of redundancy needed in these measures.

3. One problem with previous trials of geophysical methods for cavity detection has been that field programs were not designed for the detection of relatively small, localized structures. Another is that there has not been sufficent evaluation of the signatures produced by geophysical tools when used in the vicinity of cavities of known size and location. Thus, the manner in which the presence of cavities would be revealed in the data has not been known or at least appreciated for many of the methods.

Purpose

4. The purposes of the investigation reported herein were (a) to plan and construct a controlled Cavity Test Facility for use in preliminary evaluation of geophysical methods as cavity location or delineation tools and (b) to evaluate several geophysical techniques to determine whether signatures could be obtained that would help to either locate a cavity or, once located, to determine its size, depth, or shape in plan view (i.e., to delineate it).

<u>Scope</u>

5. As part of this investigation, a Cavity Test Facility was designed and constructed at the U. S. Army Engineer Waterways Experiment Station (WES) and used for the evaluation of several existing geophysical methods. Site conditions in the vicinity were documented and the following geophysical test methods were used to survey the area:

    <u>a</u>. Seismic studies

        (1) Surface refraction surveys

        (2) Surface reflection surveys

        (3) Wave-front surveys

        (4) Crosshole surveys

        (5) Sonar investigation

    <u>b</u>. Resistivity studies

        (1) Wenner profiling

        (2) Schlumberger sounding

        (3) Bristow-Bates surveys (pole-dipole)

        (4) Dipole-dipole surveys

        (5) Subsurface resistivity logging

    <u>c</u>. Radar studies

        (1) Continuous wave-frequency modulation (CW-FM) profiling

        (2) Pulse profiling

Results of these surveys were analyzed to determine if trends or anomalies in the data could be correlated to cavity location and size.

PART II: WES CAVITY TEST FACILITY

General Description

6. The criteria guiding the planning for the facility were that (a) the site should be easily accessible, (b) the cavities should simulate voids in an otherwise relatively homogeneous medium, and (c) the facility should provide a realistic range of cavity sizes and depths. Item (a) dictated that the facility be located at or near WES despite the fact that no solution-susceptible formations exist in the area. An isolated location at WES was selected for the Cavity Test Facility (see Figure 1). Soil at the location is the loess that is typical of the Vicksburg area. The stratigraphy of the area is varied, but the general succession from the surface downward is loess, Pleistocene sands and gravels, terrace deposits (mixed clays and silts), Bucatunna formation, Byram Marl, and Glendon limestone. In some places, the Pleistocene sands and gravels are missing. The loess varies considerably in thickness, depending on the topography, but typically is about 15 m* thick. The depth to the water table in the area is greater than 9 m.

7. Figures 2 and 3 show a plan and a north-south section view of the facility illustrating the general geometry of the four cavity sites. The specific characteristics of the four sites are tabulated below:

Site	Geometry (Horizontal Cylinders)	Depth to Top
I	1.22 m diam, 6.1 m long	6.1 m
IIA	0.3 m diam, 0.3 m long	3.0 m
IIB	0.6 m diam, 0.6 m long	6.1 m
IIIA	0.3 m diam, 6.1 m long	3.0 m
IIIB	0.6 m diam, 6.1 m long	6.1 m
IV	1.22 m diam, 1.22 m long	6.1 m

---

* A table for converting U. S. customary to metric (SI) units and metric (SI) to U. S. customary units is found on page 3.

It was felt that this arrangement would allow opportunity to evaluate size, shape, and depth discrimination with the geophysical methods as well as vertical discrimination and resolution. The sizes and depths were also considered appropriate and realistic simulations of commonly encountered field conditions.

Construction Details

8. Figure 4 illustrates the instructions given to the construction forces for the excavation of the site. All four excavations were to have 1-on-1 slopes in the east-west direction and 1-on-2 to 1-on-3 slopes in the north-south direction. Figures 5 and 6 are photographs of the construction in progress for Cavity Site I. They indicate that the instructions as to slope were not closely adhered to by the construction forces.

9. The cavities were formed by emplacing closed-end polyvinyl chloride (PVC) pipes of varying lengths and diameters in excavations, which were then backfilled. Fill material was compacted around and immediately above the PVC pipes. The remainder of the fill, however, was placed without compacting, and the test sites were leveled.

10. A grid pattern of nominal 0.12-m-diam by 9-m-deep boreholes was drilled (augered) at the facility for use during subsequent investigations (open circles in Figure 2). Also, vertical plastic pipes were connected to the cavities to allow them to be filled with water.

Subsurface Investigations

11. In addition to the grid pattern of boreholes discussed previously, three boreholes were drilled to depths of about 18 m at Cavity Site I at locations shown in Figure 7 after completion of construction. Soil samples were taken for visual classification and density and water content determinations, to support any analysis that might be desired in the geophysical investigations. Results are shown in Figures 8 and 9.

8

12. As indicated in Figure 8, water was encountered in Boring No. 1 at 9.5 m and Boring No. 3 at 14.5 m. The water level in a piezometer 30 m south of Cavity I was at the 8.8-m depth. As indicated by Figures 5 and 6, no water was present in the cavity excavations. At the time of construction and during the investigations reported herein, the water table at the site was at least 9 m deep. This is 1.7 m below the depth of the deepest cavities.

13. Borehole nuclear logs were run in Boring No. 1 (Figure 10). The logs were obtained solely for qualitative comparison purposes. The natural gamma log (Figure 10a) generally reflects clay content of the soil, with higher count denoting higher clay content. Gamma-gamma logs generally indicate formation bulk density, with count rate decreasing with increasing density (Figure 10b). Finally, the neutron log (Figure 10c) indicates water content above the water table and porosity below the water table, with higher count rates indicating smaller water content values. A void behind the casing possibly is the cause of the large excursion to the right in both the gamma-gamma and neutron logs at 3-m depth. The transition that occurs over the depth range of 7.7 to 9 m coincides approximately with the water table indicated in a nearby piezometer, although 7.7 m also coincides with the bottom of the fill material. The abrupt transition to lower values that occurs in the gamma-gamma and neutron logs at 14 m is not easily explained in terms of the boring logs and water content and density data. The change in character of the material at 15 m indicated on the boring logs does not seem sufficient to explain the geophysical log response.

PART III: SEISMIC INVESTIGATIONS

General

14. Seismic studies conducted at the Cavity Test Site consisted
of surface compression- (P-) wave refraction surveys, crosshole shear-
(S-) wave surveys, shallow seismic reflection surveys, "Meissner wave-
front" surveys, and a sonar investigation. The seismic refraction
method is adequately documented in many sources, and standard field
procedures were followed at the site (Headquarters, Department of the
Army 1978). Field, data reduction, and interpretive procedures for the
crosshole method are described by Ballard (1976) and Butler, Skogland,
and Landers (1978). The Meissner wave-front technique, field procedures,
and interpretive procedures are described by Meissner (1961), U. S. Army
Engineer Division, Missouri River (1971), and Franklin (1977). All
tests were conducted with air-filled cavities.

Results of Surface Seismic Refraction Surveys

15. The surface refraction surveys were conducted in the vicinity
of Cavity Sites I and II, with the majority of the reversed-profile
lines over and near Cavity Site I (see Figure 11). Time-distance plots
for each of the profile lines are presented in Figures 12-19. There are
apparently three velocity zones at the site: the fill material with a
P-wave velocity of about 270 m/sec, the undisturbed material down to
about 5.5 m with a P-wave velocity of about 340 m/sec, and the undis-
turbed material below about 5.5 m with a P-wave velocity of about
1390 m/sec. The nature of the irregular refractor located from 4.8
to 6.0 m in depth is uncertain, since the water table is considerably
deeper.

16. Detection of cavities by the conventional refraction method
relies on detecting time discrepancies caused by the seismic waves
passing through or around the void. The P-wave velocity in air is about
305 m/sec. Due to the relative closeness of the fill material velocity

10

and upper undisturbed material velocity to the velocity in air, it is unlikely that a delay could be detected. In fact, if the low fill velocity extends to the depth of the cavity, the waves would preferentially pass through the air-filled cavity. Figure 20 shows a section view of Site I along refraction line A. The refractor interface for line A is at approximately 5.9 m; and if it is assumed that the interface is continuous across the fill region, it is seen that the refracted paths would at best graze the top of the cavity. The refracted paths to the geophone positions are all drawn at θ_{12c} , and none of the rays even pass through the cavity when projected downward. Since the P-wave velocity in the fill in the immediate vicinity of the cavity is not known, the true ray paths in the fill-cavity region cannot be depicted (although in any event the undisturbed-fill velocity contrast will be small). However, with the assumption of a continuous interface across the fill region, it is seen that the delays should be greatest for geophones 10, 11, and 12 in one profile direction and for geophones 6, 7, and 8 in the reverse direction (see Figure 20) for reasons that have nothing to do with the presence of the cavity. The delay times are, in fact, due to the excavation. The time-distance data in Figure 12 are entirely consistent with this model, and the data can be explained solely in terms of the lower fill-material velocity. Line B, depicted in Figure 21, involves a yet more difficult geometry, but again the time-distance data (Figure 13) cannot be directly interpreted to show the presence of the cavity, and the delays are seen from Figure 21 to be primarily due to the geometry of the backfill zone.

Results of Crosshole Seismic Surveys

17. Crosshole S-wave surveys were conducted near Cavity Site I. Figure 7 shows the borehole layout. With borehole 1 containing the source, tests were conducted between boreholes 1 and 2 and boreholes 1 and 3. A section view between boreholes 1 and 3 is shown in Figure 22. Originally, 11 source positions and 11 receiver positions were planned, requiring 121 separate test records. Unfortunately, this complete test

11

program has not been completed. A complete set of opposed source-receiver records was obtained, e.g., S_{11} to R_{31}, S_{12} to R_{32}, etc., where S and R refer to source and receiver, respectively, the first digit of the subscript refers to the borehole number, and the second digit of the subscript refers to the position within the borehole. With the source at position S_{12}, records were also obtained for receiver stations R_{32} to R_{38}. The shear-wave velocity profile for Cavity Site I, interpreted from the opposed source-receiver records, is shown in Figure 22 also. This profile represents mean values from records obtained using both an impulsive and a vibrator source at each depth.

18. Three concepts guided the original crosshole survey planning and the manner in which the recores were examined: (a) for the opposed source-receiver records, there may be differences in arrival times and/or character of the signal for tests above the cavity, in line with the cavity, and below the cavity; (b) for the source in a fixed position and with the complete suite of receiver positions, after correction for source radiation pattern and direct path distance, the peak amplitudes observed at the receiver positions should exhibit a pattern characteristic of the cylindrical-diffractor; (c) since the air-soil interface of the cavity should have a reflection coefficient of unity (with 180-deg phase shift), for cases where the reflected travel time is sufficiently long compared to the direct travel time for resolution on the records, it should be possible to observe reflections from the cavity. Figure 23 presents opposed source-receiver records for six depths (see Figure 22 for borehole-cavity geometry). All records were obtained using a nominal vibrator frequency of 100 Hz (varied from 100 to 108 Hz). The increased travel time and diminished amplitude of the record at 7.0-m depth are conspicuous (depth to center of cavity = 6.7 m). The only other obvious change in wave form is the signature distortion of the record at 7.8 m. These initial results with the opposed source-receiver configuration are encouraging.

19. The tests with fixed source and varying receiver positions were not completed to a sufficient extent to allow identification of

cavity diffraction patterns. However, with the source fixed at position S_{12} (1.52-m depth) and varying receiver positions from R_{32} downward, the travel time of direct and reflected S-waves are sufficiently different to allow identification of the reflected event (SS). The critical parameter affecting diffraction and reflection (from a localized reflector) is the cavity diameter to wavelength ratio D/λ. For a nominal velocity of 180 m/sec and a cavity diameter $D = 1.22$ m, D/λ values for varying source frequencies are presented in the following tabulation:

f, Hz	λ, m	D/λ
70	2.57	0.47
90	2.00	0.61
110	1.64	0.75
130	1.38	0.88
150	1.20	1.02
170	1.06	1.15
190	0.95	1.29
210	0.86	1.42
230	0.78	1.56
250	0.72	1.69
500	0.36	3.38

The key concept is that the wavelength in the medium must be of the order or less than the effective diameter of the localized structure or the wave will not "see" (i.e., be diffracted or reflected by) the structure. Thus, for the present case, this requires $D/\lambda > 1.0$ or $f > 150$ Hz. For P-waves, it has been observed experimentally that no observable diffraction effects are noted for $D/\lambda < 0.2$ and that in the presence of noise, detection would be improbable for $D/\lambda < 0.7$ (Dresen 1973). Similar results are anticipated for S-waves; and if this is so, then the tabulation above indicates that observation of the SS event is most likely on records for which $f > 150$ Hz. Unfortunately, these concepts were not adequately appreciated when the crosshole surveys were conducted. Thus, the tests were not conducted with the specific goal of observing reflections.

13

20. It is possible, knowing the site S-wave velocity profile (Figure 22), for one to calculate approximately when the S-wave reflected from the cavity (SS event) should occur on a record. The results of such calculations are given in the following tabulation:

Source Depth m	Receiver Depth m	Direct Arrival Time, msec	Reflected Arrival Time, msec
1.52 (S_{12})	1.52 (R_{32})	38.1	58-63-69
	3.05 (R_{33})	38.0	51-56-61
	4.57 (R_{34})	38.8	47-50-56
	6.09 (R_{35})	43.5	45-46-63
	7.62 (R_{37})	48.3	46-47-55
3.05 (S_{13})	3.05 (R_{33})	33.7	46-46-54

The direct arrival times are calculated using mean travel path velocities. The three times for the reflected events are obtained by using the maximum, mean, and minimum velocities along the probable travel path and rounding to the nearest millisecond. It is apparent that discrimination of the SS event from the direct arrival for receiver positions below R_{34} would be improbable. Examination of the higher frequency vibrator test records and also the impulsive source records revealed a few possible reflected events. Figures 24a and b (for S_{12} to R_{32}) at 220 and 260 Hz, respectively, both have events at times consistent with being SS events. Figure 24c, at a lower frequency (120 Hz), shows no reflected events. Figure 25a (for S_{12} to R_{33}), using an impulsive source, shows the rather speculative identification of several events; however, lack of predictable source wave form precludes positive event identification in this case. Figures 25b and c at lower frequencies do not show identifiable SS events. Thus, the use of reflected S-events from crosshole records cannot be adequately evaluated from the present results, although the use of a controlled, high-frequency S-wave source looks very promising.

Shallow Seismic Reflection Survey

21. A shallow seismic reflection survey was conducted over Cavity

Site I (Kronig 1977). A 12-geophone array and a 50-Hz, low-cut filter were used to attenuate high-amplitude, low-frequency surface waves. The wavelength of the interfering surface waves from the hammer-impact source was determined to be 2.5 m; thus, geophones in the array were placed 0.23 m apart.

22. Figure 26 illustrates the survey plan. It was intended that a five-fold common depth point (CDP) stack (Sheriff 1974) be conducted at each station. If conducted properly (including corrections for statics and normal move-out), reflected signals should grow in amplitude with each stack while noise should diminish. Thus ten single, common depth point records would result from the plan shown in Figure 26. This should not be confused with a CDP traverse in which the common depth point itself varies along a profile line.

23. The survey as actually conducted, however, was not a true CDP stack. As shown in Figure 27, the geophone array remained fixed while the impact station varied, i.e., the CDP actually changes during the stack. Mooney (1976) refers to this procedure as "pseudo-CDP," since it depends on the planarity and continuity of the subsurface reflector for success. Thus, for a localized structure, the "pseudo-CDP" stack is not strictly valid. However, since the horizontal variation of reflection points (from a hypothetical horizontal reflector) is 0.6 m for the geometry in Figure 27 (less than half the cavity diameter), it is still possible that enhancement will occur during stacking due to the duration of the reflected pulse.

24. Considering the P-wave velocities from the refraction surveys, the cavity-reflection event should occur at 30 to 40 msec (record time). Figures 28 and 29 show records from Stations 1 and 2 (Figure 26).* Each record (from the top down) is the sum of itself plus the preceding records. Thus, the bottom records in Figures 28 and 29 are the sum or stack of records from five impact stations (see Figure 27). The vertical dashed line is drawn at 35 msec (mean value for the expected arrival

---

* Records from the remainder of the stations are contained in Appendix A.

15

time of the cavity reflection event) for both Stations 1 and 2. In-
deed, enhancement of a trough occurs at 35 msec. This trough could
represent the cavity-reflection event. There are peaks and troughs
on these as well as the other records from the survey that show enhance-
ment during stacking and that could represent reflections from inter-
faces as defined by the refraction survey (Kronig 1977).

Results of Wave-Front Surveys

25. Wave-front surveys using the Meissner technique (Meissner
1961) were conducted at Cavity Site I. Figure 30 illustrates the geom-
etry for an east-west survey across the cavity, and Figure 31 presents
the results in the form of an arrival time contour plot. The contour
lines represent lines of equal travel time of the wave front, and the
grid represents the hypothetical reciprocal positions to which measured
first arrival times are assigned. There is no obvious perturbation of
the contours indicative of the cavity.

26. Another wave-front survey was conducted in a north-south
direction using a borehole west of Cavity Site I. This survey line
passed over undisturbed material. Figure 32 presents the results.
Accepting this contour map as standard or typical of the site, an
anomaly contour map (Figure 33) is produced when the arrival times in
Figure 32 are subtracted from those in Figure 31. Comparing this
anomaly map with maps produced by analytical model studies involving
cavities and grikes, Franklin (1977) demonstrated that the anomaly due
to a cavity of this size would not be evident. However, an 8-msec
anomaly would be produced by the backfilled trench. Thus, again, any
anomaly due to the cavity would be indistinguishable from the anomaly
due to the trench (as in the refraction surveys).

Sonar Investigation

27. In an attempt to detect the cavities with higher frequency
seismic (acoustic) waves, a sonar survey was conducted at the Cavity

16

Test Facility (Unterberger 1977). The system, called SONAR II, uses a single transducer array* as source and receiver. The output is a pulse of 24-kHz waves with 0.25 msec duration. The test geometry and procedure is essentially equivalent to vertical seismic reflection profiling. Surveys were conducted over Cavity Sites I and III. Because of the uncertain nature of the P-wave velocity variation in the fill material, it is difficult to predict the time at which a reflected signal should be observed. Thus, it is preferable to attempt to bound the expected arrival time (due to uncertainty in the true velocity profile above the cavity) as in the following tabulation:

Assumed Velocity Structure	Reflection Time msec
270 m/sec--0-5.95 m[†] (apparent fill velocity)	44.1
340 m/sec--0-5.95 m (apparent undisturbed profile)	35.0
270 m/sec--0-5 m (nominal P-wave refraction profile)	38.5
1390 m/sec--5-5.95 m	
300 m/sec--0-5 m (profile used by Unterberger 1977)	34.6
1500 m/sec--5-5.95 m	

[†] 0.15 m graded off surface prior to tests.

Thus, events occurring between 34 and 44 msec could be reflections from the cavity.

28. Figure 34a is a sonar record from directly over the cavity at Site I. The record is a photograph of an oscilloscope screen on which the transducer output voltage is displayed as a function of time. There are at least five signals present from 34 to 44 msec. The indicated signal at 35.5 msec is the best candidate for the cavity reflection (Unterberger 1977). However, it is not necessarily prominent with respect to the rest of the events present. It is interesting that the

---

* Twenty-one lead titanate zirconate transducers (2.5 cm diam, 2.5 cm long) arranged in a "circular" array. The array is coupled to the soil via a castor oil medium.

peaks between 25 and 45 msec are roughly equally spaced; this could be an indication of secondary "layering" resulting from the backfilling process. Figure 34b is a sonar record from directly over the cavity at Site III (2.9 m to top of cavity). In nominal 300 m/sec material, the reflection is expected at 19.3 msec; and, indeed, there is a low amplitude signal at 19.3 msec. These results are encouraging but are certainly not dramatic demonstrations of cavity detection.

Summary of Seismic Investigations

29. The following statements summarize the results of the seismic investigations:

   <u>a</u>. <u>Surface refraction surveys.</u> Time delays were observed for lines over Cavity Site I that could be attributed to the backfill material. No effect was observed that could be interpreted as directly due to the cavity.

   <u>b</u>. <u>Crosshole surveys.</u> Diminished amplitude and slightly increased travel time were observed for the crosshole geometry in which the cavity was directly between source and receiver. Some success was achieved in identifying cavity-reflection events on crosshole records from a high-frequency controlled S-wave source.

   <u>c</u>. <u>Seismic reflection survey.</u> A possible cavity-reflection event was observed using enhancement techniques to stack records obtained using "pseudo-CDP" field procedures.

   <u>d</u>. <u>Wave-front surveys.</u> A wave-front anomaly plot, obtained from wave-front surveys over and near Cavity Site I, showed a significant anomaly due to the backfilled region, but no specific indication of the cavity.

   <u>e</u>. <u>Sonar investigation.</u> Sonar records from vertical probing over Cavity Sites I and III showed reflections at times consistent with the cavity depths, but also showed numerous other events of equal or larger amplitude from unknown sources.

PART IV: RESISTIVITY SURVEYS

Surface Resistivity Methods

30. Surface resistivity surveys* using the Modified Bristow or
Bristow-Bates technique, Wenner profiling, Schlumberger sounding, and
dipole-dipole methods were conducted over Cavity Sites I and III. The
resistivity surveys were aligned in a direction normal to the long axis
of the cavities (except for two dipole-dipole surveys parallel to the
long axis).

Bristow-Bates technique

31. The Bristow-Bates technique (Bates 1973) uses essentially a
pole-dipole geometry. The first Bristow-Bates survey at Cavity Site III
was conducted using a potential electrode spacing (PP) of 10 ft (Fig-
ure 35). The Gish-Rooney resistivity instrument was used with copper-
clad steel stakes as the electrodes. A current sink (C_2) was placed at
about 500 ft from the C_1 current electrode. The maximum length of line
that could be run was 150 ft because of the presence of steel and fabric
test strips on both sides of the facility. Segments for the first sur-
vey were 100 ft long; i.e., resistivity measurements were made at nine
positions at 10-ft spacings. Current electrode C_1 was moved 50 ft along
the line to achieve the necessary overlap of measurements (see Fig-
ure 36). Field data for the first survey are shown in Plates B1-B3.**
Electrode spacings were measured using nonconducting measuring tape,
and resistance data were converted to apparent resistivities $(\rho_a$, see
Figure 35) and plotted in ohm-centimetres versus electrode pair distance
from the C_1 electrode (see Appendix B). Interpretations were based on
deviation of resistivity values from a baseline curve. Peaks, or anoma-
lously high values, are interpreted as resistive zones within the "shell"
of earth measured between the potential electrodes. Anomalously low

---

* Mixed U. S. customary and metric units are used in this Part due
to the inconvenience and awkwardness of converting field data and
survey line references.
** Field data for the Bristow-Bates surveys are contained in
Appendix B (Plates B1-B32).

values are interpreted as conductive zones. The buried cavities sur-
veyed are air-filled and should be represented by anomalously high
values. Study of the curves obtained in the initial survey (Plates B1-
B3) indicated that more data points were needed to establish the baseline
for the curve, which would permit better delineation of highs and lows.
Subsequent surveys were therefore run with segments consisting of 18
points (PP = 5 ft) instead of the previous nine. In a situation of
homogeneous, isotropic earth, the baseline should be a vertical line
(resistivity versus distance of potential electrode array from C_1). The
thick loess section in which the test cavities are buried should approxi-
mate this situation, except for the excavated and backfilled regions.
It was not known initially how this disturbed zone would affect measure-
ments, if at all. Subsequent surveys run at smaller PP spacings showed
that the effect of the disturbed zone was substantial, as discussed
below.

32. An interpretation of the data collected in the first survey
is given in Figure 36. No more than two arc interceptions result for
either high or low anomalies, except for the apparent three-arc
intersections at a depth of about 60 ft. The three-arc intersection
is considerably below the cavities and is presumed to be a false indi-
cation caused by near-surface anomalies, as discussed later (para-
graphs 36 and 37). It is desired to have at least three interceptions
for a reliable interpretation (Bates 1973). Failure of the first survey
to locate the cavities was attributed to (a) failure to establish a
sufficient baseline from which to select anomalies, (b) use of potential
electrode spacings that were too large, considering the diameter of the
target cavities, and (c) the effect of the disturbed zone, which may
mask the existence of cavity-related highs and lows.

33. The second survey at Cavity Site III was modified based on
results of the first survey and was run on the same line, using a 5-ft
PP spacing and segments of 18 points (100-ft segments with the C_1 elec-
trode moved 50 ft for each segment). The 5-ft spacing resulted in a
much smoother, better defined baseline (Plates B4-B8) from which pos-
sible anomalies were picked and plotted for the interpretation. The

20

interpretation (Figure 37) did not locate the known cavities, although a point of intersection of three high anomaly arcs occurred at a depth of about 47 ft, 8 ft west of the cavity axis. There is no subsurface information available to indicate that the arc intersections represent an actual anomaly, and for reasons explained in paragraphs 36 and 37, the apparent anomaly is presumed to be a false indication caused by near-surface resistivity variations.

34. What is striking about the data of the second survey is the abrupt step from one baseline resistivity value to another as shown in Plates B5 and B6. Plate B5 shows the segment run from the 100-ft position to the 200-ft position and indicates that the measuring potential electrodes cross from a zone of relatively high resistivity (about 7000 ohm-cm or 230 ohm-ft) to a zone of low resistivity (about 3000 ohm-cm or 98 ohm-ft) at the 125-ft position and back to a high zone at the 155-ft position. Plate B6, which shows the segment run from the 150-ft position to the 50-ft position (opposite in direction to that of Plate B5), indicates the measuring electrodes crossed from a zone of relatively low resistivity (about 300 ohm-cm) to a high zone at the 125-ft position. The 155- and 125-ft positions plot symmetrically about the axis of the cavity burial area and coincide with the approximate boundaries of the excavated or disturbed zone of material. The disturbed and remolded loess of the excavated zone exhibits lower resistivity. The potential electrode measuring circuit is strongly influenced by resistivities of surface materials, and it is apparent that, in this case, the measuring electrodes are detecting the presence of the disturbed zone of material and that the resistivity of the disturbed zone differs from that of the undisturbed material. Referring to Plates B1-B3, it is now apparent that most of the anomalies recognized in the first survey were actually an expression of the disturbed zone. This illustrates a problem that variable overburden materials present in the use of the Bristow-Bates technique. Failure of the second survey to locate the cavities was attributed to (a) potential electrode spacing that was too large, (b) masking effects of the disturbed zone, and

21

(c) lack of sensitivity (lack of power) of the instrument at the electrode spacings used.

35. A Keck IC-69 resistivity meter was used to run a third Bristow-Bates survey at Cavity Site III with a 2-ft potential electrode spacing. The survey line was the same as that used for the other (5- and 10-ft electrode spacing) surveys. The third survey was run in 40-ft segments with the current electrode at the 110-, 130-, 150-, and 170-ft positions, respectively, along the survey line (see Figure 38). There were no arc intersections that indicated locations of the cavities in this survey. The data do indicate, however, the location of the east and west boundaries of the disturbed or excavated zone. By noting the gradual increase or decrease of the baseline values of the curves as the potential electrodes are advanced 2 ft at a time, it can be concluded that the excavation boundary is sloping toward the center line of the test area. A vertical boundary between high and low resistivity material would be expected to produce a sharp break in the curve regardless of electrode spacing. A sloping boundary, however, creates a situation of a gradual decrease in the measured apparent resistivity values as more and more lower resistivity material near the potential electrodes comes into the section. Plate B11 illustrates this situation very well. Note the gradual rise from one baseline resistivity value to a higher value from the 152-ft position to the 160-ft position.

36. Two distinct high anomalies were indicated in the third survey by intersections of fairly strong arcs 2 ft east and west of the center line, at the ground surface. These positions are expressed on the surface by a slightly raised ground surface, indicating possibly a less compacted zone of material within 2 ft either side of the center line. It is not known why the boundaries of this zone are expressed specifically by high anomalies, but the symmetry and position of the anomalies with respect to the center line cannot be overlooked. The several surface anomalies exhibited in the final survey emphasize again that the measuring circuit (potential electrode pair) is influenced strongly, if not dominated, by surface and near-surface phemonena at small potential electrode spacings, rather than by material within the "bowls" described

by the arcs. A possible exception is the anomaly indicated in Figure 38 at about the 134-ft position, lying approximately 12 ft below the surface. It is indicated by a three-arc intersection--one arc corresponding to a very weak anomaly, and the other two are part of the intersections of the surface anomalies. One is led to conclude that the apparent buried anomaly is a false indication.

37. Bristow-Bates surveys were also run over Cavity Site I, using 10-, 5-, and 2-ft potential electrode spacings. Field data for the surveys are presented in Plates B16-B32. Interpretations of the data are shown in profile in Figures 39-41. Results were very similar to those obtained over the 2-ft cavity. Only surface-expressed anomalies were detected. There were no subsurface arc intersections that indicate the presence of the cavity. Figure 40 indicates the presence of a resistivity high directly above the cavity. The anomaly corresponds to the position of two small-diameter plastic access pipes leading to the large buried cylinder. As with the other surveys, the disturbed or excavation zone again was well depicted as a zone of low resistivity (Figures 39-41).

Wenner profiling

38. Constant spacing (a-spacing) Wenner profiling surveys (Figure 42) were conducted over Cavity Sites I and III. Results of the survey over Cavity Site III are presented in Figure 43 for 5- and 10-ft a-spacings. The horizontal scale in Figure 43 is referenced to the same survey line used in the Bristow-Bates surveys over the site (Figure 36). These surveys were conducted primarily to verify the low resistivity zone and its correspondence with the backfilled region. The interpreted low velocity zone (Van Nostrand and Cook 1966) in Figure 43 corresponds quite well with the known excavation limits and the results of the Bristow-Bates surveys.

39. Results of the survey over Cavity Site I using 10-, 25-, and 50-ft a-spacings are shown in Figure 44. It is doubtful if either of the two smaller a-spacing curves represents sampling to sufficient depths to include the cavity. At such a wide a-spacing, however, a greater

23

volume of soil is averaged into the resistivity measurement, so that
any effect of the cavity is decreased. The relatively diminutive value
of the resistivity low attributed to the disturbed soil zone on the
50-ft a-spacing profile is another result of too great a volume of soil
being measured. All three curves indicate the presence of the disturbed
soil zone by the "trough" of low resistivity near the centers of the
profiles, similar to profiles for Site III (Figure 43).

Schlumberger sounding

40. An east-west Schlumberger sounding was performed over Cavity
Site I with the potential electrode pair centered over the cavity. L-
spacings (see Figure 45) ranged from 5 to 130 ft. The results (Fig-
ure 46) can be interpreted in two ways: (a) a four-layer structure of
high, low, high, low apparent resistivity (12), where ρ_1 = 93 ohm-ft
(28 ohm-m) , ρ_2 = 60 ohm-ft (18 ohm-m) , ρ_3 = 470 ohm-ft (143 ohm-m) ,
ρ_4 = 40 ohm-ft (12 ohm-m) , and layer 1 thickness E_1 = 4 ft (1.2 m) ,
E_2 = 6 ft (1.8 m) , and E_3 = 11 ft (3.4 m) or (b) more probably, a
structure of approximately constant low resistivity in the disturbed
material over the cavity (with a very thin surface layer of higher
resistivity material) and as a two-layer structure of high then low
apparent resistivity in the undisturbed material outside the excavated
zone. In this interpretation, it is assumed that the hump in the sound-
ing curve in the middle L-spacing range is caused by current flow en-
countering the higher apparent resistivity material of the undisturbed
zone. When the current electrodes are placed farther apart, the current
penetrates to the water table. This produces the final drop in apparent
resistivity at large L-spacings.

Dipole-dipole surveys

41. Dipole-dipole surveys (see Al'pin et al. 1966) were run from
east to west across Cavity Sites I, II, and III and from north to south
across Cavity Sites I and III (Kronig 1977). The electrode configura-
tion and method of surveying are illustrated in Figures 47 and 48.
Depth of penetration with this form of dipole-dipole surveying is esti-
mated to be 0.7 to 0.9 times the distance n × r (see Figure 47). The
apparent resistivity data are tabulated to permit easy contouring of a

24

cross section through the site along the survey line (Figures 49-53). The vertical spacing in the tabulation is constant but arbitrary, and horizontally the data points are placed at the midpoints of the array.

42. Traversing east to west across the three cavities, the transition from undisturbed to disturbed material can be detected, with varying degrees of clarity, by the lower apparent resistivity values in the disturbed material. The central region of the surveys produces generally low resistivity readings compared to the outer, undisturbed regions. In traversing north to south over Cavities I and III, while there are sporadic high resistivity readings, the sampled material is generally of low resistivity, as expected, since in the north-south direction, the surveys cross undisturbed material only at the end.

43. The east-west survey across Cavity III (Figure 52) clearly reveals the sharp contrast between the high (undisturbed) and low (disturbed backfill) resistivity zones. The presence of the backfill anomaly can be seen in all the east-west surveys. There are high apparent resistivity values within the central low resistivity zone that possibly indicate the cavity's location. However, Cavity I, the largest cavity, indicated no discernible resistivity high (Figure 50).

44. The interpreted shape of the disturbed-undisturbed interface, distinguished by the transition from low to high apparent resistivity values, is generally distorted, and in Figure 51, the slope is in the opposite direction from the actual slope. The anomalous high apparent resistivity values in the disturbed zone (see Figures 49 and 51), which possibly indicate the influence of the cavity, do not line up directly over the cavity. This offset can be explained by recognizing that data points are plotted, as a compromise, at the midpoint of the dipoles, even though the anomalous sampled material may be located to either side of the midpoint. Thus, this method shows some promise of detecting the presence of cavities and geologic boundaries, but must always be expected to be imprecise on the actual location of the anomalies.

25

45. An electrical resistivity device capable of conducting various types of single-hole and crosshole resistivity surveys has been designed at WES and prototype-tested at the Cavity Test Facility. The power supply is a 12-volt high-capacity battery, which is commutated at about 10 Hz, with dead times each half-cycle to prevent polarization effects at the electrodes. The 10-Hz square wave is centered at about 0 volts. The downhole probes consist of a 0.04-m-diam (d) by 0.15-m-long (L) solder-wrapped electrodes separated on either end of 0.05-m insulating sections from 0.76-m-long guard sections. A 0.15-m-long and 0.04-m-diam solder-wrapped electrode serves as a surface or mud-pit electrode. The measuring system is a Wheatstone bridge circuit using a microammeter as a null indicator and a precision rotary potentiometer to indicate the required null resistances. Seven different systems are possible: (a) single-hole, single-electrode resistivity; (b) single-hole, differential resistivity; (c) single-hole, focused resistivity; (d) crosshole, single-electrode resistivity; (e) uncontrolled guard, crosshole resistivity; (f) controlled Kelvin guard, crosshole resistivity; and (g) crosshole potential measurement (see Keller and Frischknecht 1966).

46. Although many problems were encountered with the instrumentation and field procedures, sufficient data have been collected using the single-hole point resistivity and crosshole point resistivity systems to be worthy of reporting.* A borehole 7.6 m to the east and a borehole 7.6 m to the west of Cavity I were used for the field tests. Several single-hole, single-electrode resistivity runs were made in each borehole, and then crosshole, single-electrode resistivity measurements were made. The conversions from measured resistances ($\Delta V/I$) to resistivities was made by the equation $\rho_a = K_G(\Delta V/I)$, where $K_G = 2.73$ $L/\left[\ln(2L/d)\right] = 2.03$ (see Keller and Frischknecht 1966). The results

---

* Personal communication, J. B. Warriner, EG&RMD, WES, August 1978.

are presented in Figure 54, where the dashed curve is the crosshole resistivity curve, the solid curve is the average of all single-hole measurements, and the horizontal bars represent the scatter in single-hole values at each depth. The crosshatched regions represent depths for which the crosshole curve significantly deviates from the average single-hole curve. At first, it seems that an anomaly occurs at about the right depth to be due to the cavity; however, since both the single-hole data and the crosshole data exhibit similar patterns and since the sign of the anomaly is wrong to represent an insulator, the anomaly centered at 7.0 m is probably not due to the cavity. It is difficult to formulate a consistent explanation for either anomaly. It is possible that the relatively more compacted fill around the cavity might contribute to the difference in the two curves and produce the lower anomaly. The anomaly at 4.3 m is possibly related to the observed refracting horizon in seismic surveys, although in general the refracting horizon was somewhat deeper. It should be noted that single-hole and crosshole data contain anomalies that are only about ±10 percent of the mean value. The other resistivity procedures produced more substantial anomalies, although clearly the geometries with respect to the fill zone are very different.

Summary of Resistivity Surveys

47. Five electrical survey techniques were attempted: (a) Bristow-Bates (pole-dipole), (b) Wenner profiling, (c) Schlumberger sounding, (d) dipole-dipole, and (e) crosshole resistivity. The first four techniques consistently produced anomalies that could be related to the backfill zone. The Bristow-Bates and dipole-dipole techniques did reveal some anomalies that were possibly cavity related; however, neither technique showed these latter anomalies consistently from one survey to another.

48. The data obtained indicate the following:

    a. Interpretation of the Bristow-Bates technique can be complicated by large lateral variations in resistivity of

near-surface material; for these situations, it is imperative to increase data redundancy by decreasing current station spacing along the survey line.

b. More data points should be obtained along survey lines for the Wenner profiling technique; for a = 40 to 50 ft (appropriate for Cavity Site I), data points should be spaced 10 ft or less along the survey line.

c. The dipole-dipole technique, while sensitive to horizontal variations in resistivity, does not accurately delineate interfaces via the approximate interpretation method used in this study.

PART V: RADAR SURVEYS

General

49. Surveys were conducted at the Cavity Test Facility with three different radar systems: (a) a 4.2-GHz continuous wave-frequency modulated (CW-FM) radar system; (b) a 100-MHz pulse radar system; and (c) a 300-MHz pulse radar system. These surveys were part of two contract investigations (Unterberger 1977, Benson 1977) and were considered to be feasibility studies.

CW-FM Radar Probing Results

50. The CW-FM radar system, called ECHO II, is essentially a modified airborne radar altimeter (Unterberger 1977). Since it is a CW system, it does not suffer from minimum range problems as do pulse radars. Also, since the system operates at a microwave frequency (4.2 GHz), the wavelength in the loess is of the order of 4 cm; hence, resolution should be excellent for objects the size of the cavities. The output frequency is modulated about the base frequency (4.2 GHz) at 120 Hz in a linear ramp (triangular modulation). The return signal is mixed with the transmitted signal and fed to a frequency analyzer. Beat frequencies other than 120 Hz or its harmonics indicate return signals from subsurface structures. Since the beat frequency and the speed of electromagnetic waves in the soil are known, the depth to the object causing the return signal can be calculated, at least in principle.

51. An east-west profile line of 21 stations, 1.52 m apart, was surveyed at Cavity Site I. All 21 stations were probed, and with only small variations, all spectral analysis records resembled Figure 55. No signals were observed other than harmonics of the 120-Hz frequency. In an attempt to bound the probing range of the system, a test was conducted probing horizontally through 1.5 m of surface loess material. Again, no return signal was detected. The failure of the system to achieve even small penetration depths can best be attributed to extremely

high attenuation in most soils at microwave frequencies. As indicated in Unterberger (1977), a lower frequency system (about 30 MHz) would have greater depth of penetration than the ECHO II system. However, because the wavelength would be about 6 m, small cavities could not be located.

Pulse Radar Profiling Results

52. A pulse radar system was utilized to obtain "continuous" real-time subsurface profiles over Cavity Sites I and III (Benson 1977). The system utilized two different antennae: (a) a monostatic* nonshielded antenna with a center frequency of about 100 MHz and 10-nsec pulse width, and (b) a bistatic** shielded antenna with a center frequency of 300 MHz and 3-nsec pulse width. The system was utilized in a "towed traverse" mode, with a speed of about 0.73 ft/sec (1.2 mph). All traverses were made from east to west. A total of 38 different trials were made over Cavities I and III.

53. Figure 56 is a profile (time section) made by moving the radar from east to west over Cavity Site III (3.05 m to top of upper cavity). The ideal cavity-disturbed zone appearance on the time section should be as shown in Figure 57, which shows a radar profile over two pipes buried in V-shaped trenches in limestone; however, such a structure is not observed in the time section of Figure 56. Several enhancement techniques were attempted with no success, such as varying the electric field vector polarization relative to the cavity axis, changing antennae, filling the cavity with water, and using various data processing schemes. While some of the records did reveal some features that can be seen to repeat on more than one scan, they do not reveal the unambiguous type of record indicative of the presence of a cavity seen in Figure 57.

---

* A single antenna used for both transmitting and receiving.
** Separate antennae used for transmitting and receiving.

54. In an effort to determine the depth of penetration of the radar system, traverses were made over several shallow culverts and pipes at WES. Figures 58 and 59 show time sections for traverses over 0.305-m-diam culverts at 0.305-m and 0.61-m depths, respectively. Both profiles show clearly the classical pattern produced by a "point source" target, and in Figure 58, the disturbance due to the trenching is also clearly seen. However, traverses over a 0.76-m-diam culvert at 1.83-m depth showed no evidence of the culvert. Horizontal probing through 0.305-m- and 0.61-m-thick loess blocks revealed the loess-air interface by use of the 300-MHz system, although the reflected signals were weak.

55. Possible explanations cited in Benson (1977) for the inability to detect cavities (or pipes) at depths greater than about 1 m in the loess are as follows:

    a. The material may be anisotropic and act as a depolarizer on the wave. (This is unlikely, however, as the material appears quite homogeneous and is composed of a fine-grained crystalline material whose particle size is very small compared to the radar's wavelength.)

    b. The cavity (pipe) acts as a depolarizer. (This may be possible at Site III as the wavelength is comparable to that of the cavity. Within the possible resonance region, polarization may occur.)

    c. Another material property commonly neglected when discussing radar is that of magnetic susceptibility, which is usually considered to be zero. (The loess at the WES site does have a small magnetic susceptibility of 50 to 60 cgs units. While this value is relatively small, the massiveness of the loess deposits may influence radar performance.)

    d. Penetration may be limited due to a high attenuation (signal absorption) of the loess backfill material.

Summary of Radar Surveys

56. Successful geological application of radar appears to be very site-dependent, but even under optimum conditions, it will be limited to shallow depths of penetration for typical sites of interest. Cook (1975) reports 18 rock types (in their probable natural moisture content state)

31

for which probing depths should be in excess of 30 m at frequencies of
25 to 100 MHz; fortunately, limestone is one of these rocks. However,
for soils (particularly those with high clay contents and/or moisture
contents), the probing depths are commonly very small (<1 m) as demon-
strated in the present study. Thus, for sites with more than a very
thin soil cover, radar will likely be of limited usefulness. For sites
with exposed rock or dry, sandy soil covers, the potential for success-
ful use of radar should be much better.

PART VI: SUMMARY AND RECOMMENDATIONS

57. This report documents the construction of a Cavity Test Facility at WES and presents the results of attempts to detect the cavities using various geophysical methods. It is important to emphasize that the group of geophysical methods studied is not exhaustive. There are several very promising methods that were not used: micro-gravimetric techniques, high-resolution seismic reflection profiling, borehole gravimetry, and magnetic methods (for clay-filled cavities or cavities in high clay-content soils). Also, it is not claimed that the methods that were used at the Cavity Test Facility are necessarily the most appropriate nor that the field procedures and interpretations represent best efforts. Based upon results of data obtained at the WES test site, it became apparent that some of the methods used showed potential as tools for cavity detection provided that refinements in data acquisition and/or interpretation were incorporated. In other words, in retrospect there is much that could be done differently or additionally if the program were to continue in the future.

58. In general, the results of the attempts to detect the cavities at WES are mostly of a negative nature. Seismic refraction methods appear to be a poor prospect for detecting cavities of the sizes present at the test facility. Some success was achieved in identifying reflections from the largest of the cavities (Site I) using the crosshole or surface reflection methods. Also, it appears technically promising to detect cavities between boreholes by seismic travel time and amplitude anomalies. Surface resistivity methods were generally unsuccessful at detecting the cavities. The Bristow-Bates and dipole-dipole techniques each provided indications of anomalies that possibly correlated to cavities in one or two cases. Subsurface probing radar could not detect the cavities, probably because of its insufficient depth of penetration.

59. It cannot be overemphasized that the results presented in this report are site-specific; i.e., they hold specifically only for the WES

33

Cavity Test Facility or cavities in a loesslike material. In fact, the negative results emphasize deficiencies of the test facility itself. The Cavity Test Facility fails to fulfill the program objectives in three important ways: (a) as a result of the construction methods, the medium around the cavities is not homogeneous because the backfill zone has different seismic and electrical properties from the undisturbed media; (b) the loess material in the backfill and top 6 m of the undisturbed material has P-wave velocities close to that of air and hence the cavities do not represent a significant velocity anomaly; and (c) although the cavity sizes and depths may be realistic for simulating field conditions and as goals for geophysical capability, they represent conditions too extreme for the evaluation and development of geophysical techniques for cavity detection. Indeed, most of the methods succeeded in detecting and delineating the zone of backfilled material around the cavities, and if any effect due to the cavities were present in the data, it was indistinguishable from the anomaly due to the backfilled material. Most of the geophysical methods used succeeded in delineating the backfilled zone, and since the differences between the disturbed and undisturbed materials were actually quite small, this is encouraging. However, the physical size of this zone was large and this may be one of the reasons why it was detectable.

60. It is recommended that cavity detection research continue, but that an alternate test site be found. The present WES Cavity Test Facility will still be of value in the future, but should only be used subsequent to the development and evaluation phase of research, i.e., only after the geophysical techniques have been thoroughly tested under less extreme conditions and interpretation procedures are well understood. The possibility of a natural Cavity Test Site should be explored. A thoroughly mapped cave system in limestone or dolomite with a satisfactory range of sizes and depths of cavities would be ideal. Also, a viable possibility is to drill horizontal holes into the vertical face of a rock quarry. All such sites are likely to be remote from WES, more costly to investigate, and have a lesser amount of "ground truth" information available than for a man-made site.

61. Geophysical methods that should be investigated in the cavity detection research program are microgravimetric techniques including gravity-gradient measurements, high-resolution seismic reflection profiling, expanding spread seismic fan shooting (Sheriff 1974), investigation of cavity diffraction signatures with the cross-hole geometry, and continued study of subsurface probing radar to determine the lithology dependence of its applicability.

REFERENCES

Al'pin, L. M. et al. 1966. Dipole Methods for Measuring Earth Conductivity, Consultants Bureau, New York.

Ballard, R. F., Jr. 1976. "Method for Crosshole Seismic Testing," Journal of the Geotechnical Engineering Division, ASCE, Vol 102, No. GT 12, Proceedings Paper 12646.

Bates, E. R. 1973. "Detection of Subsurface Cavities," Miscellaneous Paper S-73-40, U. S. Army Engineer Waterways Experiment Station, Vicksburg, Miss.

Benson, R. C. 1977. "Radar Subsurface Profiling - U. S. Army Engineer Waterways Experiment Station," Technos, Inc., Miami, Fla.

Butler, D. K., Skogland, G. R., and Landers, G. B. 1978. "CROSSHOLE: An Interpretive Computer Code for Crosshole Seismic Test Results, Documentation and Examples," Miscellaneous Paper No. S-78-8, U. S. Army Engineer Waterways Experiment Station, Vicksburg, Miss.

Cook, J. C. 1975. "Radar Transparencies of Mine and Tunnel Rocks," Geophysics, Vol 40, pp 865-875.

Dresen, L. 1973. "Investigation of Diffracted Seismic Wave Amplitudes as a Method for Locating Circular - Cylindrical Cavities in Solid Rock," Proceedings of the Symposium on Sink-Holes and Subsidence, IAEG, Hanover, Germany.

Franklin, A. G. 1977. "Effects of Subsurface Cavities on Wavefront Diagrams," Symposium on Detection of Subsurface Cavities, U. S. Army Engineer Waterways Experiment Station, Vicksburg, Miss.

Headquarters, Department of the Army. 1978. "Subsurface Investigations - Geophysical Investigations," Engineer Manual EM 1110-1-1802.

Keller, G. R. and Frischknecht, F. C. 1966. Electrical Methods in Geophysical Prospecting, Pergamon Press, New York.

Kronig, D. M. 1977. Cavity Detection by Geophysical Methods, Master's Thesis, University of Minnesota, Minneapolis, Minn.

Meissner, R. 1961. "Wave-Front Diagrams from Uphole Shooting," European Association of Exploration Geophysicists, Netherlands, Vol 9, pp 50-62.

Mooney, H. M. 1976. Shallow Reflection Seismology, University of Minnesota, Minneapolis, Minn.

Sheriff, R. E. 1974. _Encyclopedic Dictionary of Exploration Geophysics,_ Society of Exploration Geophysicists, Tulsa, Okla.

Unterberger, R. R. 1977. "Radar and Sonar Probing of Subsurface at U. S. Army Corps of Engineers Waterways Experiment Station," Texas A&M University, College Station, Tex.

U. S. Army Engineer Division Laboratory, Missouri River. 1971. "Gathright Dam Site Geophysical Studies," Omaha, Nebr.

Van Nostrand, R. G. and Cook, K. L. 1966. "Interpretation of Resistivity Data," U.S.G.S. Professional Paper 499, U. S. Geological Survey, Washington, D. C.
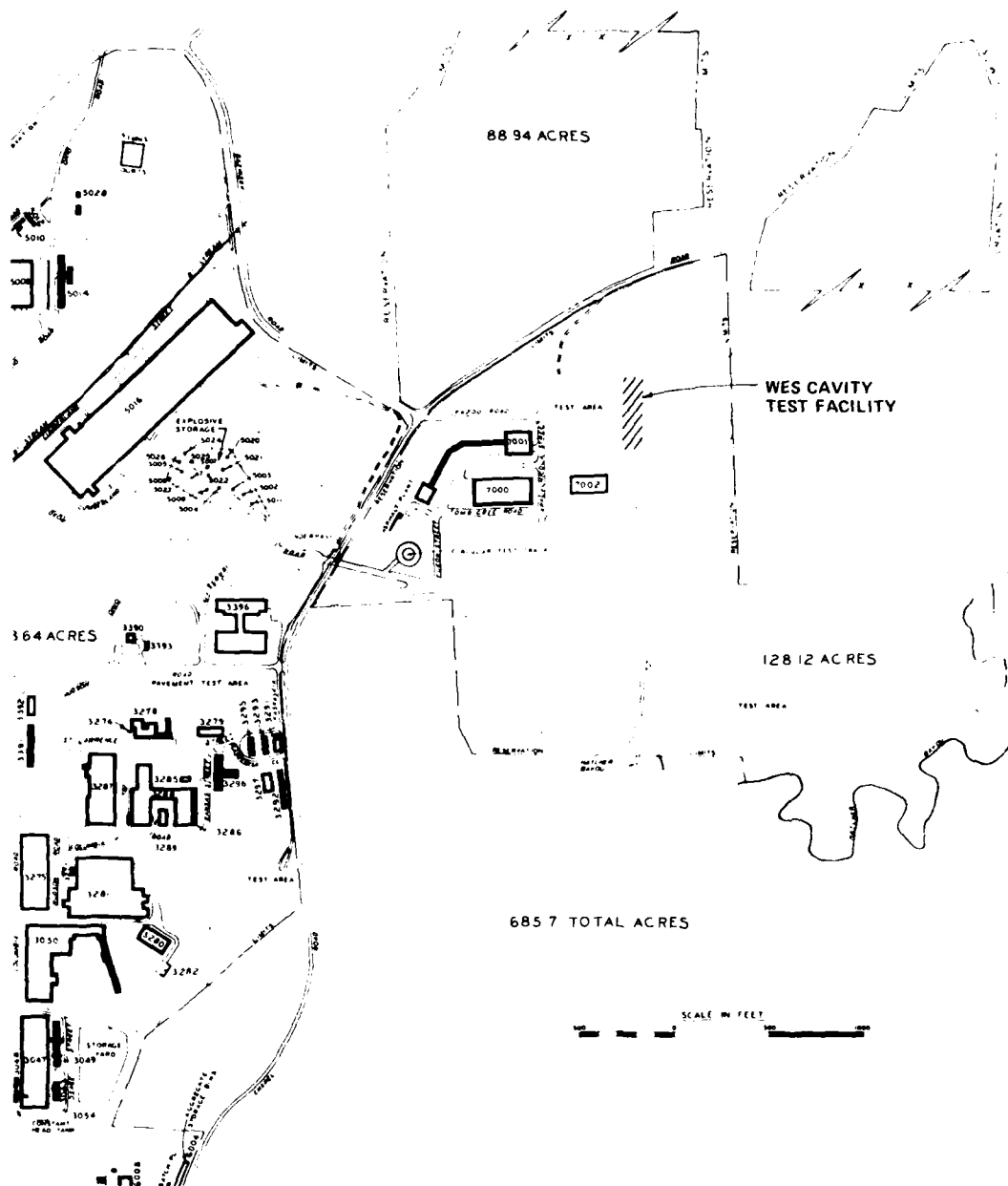
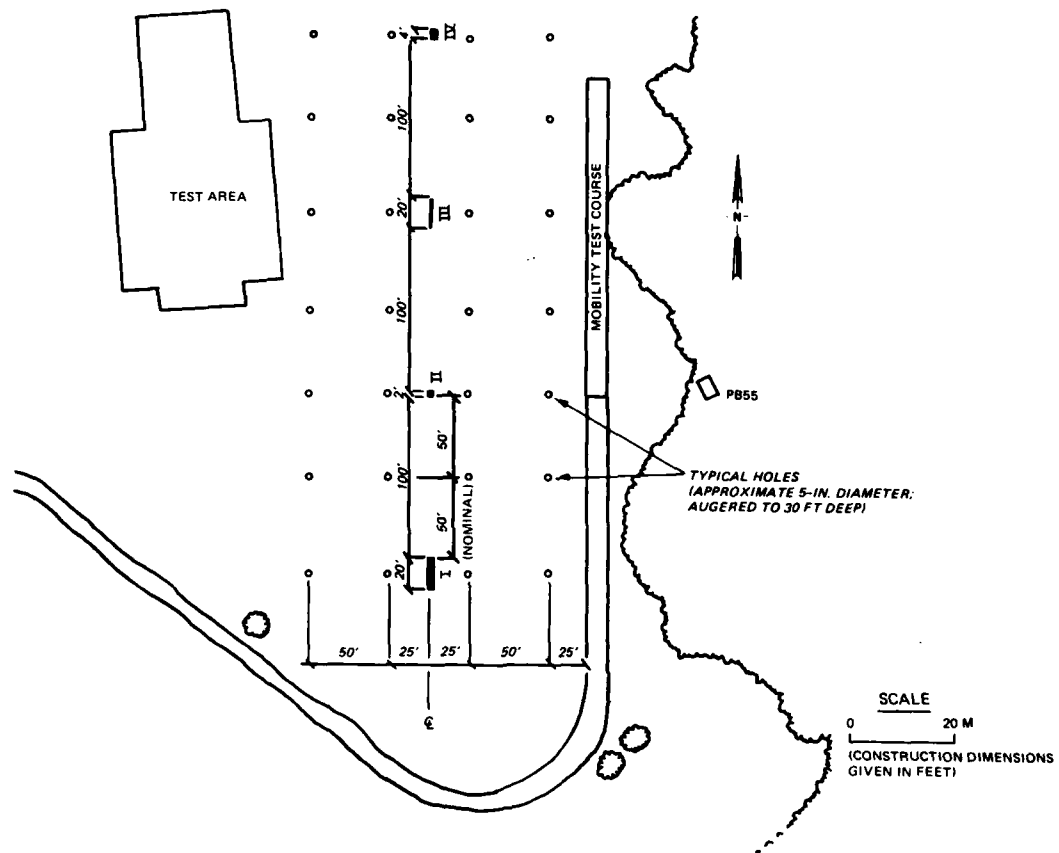Figure 1. Partial WES map showing Cavity Test Facility location
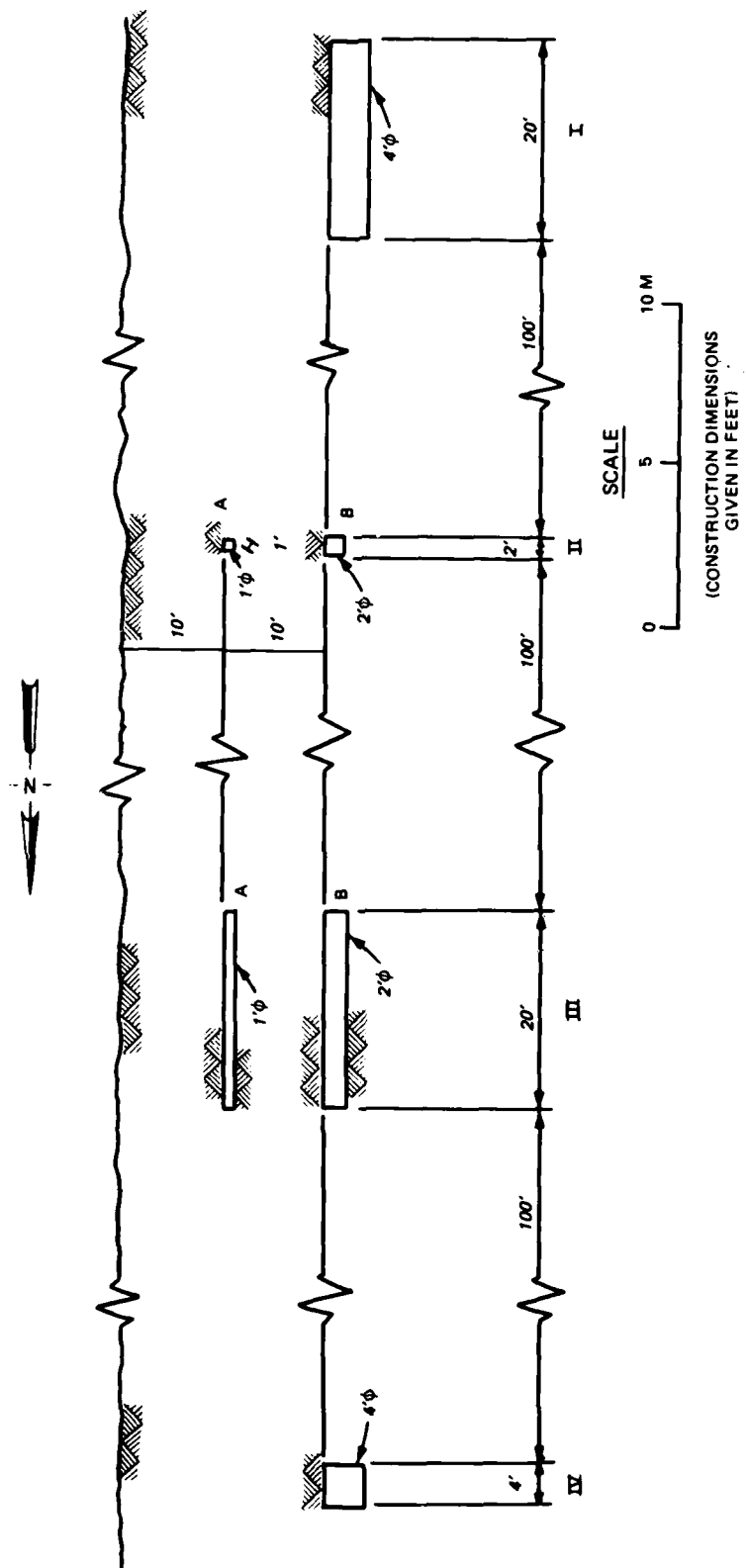
Figure 2. WES Cavity Test Facility

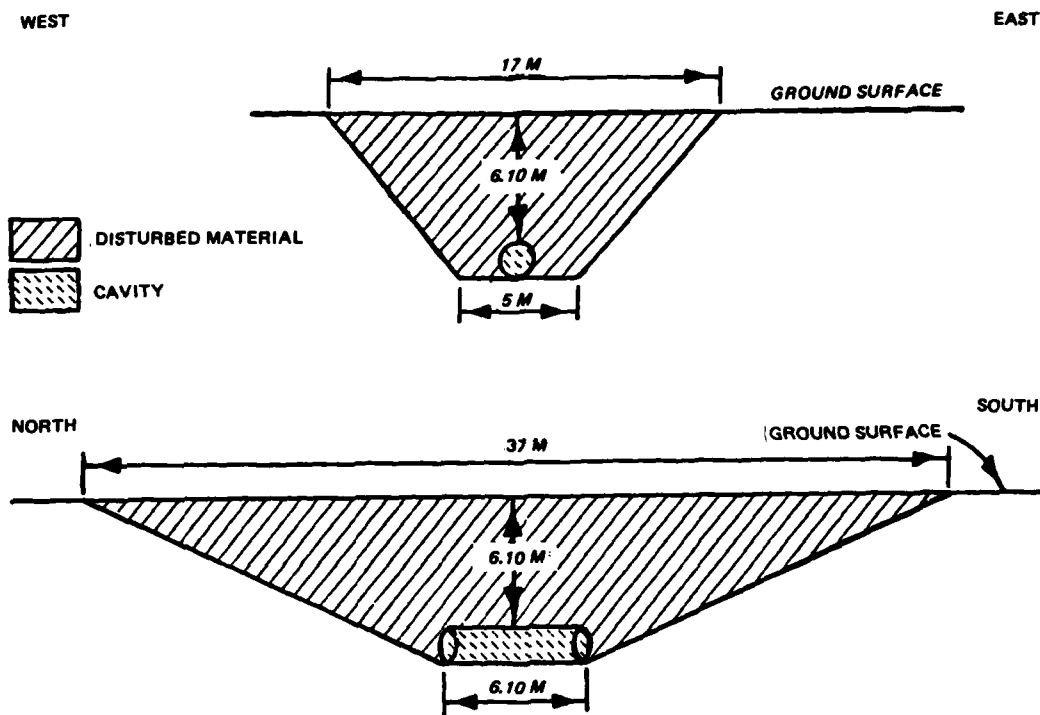Figure 3. North-south section view of Cavity Test Facility

Figure 4. Section view of Cavity Site I

Figure 5. Emplacement of PVC pipe at Cavity Site I
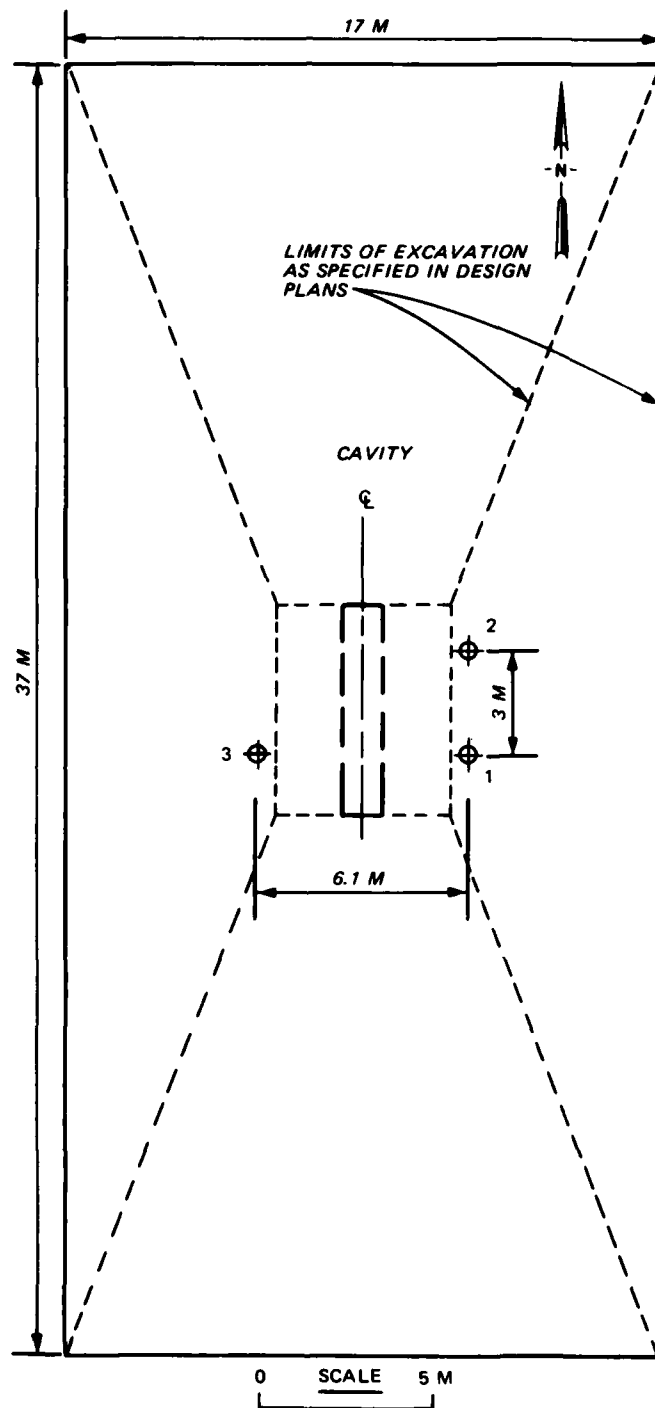

Figure 6. Backfilling operation at Cavity Site I

Figure 7. Location of boreholes
around Cavity Site I
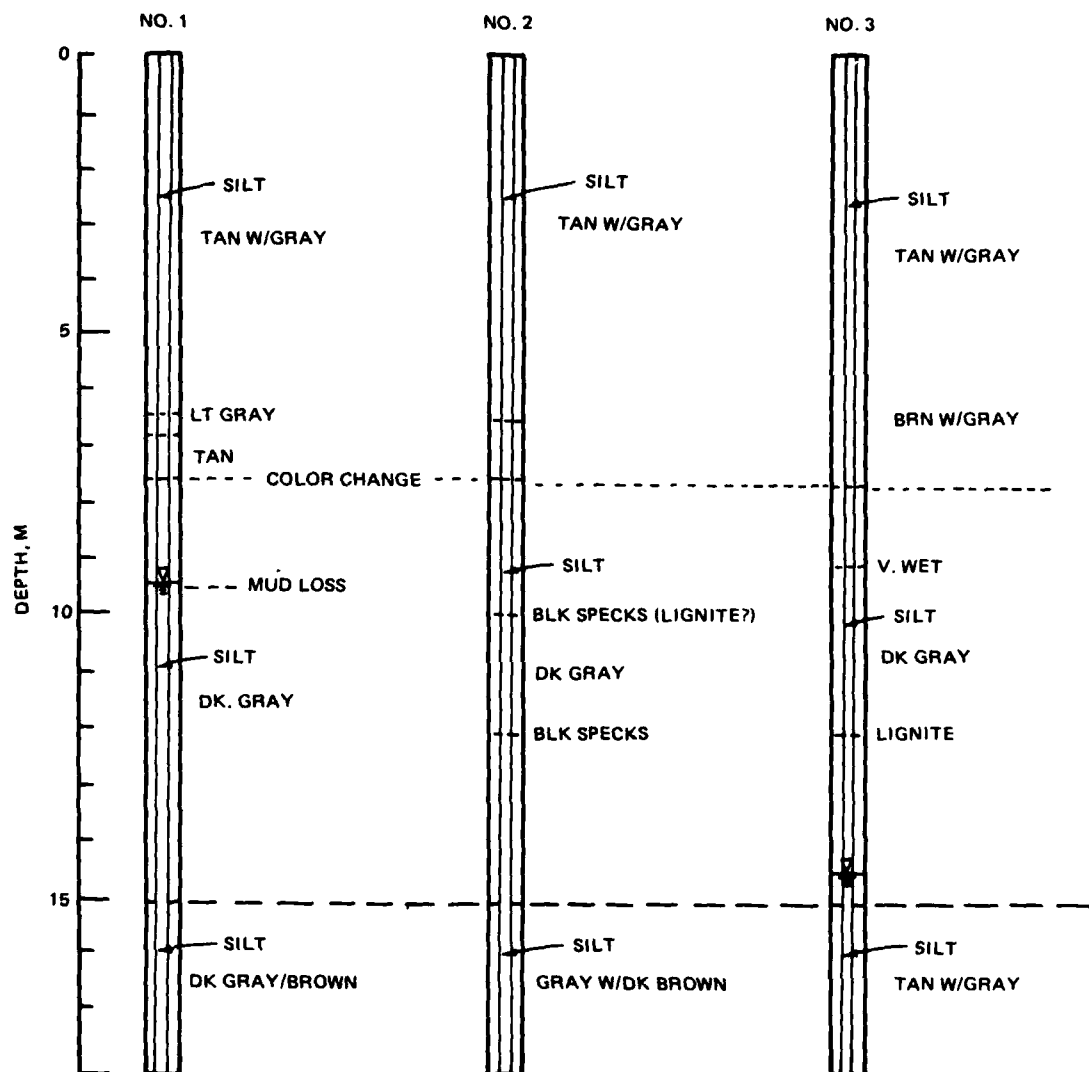
Figure 8. Boring logs from holes near Cavity Site I
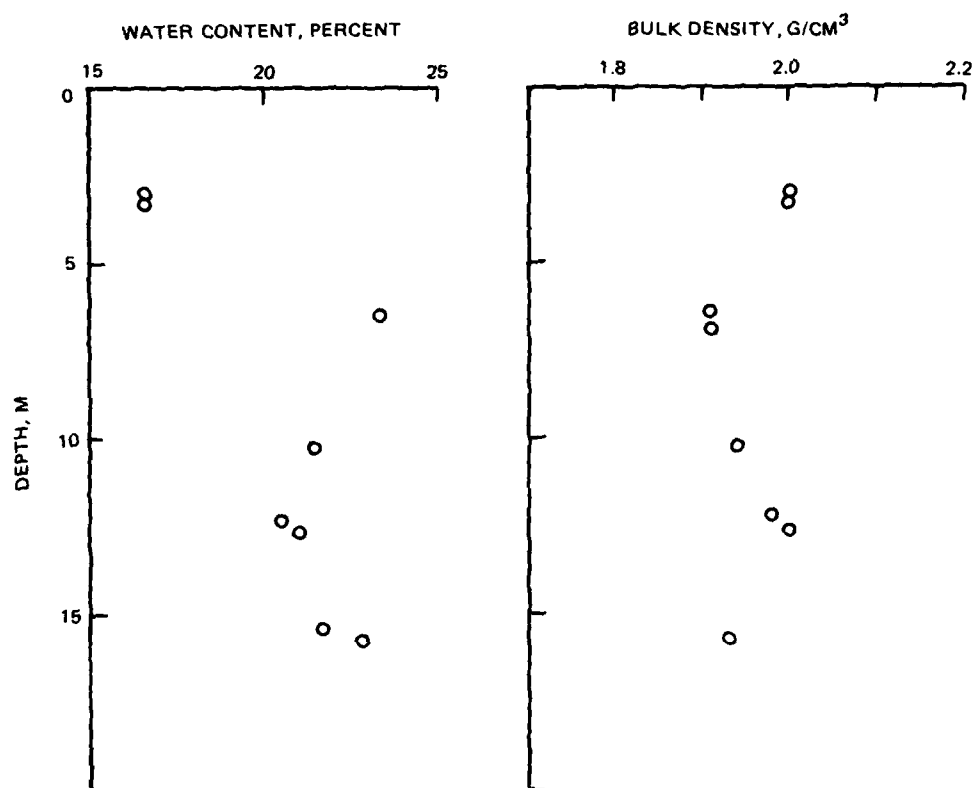
Figure 9.   Physical property data from Boring No. 1

c. NEUTRON LOG WITH 0.25-M SPACER
   COUNT RATE = 100/MIN
   TIME CONSTANT = 2.0
   LOGGING SPEED = 3 M/MIN

b. GAMMA-GAMMA LOG (DENSITY) WITH 0.3-M SPACER
   COUNT RATE = 5 K/MIN
   TIME CONSTANT = 2.0
   LOGGING SPEED = 3 M/MIN

a. NATURAL GAMMA LOG
   COUNT RATE = 100/MIN
   TIME CONSTANT = 2.0
   LOGGING SPEED = 3 M/MIN

Figure 10. Borehole geophysical logs of Boring No. 1 (count rate = (counts/min)/inch)
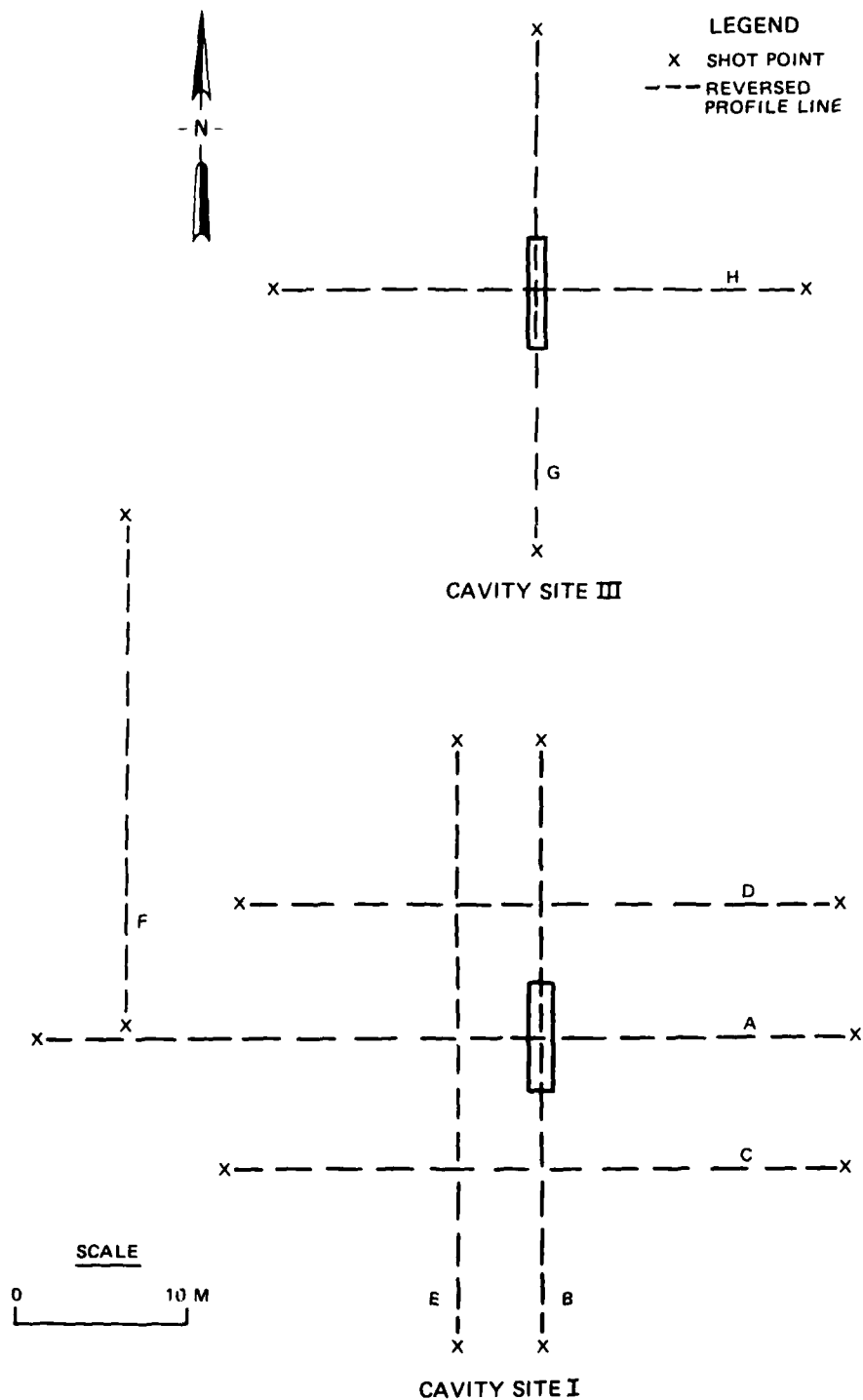
Figure 11. Layout of surface refraction surveys
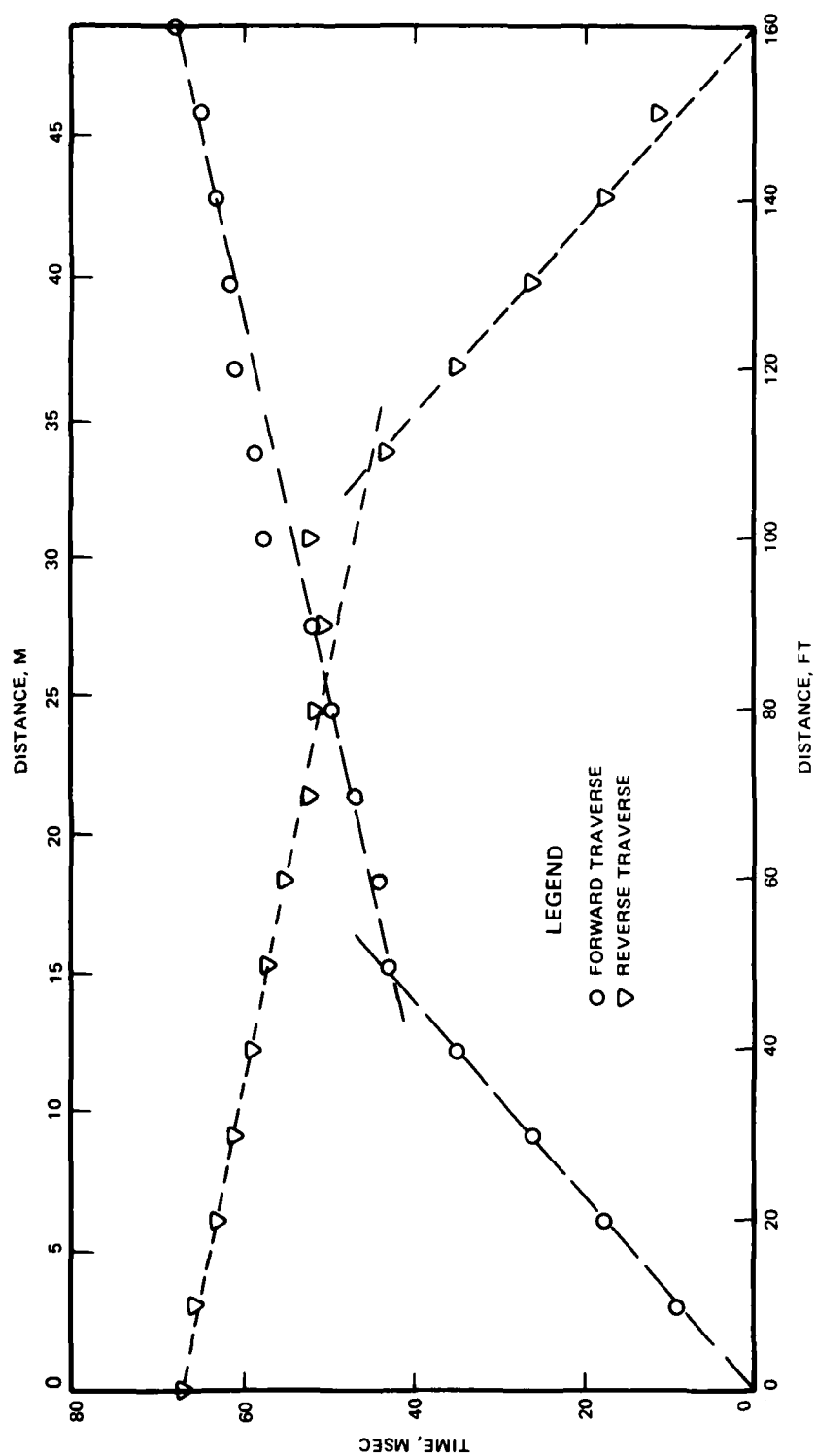
Figure 12. Time-distance plot, seismic refraction line A
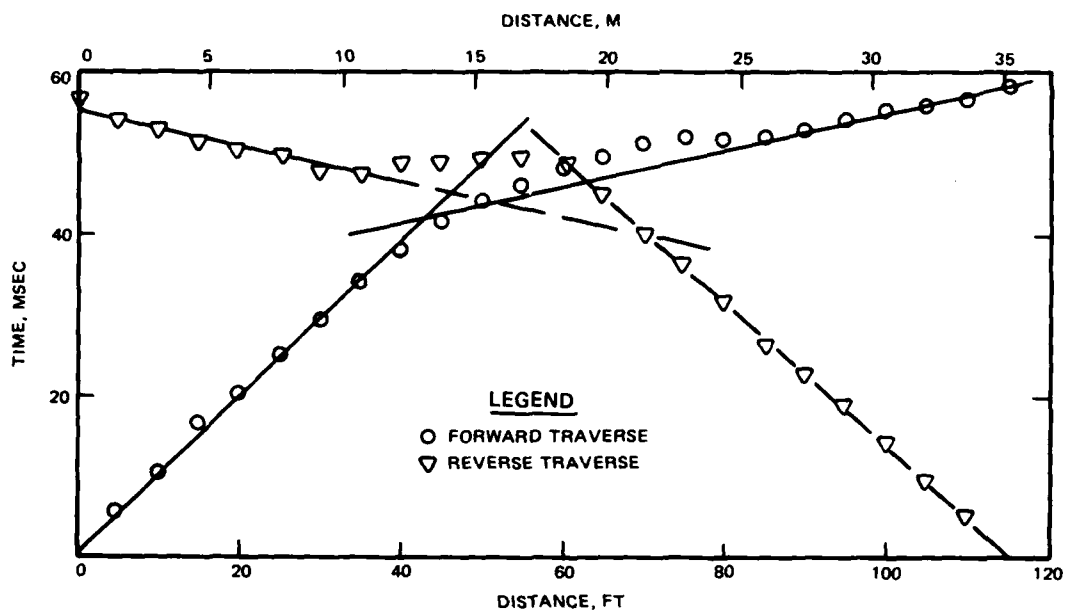
Figure 13. Time-distance plot, seismic refraction line B
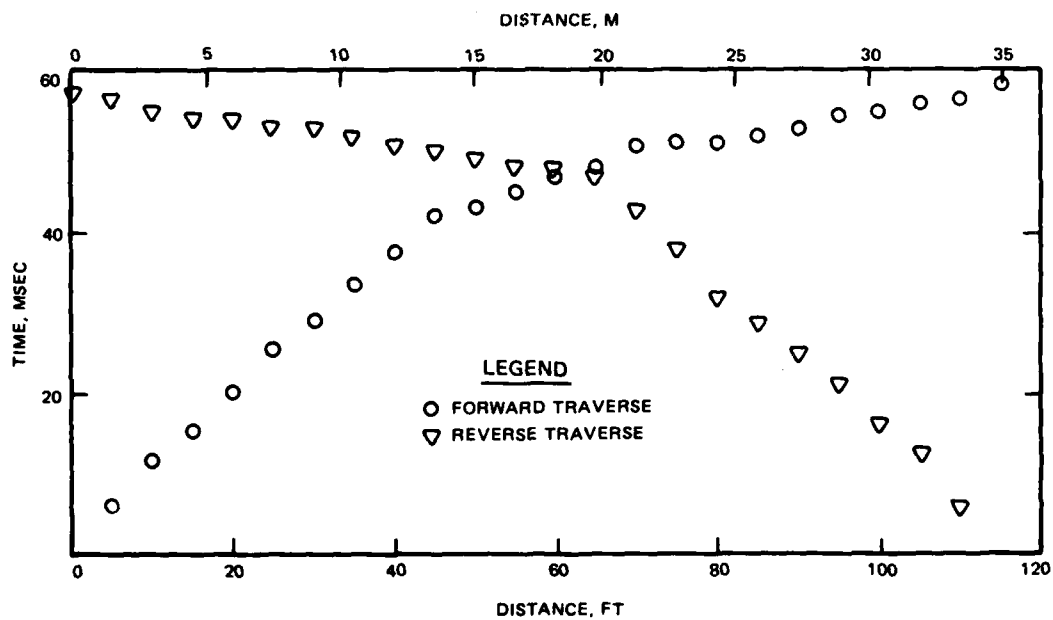
Figure 14. Time-distance plot, seismic refraction line C
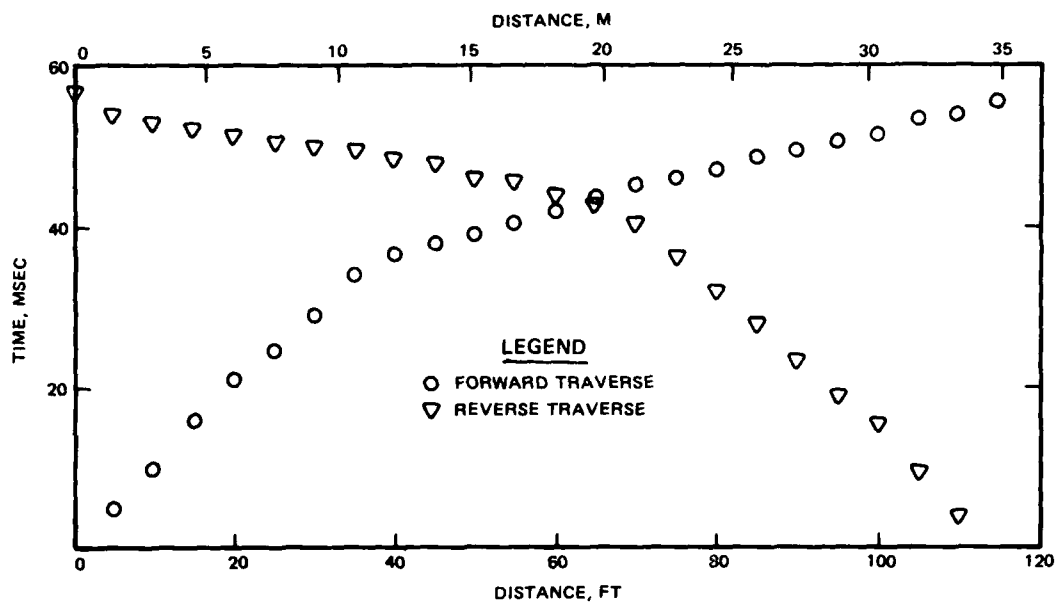
Figure 15. Time-distance plot, seismic refraction line D
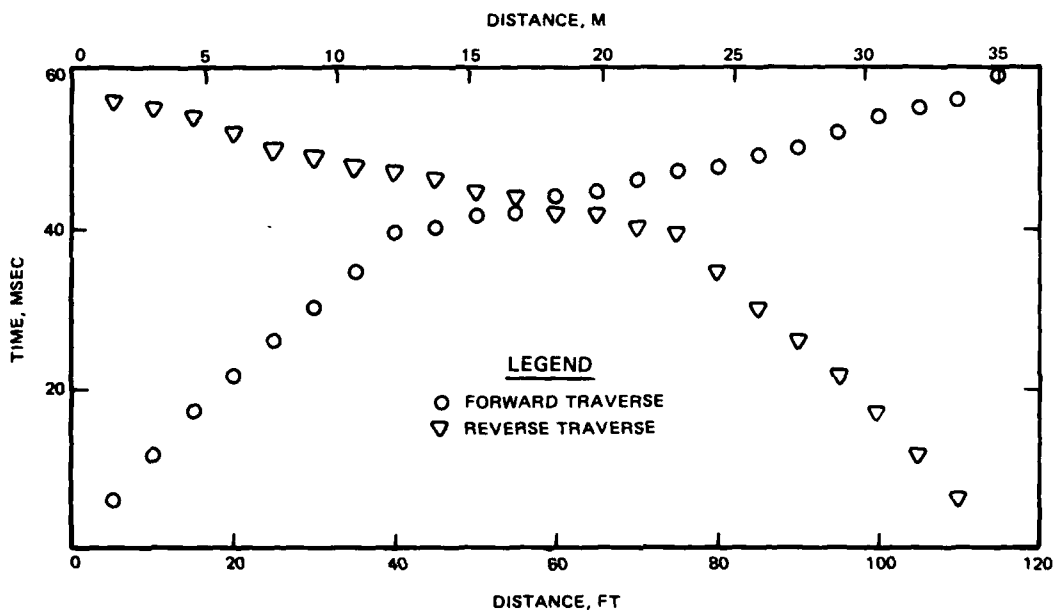
Figure 16. Time-distance plot, seismic refraction line E
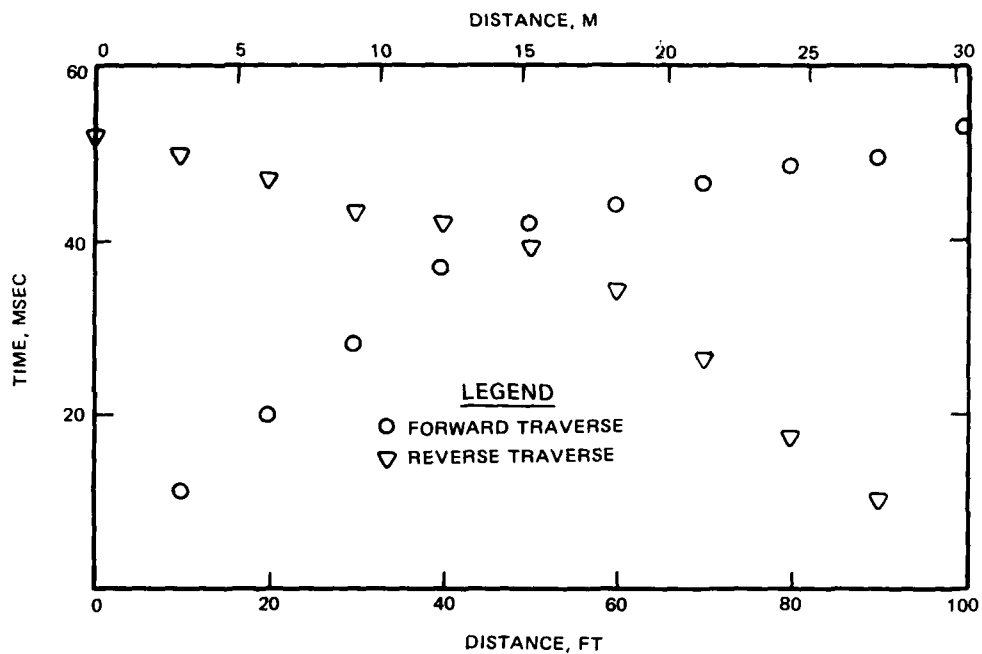
Figure 17.   Time-distance plot, seismic refraction line F
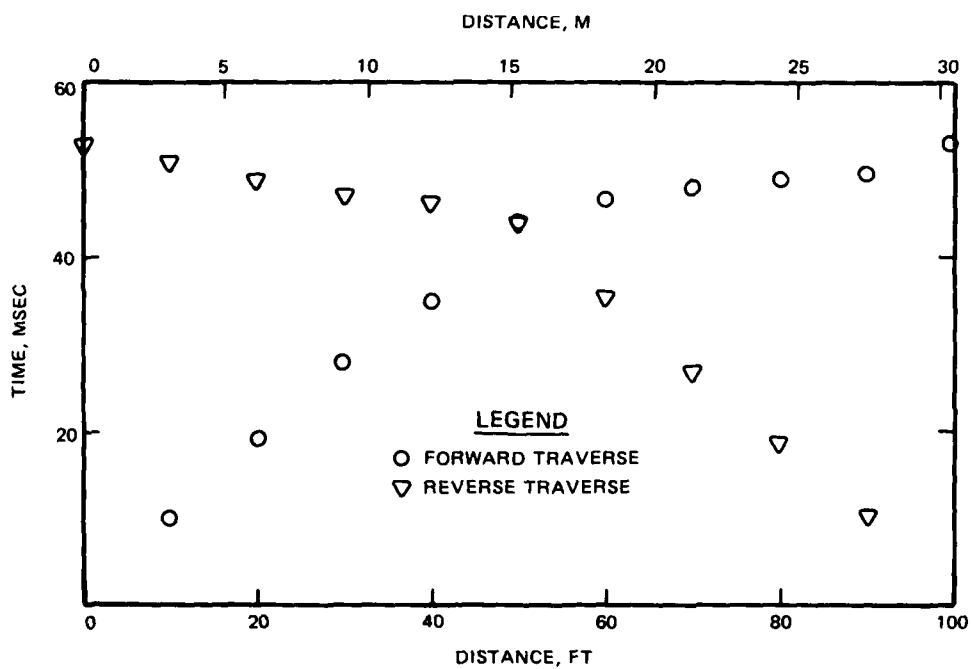
Figure 18.   Time-distance plot, seismic refraction line G
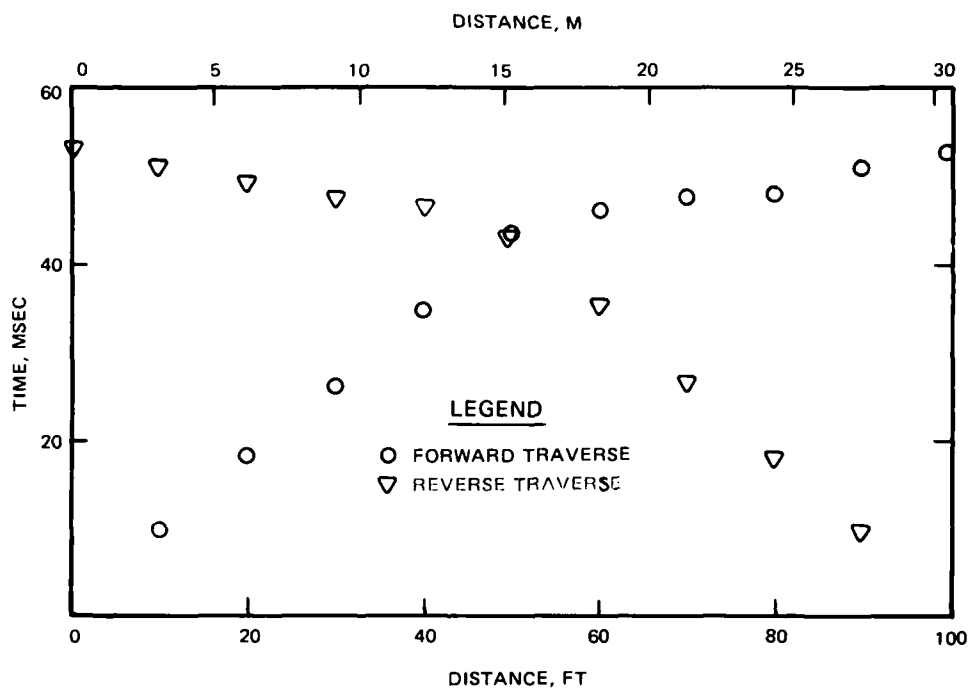
DISTANCE, M

Figure 19.   Time-distance plot, seismic refraction line H
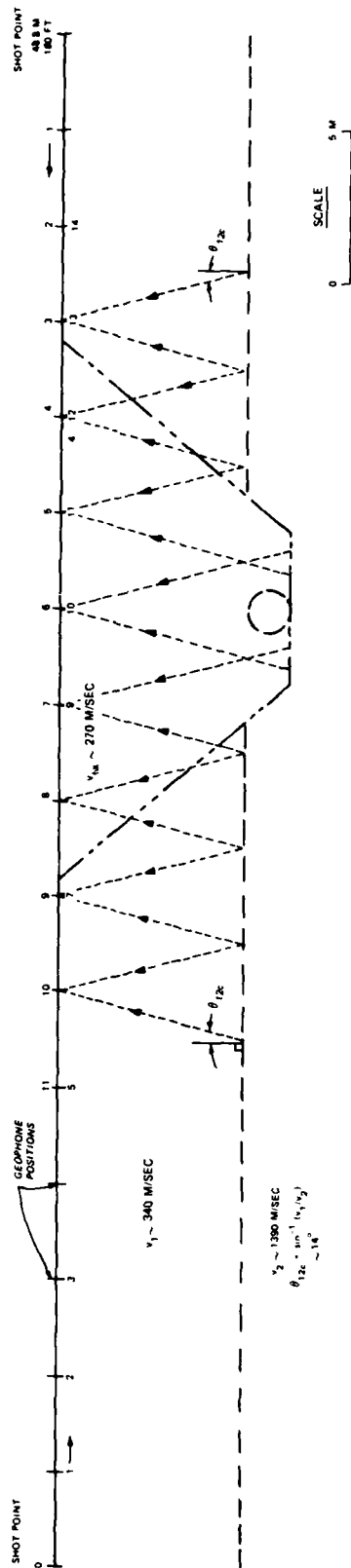
Figure 20. Section view of Cavity Site I along refraction line A, showing hypothetical ray paths
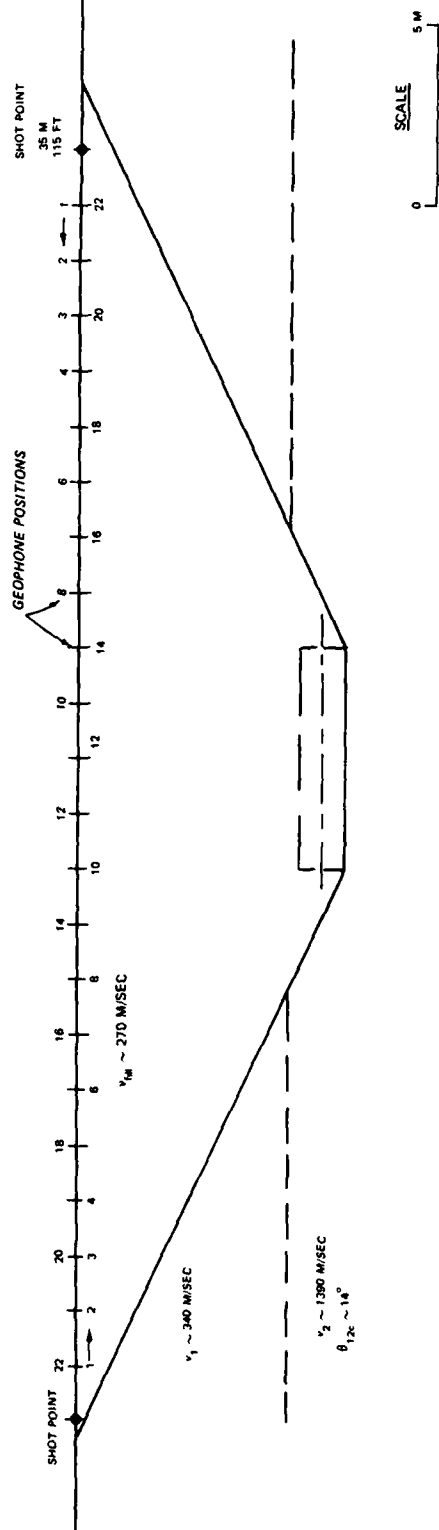
Figure 21. Section view of Cavity Site I along refraction line B
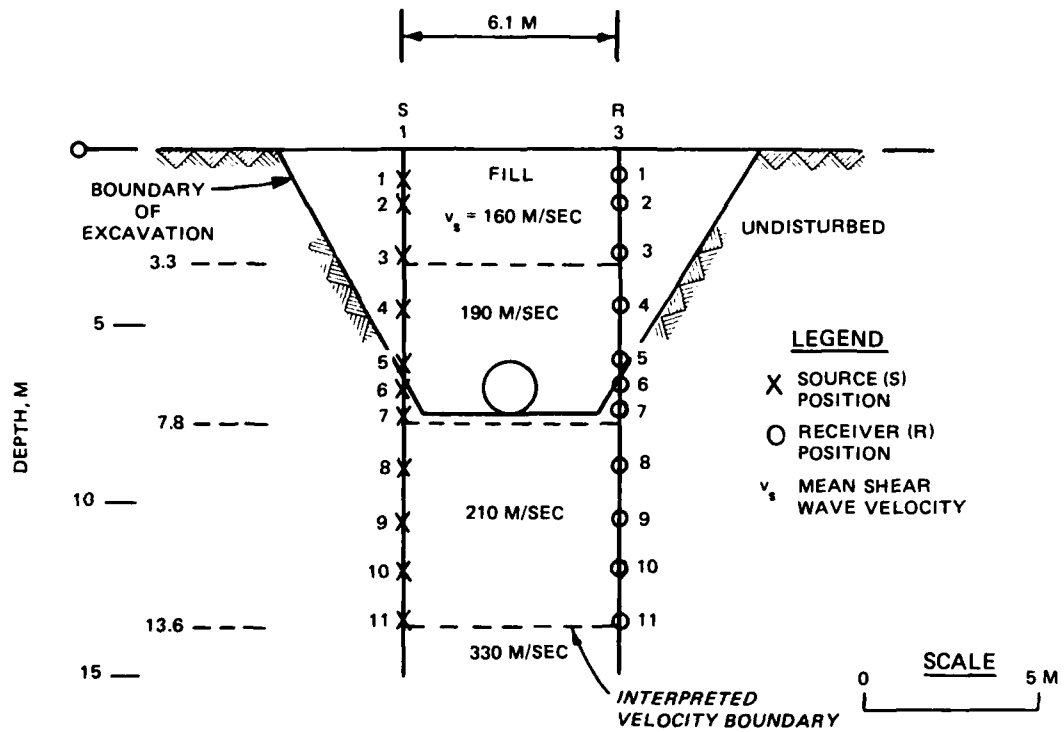
Figure 22. Section view between Borings No. 1 and 3 at
Cavity Site I, showing interpreted crosshole S-wave
velocities
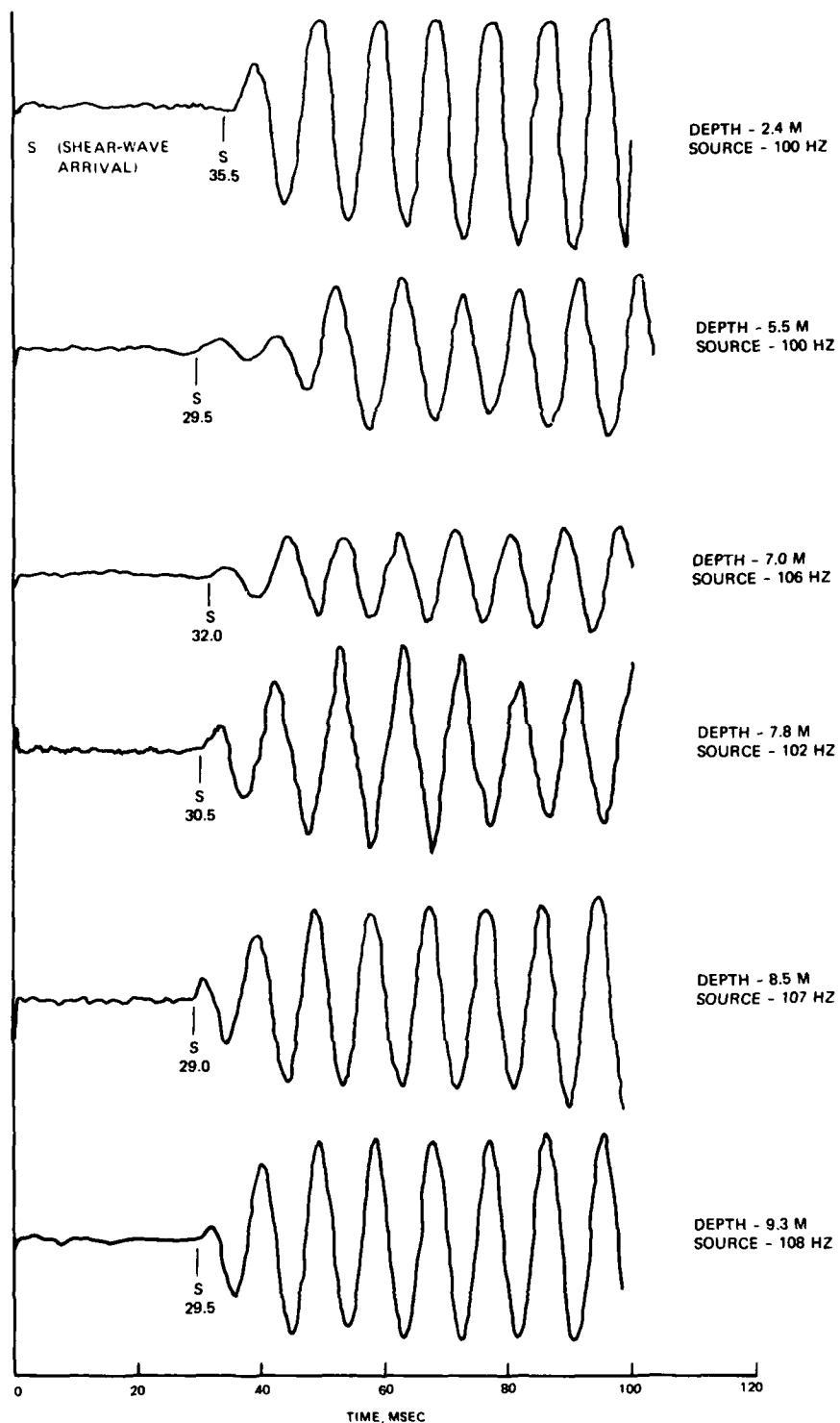
Figure 23. Set of opposed source-receiver crosshole shear-wave records at Cavity Site I; source-receiver distance, 6.1 m; depth to center of cavity, 6.7 m
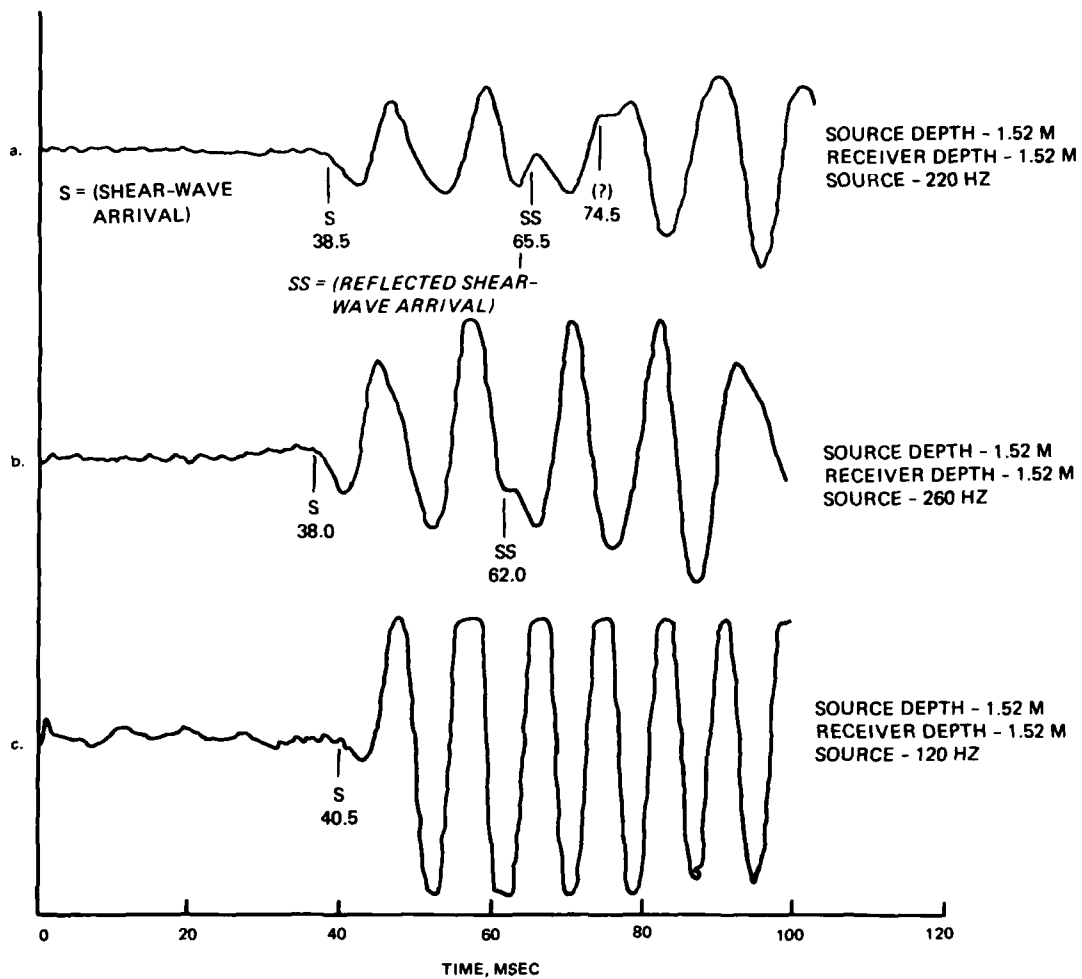
Figure 24. Crosshole seismic records, Cavity Site I;
source position S_{12}, receiver position R_{32}
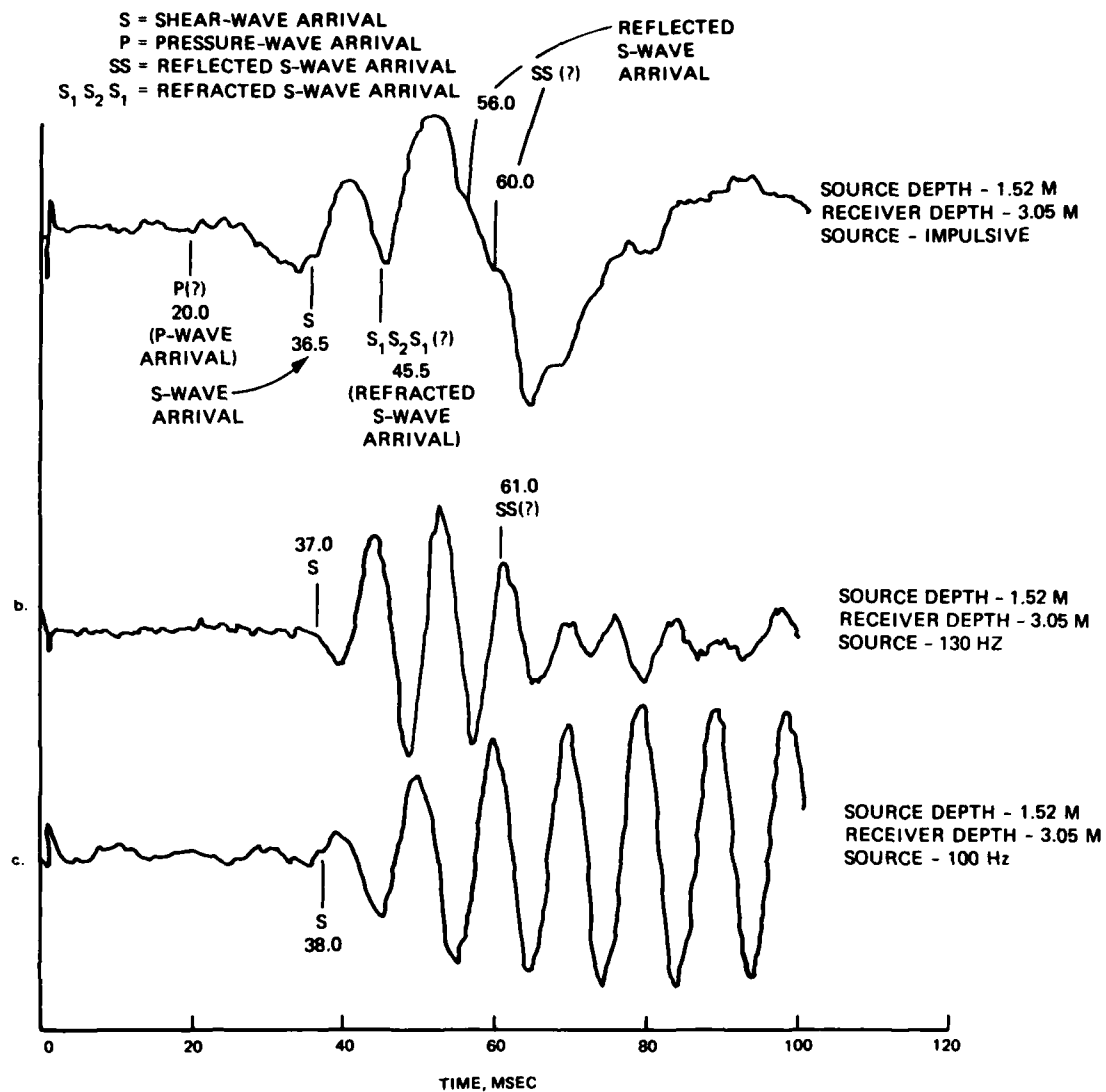
Figure 25. Crosshole seismic records, Cavity Site I;
source position S_{12}, receiver position R_{33}
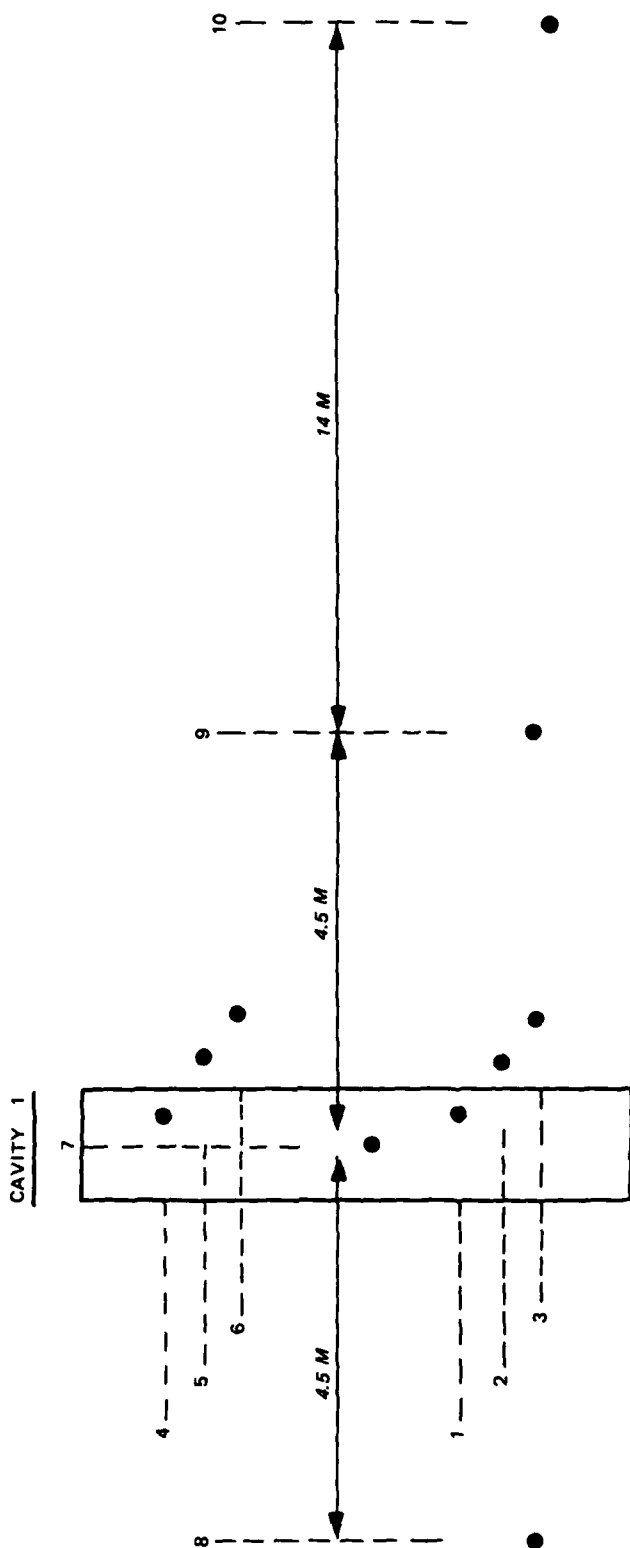
Figure 26. Location of reflection Stations 1 to 10 around Cavity I. (Dashed line illustrates 12-geophone array, 2.5 m long. Dot indicates first impact station, 0.91 m from end geophone)
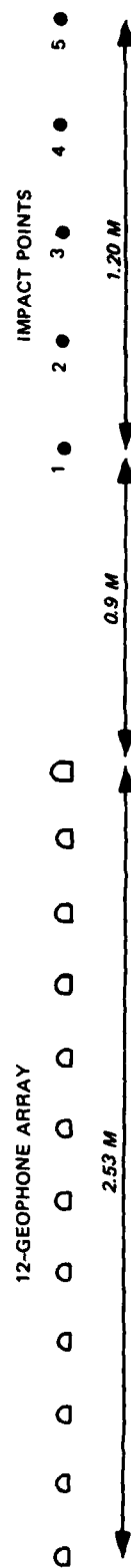
Figure 27. Geophone array and impact stations for reflection seismology. (Geophone spacing = 0.23 m; impact station spacing = 0.30 m)
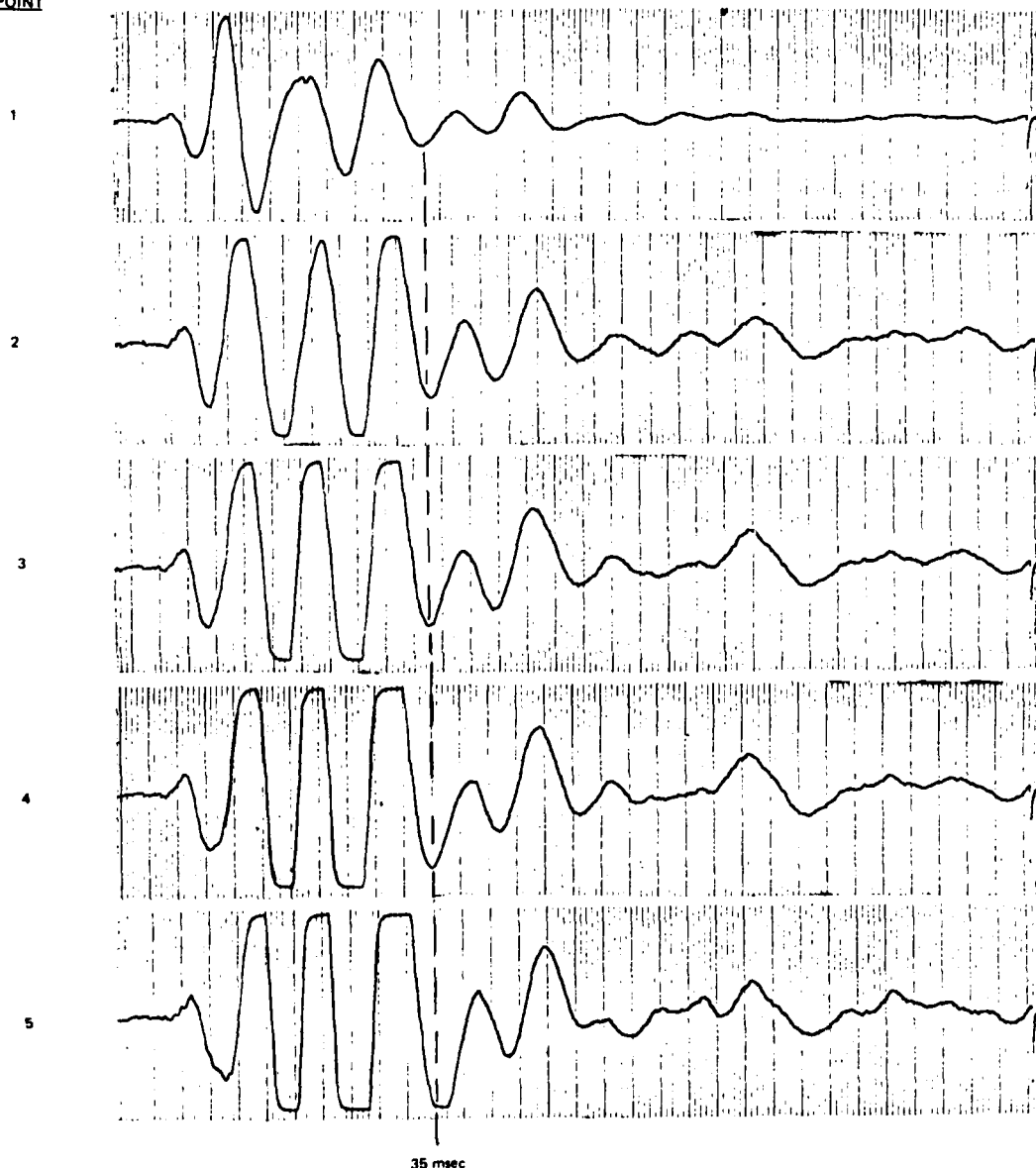
Figure 28. Station 1, seismic reflection survey. (Each
record represents sum of itself plus all preceding
records for each station)

IMPACT
POINT

35 msec

Figure 29. Station 2, seismic reflection survey
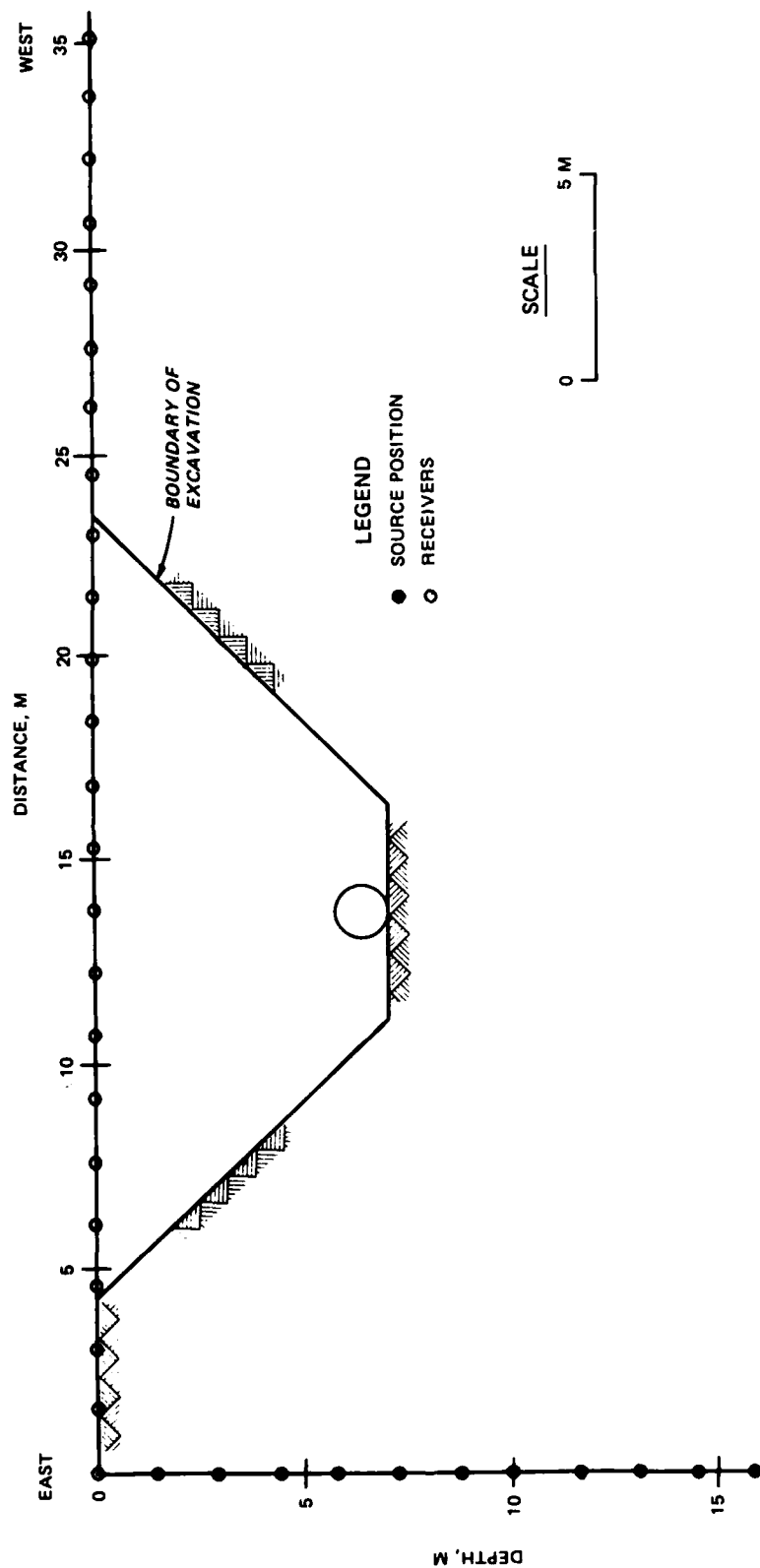
Figure 30. Geometry for wave-front survey, Cavity Site I
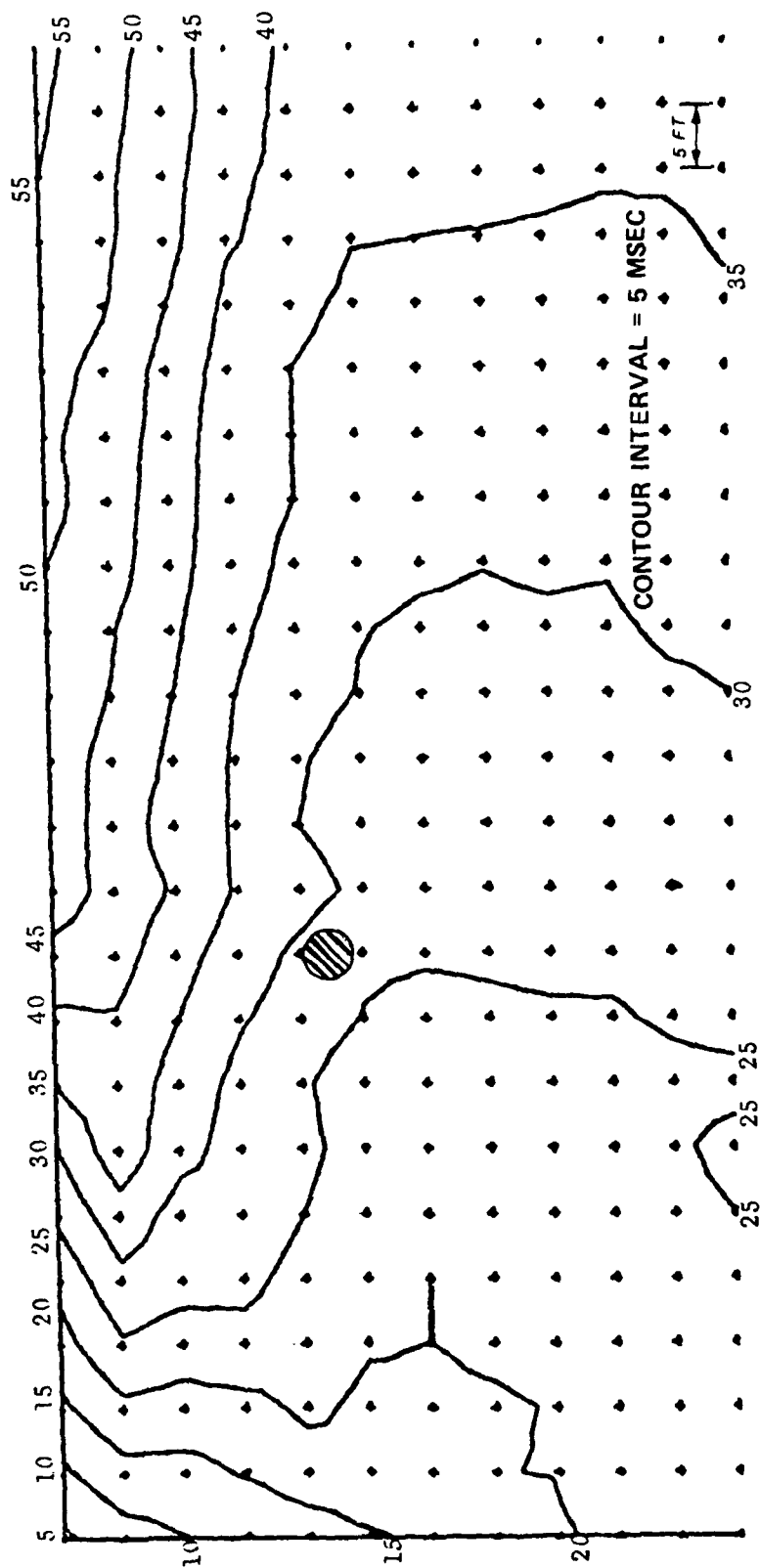
Figure 31. Wave-front survey, Cavity Site I (see Figure 30), contour interval 5 msec
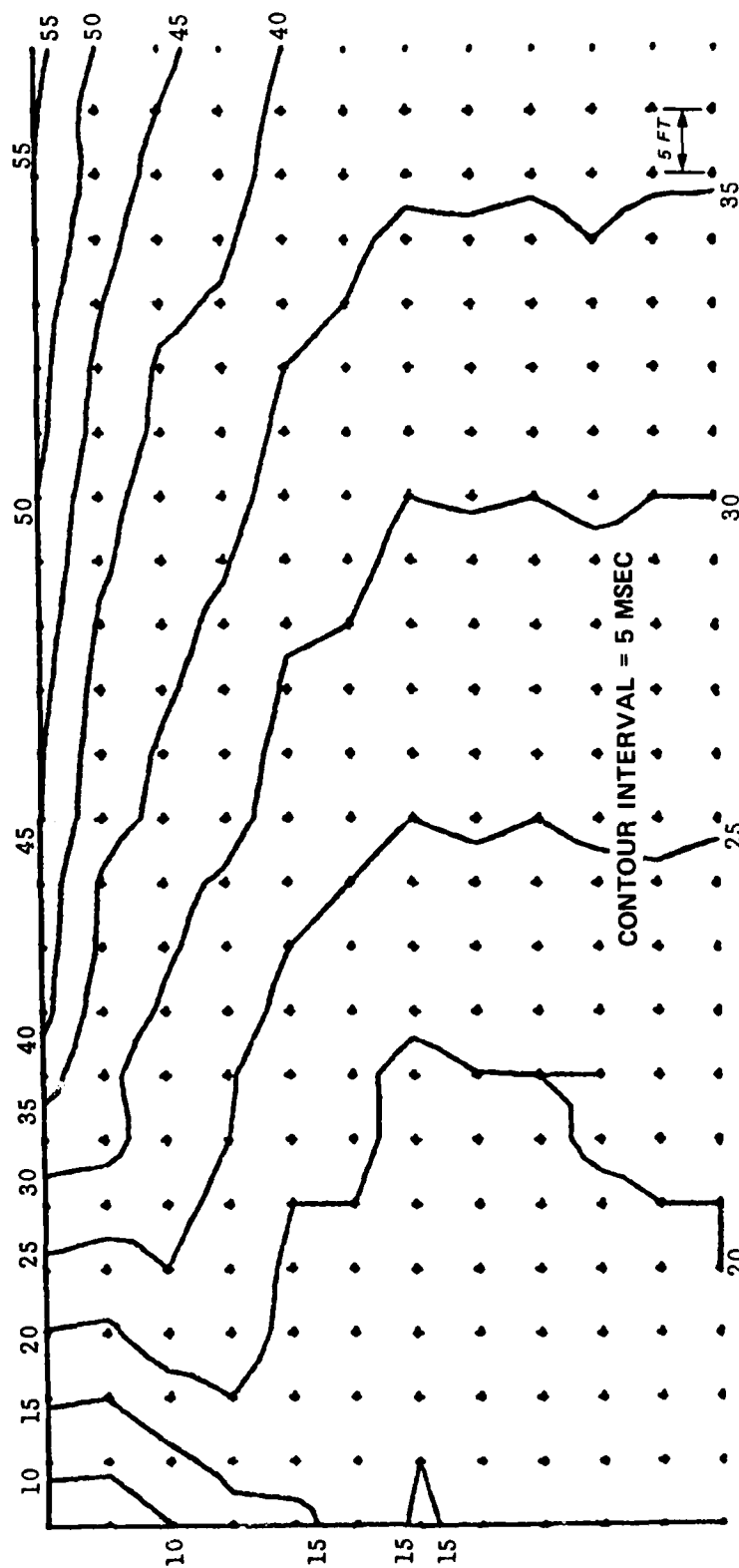
Figure 32. Wave-front survey, parallel to but offset from Cavity Site I in north-south direction, contour interval 5 msec

CONTOUR INTERVAL = 5 MSEC
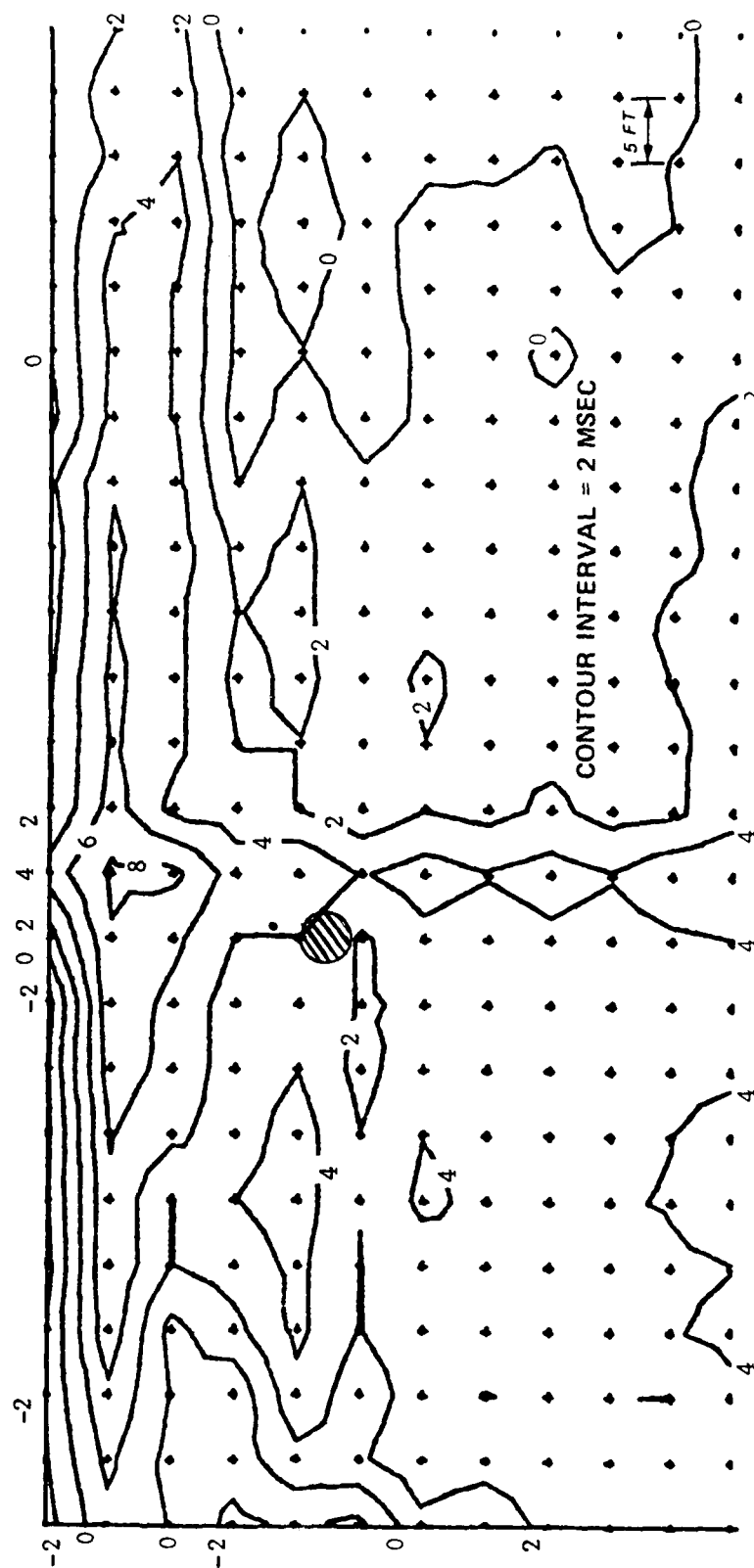
Figure 33. Wave-front anomaly diagram for Cavity Site I, contour interval 2 msec

Transducer output (arbitrary units)
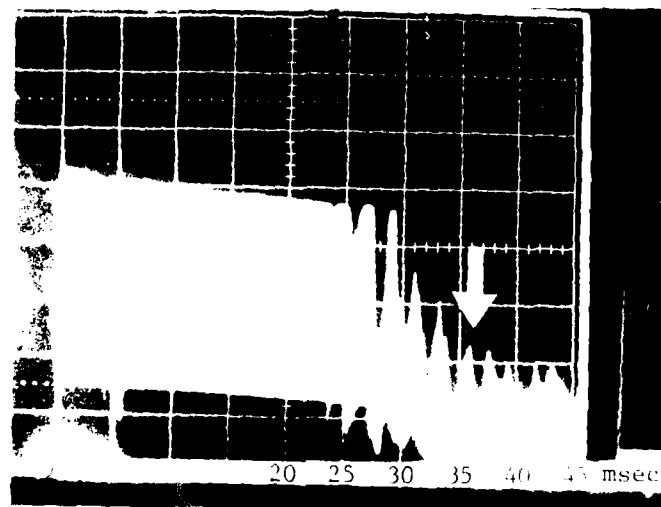
TIME, MSEC

a. Source-receiver directly over cavity at Site I

Transducer output (arbitrary units)

0   4   18   20 msec
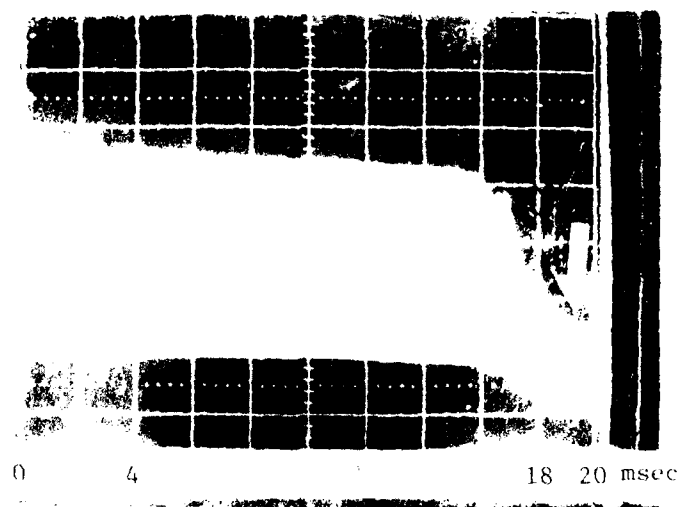
TIME, MSEC

b. Source-receiver directly over cavity at Site III

Figure 34. Sonar reflection records

$$\rho_a = 2\pi\left(\frac{R_1 R_2}{R_2 - R_2}\right)\left(\frac{\Delta V}{I}\right)$$
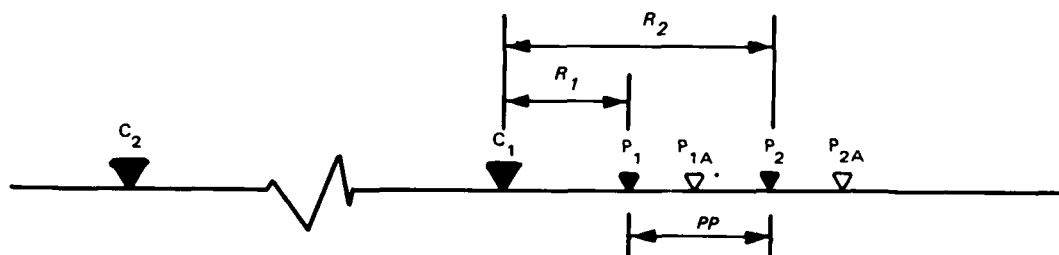
C - CURRENT ELECTRODES
P_1 - POTENTIAL ELECTRODE NO. 1
P_{1A} - SUBSEQUENT POSITION OF P_1
ρ_a - APPARENT RESISTIVITY
ΔV - POTENTIAL DIFFERENCE
I - CURRENT

Figure 35. Bristow-Bates (pole-dipole) electrode geometry
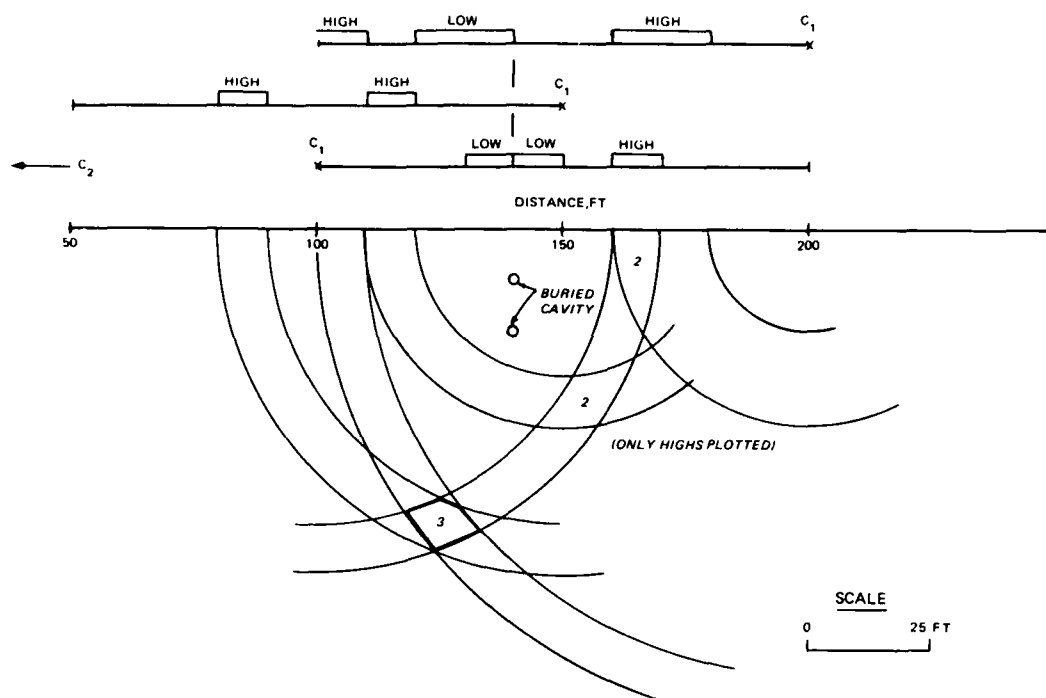
Figure 36. Bristow-Bates survey over Cavity Site III, using 10-ft potential electrode spacing (see Plates B1-B3)
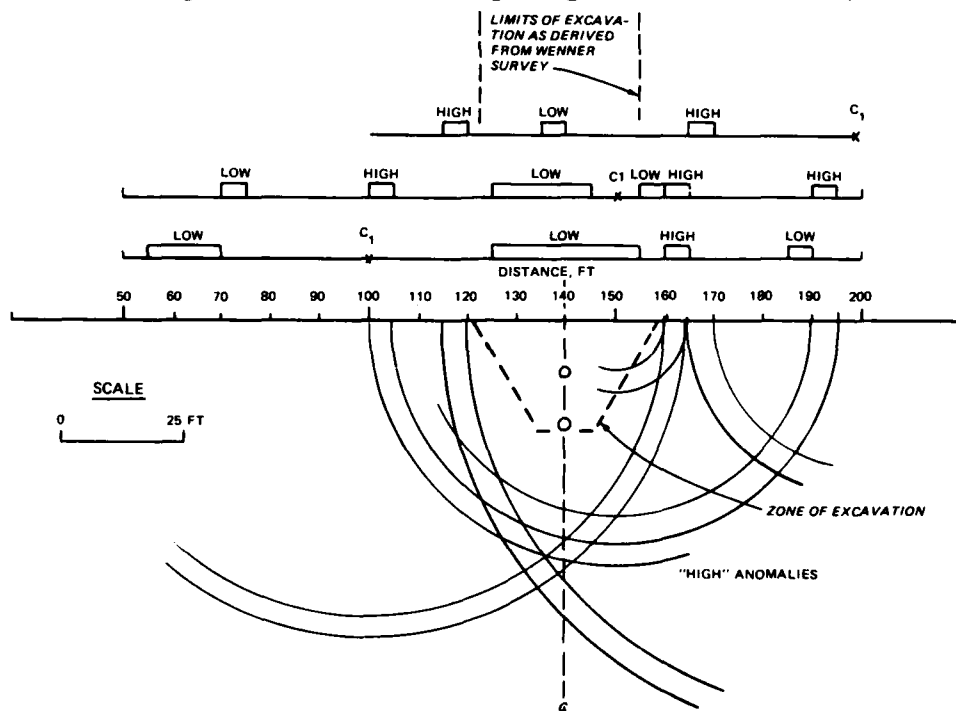
Figure 37. Bristow-Bates survey over Cavity Site III, using 5-ft potential electrode spacing (see Plates B4-B8)
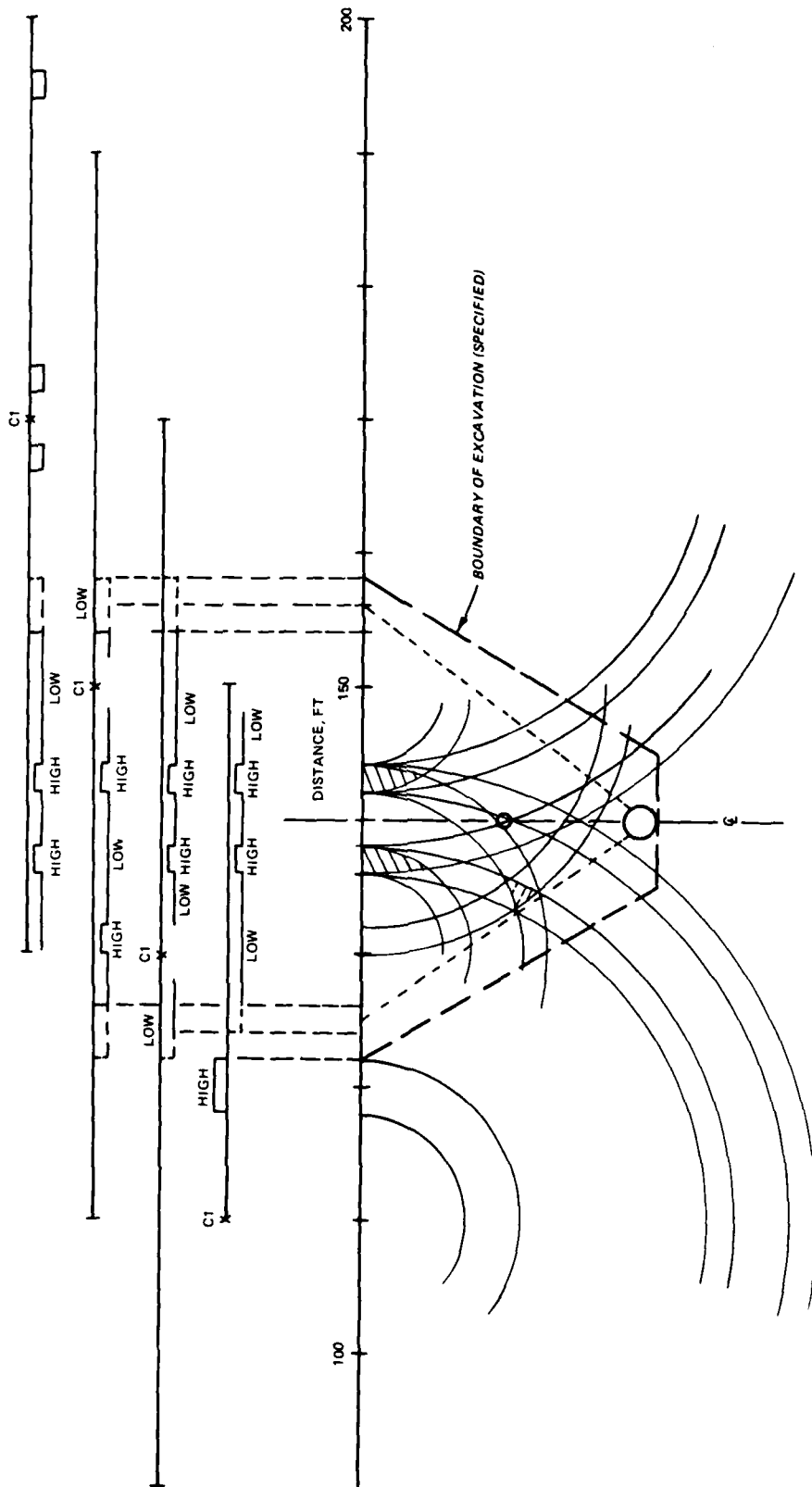
Figure 38. Bristow-Bates survey over Cavity Site III, using
2-ft potential electrode spacing (Plates B9-B15)
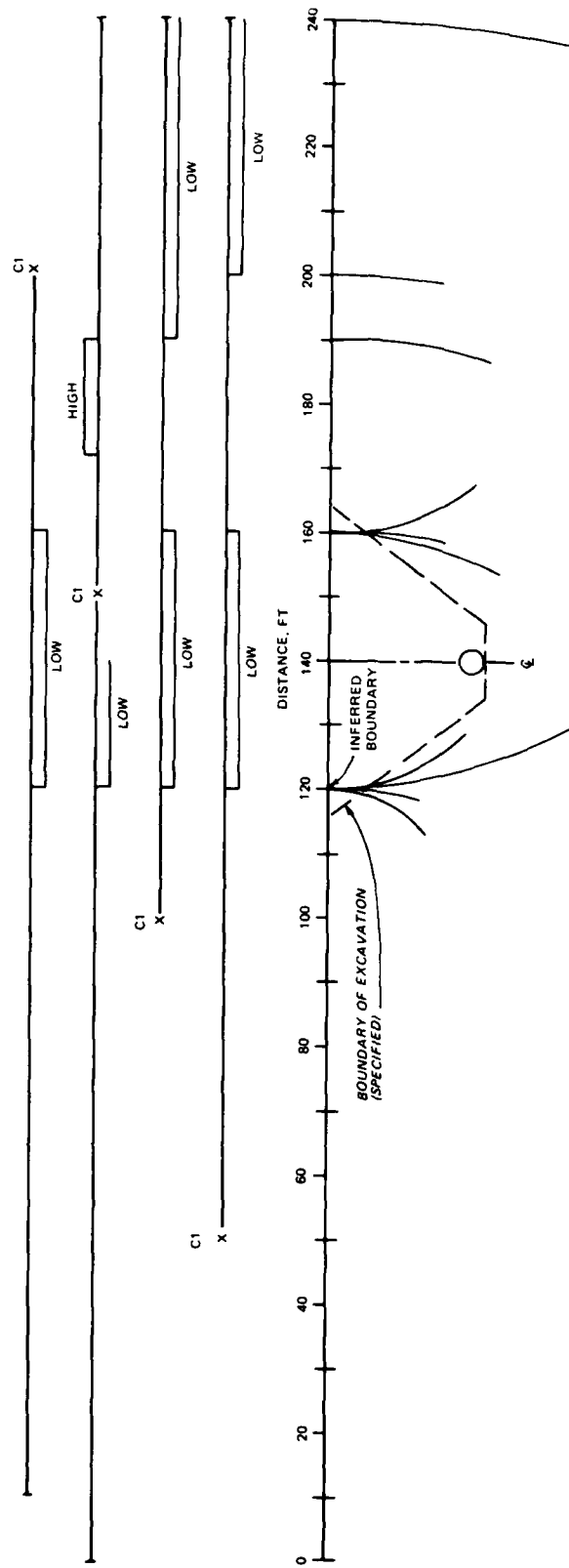
Figure 39. Bristow-Bates survey over Cavity Site I, using 10-ft potential electrode spacing (Plates B16-B20)

Figure 40. Bristow-Bates survey over Cavity Site I, using 5-ft potential electrode spacing (Plates B21-B26)
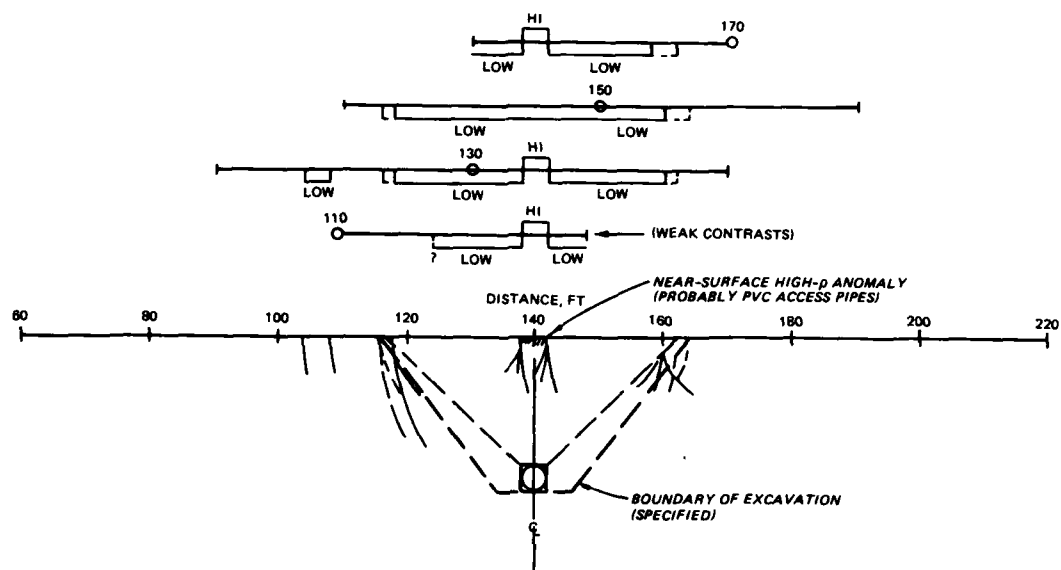
Figure 41. Bristow-Bates survey over Cavity Site I, using
2-ft potential electrode spacing (Plates B27-B32)
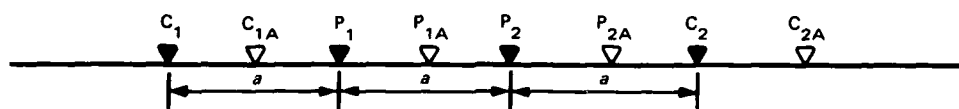
C_1, C_2 - INITIAL CURRENT ELECTRODE POSITIONS

P_1, P_2 - INITIAL POTENTIAL ELECTRODE POSITIONS

C_{1A}, C_{2A}, P_{1A}, P_{2A} - SECOND ELECTRODE POSITIONS
FOR PROFILING TO THE RIGHT
AT INCREMENTS OF a/2.

Figure 42. Wenner profiling array
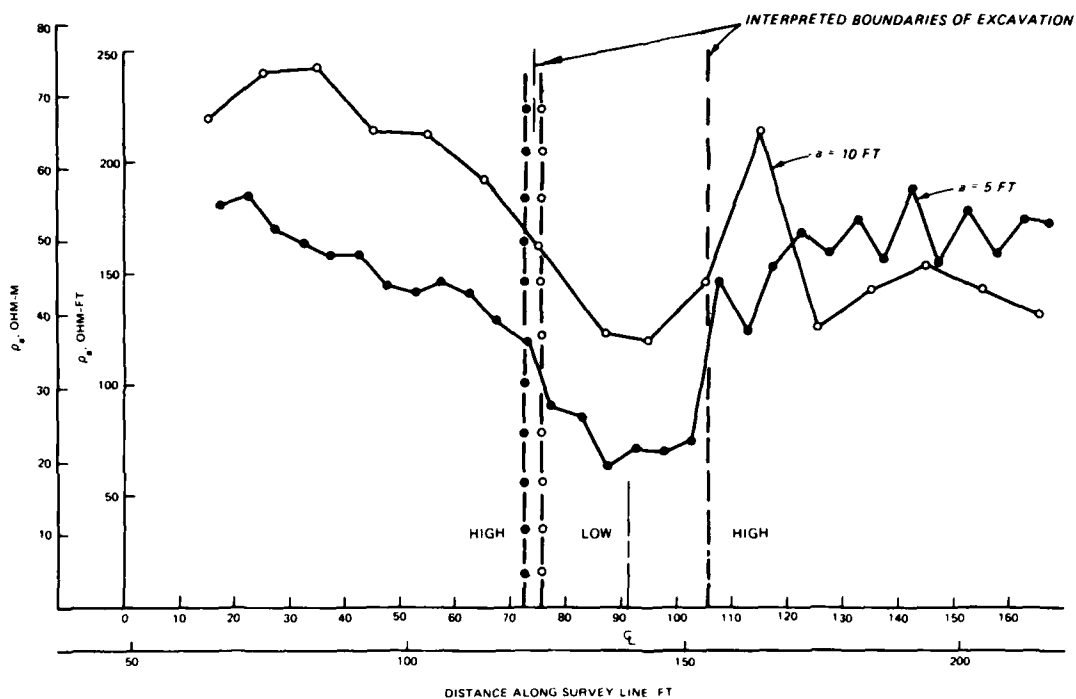
Figure 43. Wenner profiles over Cavity Site III
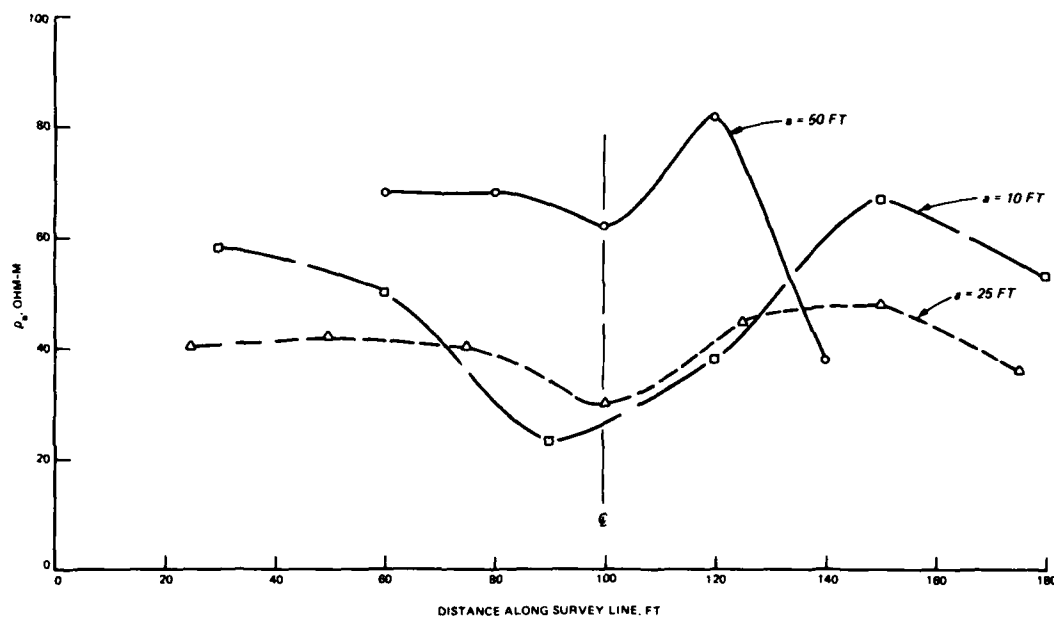
Figure 44. East-west Wenner profiles over Cavity Site I

$$\rho_a = \pi S \left[\left(\frac{L}{S} \right)^2 - \frac{1}{4} \right] \left(\frac{\Delta V}{i} \right)$$
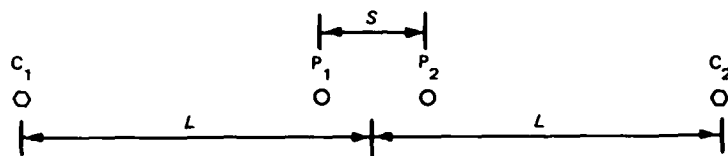
Figure 45. Schlumberger electrode configuration
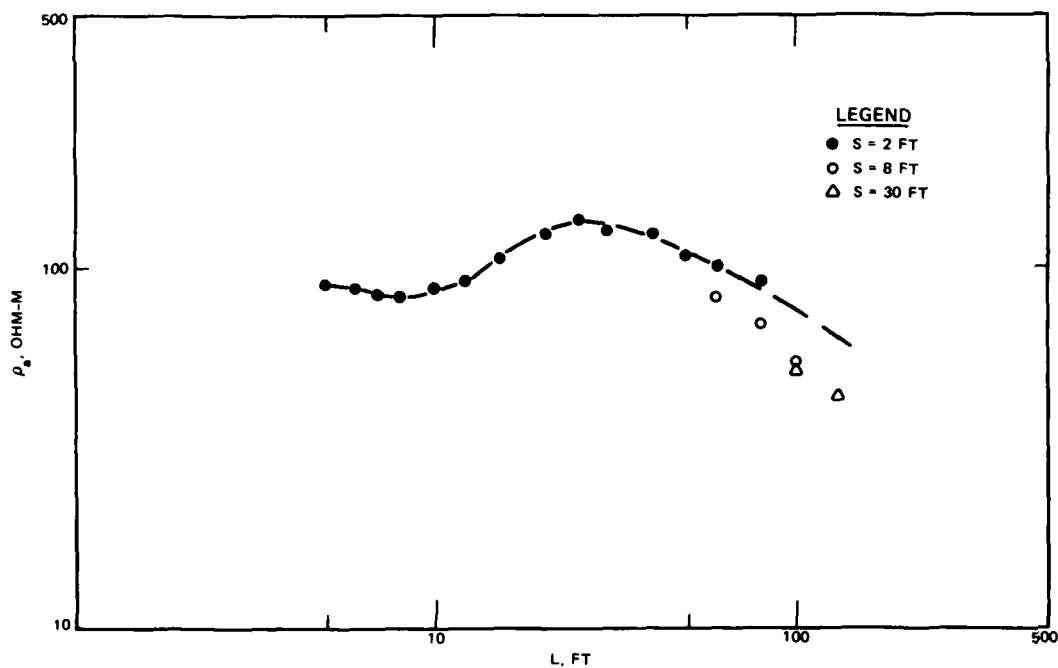
Figure 46. East-west Schlumberger sounding centered
over Cavity Site I
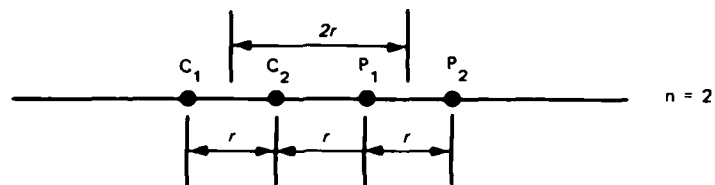
a. INITIAL STATION

b. n = 2
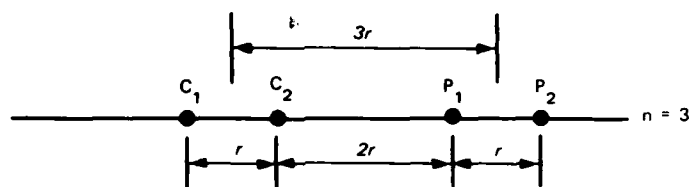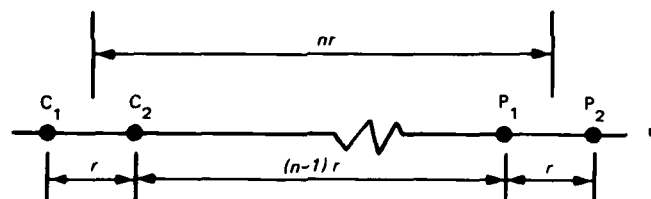
$$\rho_a = \pi r\, n(n^2 - 1)\left(\frac{\Delta V}{I}\right)$$

ρ_a - APPARENT RESISTIVITY

ΔV - POTENTIAL DIFFERENCE ($\Delta V = V(P_1) - V(P_2)$)

I - CURRENT

c. GENERAL CASE AND EQUATION
FOR APPARENT RESISTIVITY

Figure 47. Dipole-dipole configuration: a. initial
station; b. n = 2 ; c. general case and equation
for apparent resistivity
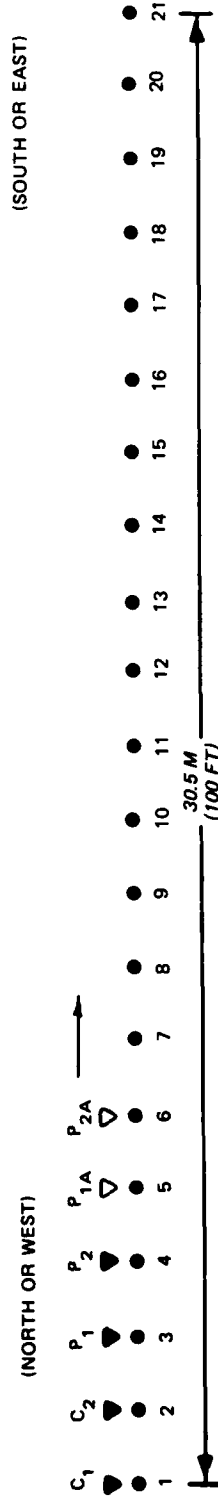
Figure 48. Dipole-dipole stations 1 to 21. (Initial reading is taken with C_1 at 1, C_2 at 2, P_1 at 3, and P_2 at 4. The two potential electrodes are moved one station for each reading until N (Figure 34) equals 7. Then C_1 is moved to Station 2, C_2 is moved to Station 3, and the process repeated. Station spacing = 1.52 m. Cavity center under Station 11)

Test Geometry (N-S Profiles) — 1 11 21 — 5 FT

stations — N ... S

Stations: 1 2 3 4 5 6 7 8 9 10 11 12 13 14 15 16 17 18 19 20 21

n values, Depth

```
 2      56  90  62  42  40  17  22  24  20  22 (52)·26  17  21   9  27  12  20
 3      70  69  33  43  25  17  18  19  18  25  30  15  20  13  15  20  18
 4      57  36  36  30  25  19  15  30  19 (54)·16  19  14  23  17  34
 5      31  38  27  30  30  14  16  22  23  17  30  17  25  26  33
 6      35  28  25  35  30  18  19  21  16  22  34  26  30  39
 7      29  26  29  34  29  19  24  18  18  13 (66)·30  48
```

* ANOMALOUS RESISTIVITY VALUES

Figure 49. North-south dipole-dipole survey over Cavity Site I; apparent resistivity in ohm-metres; cavity center at Station 11

Test Geometry (E-W Profiles) — 1 5 11 17 21

stations — W ... E

Stations: 1 2 3 4 5 6 7 8 9 10 11 12 13 14 15 16 17 18 19 20 21

n values, Depth

```
 2      51  58  41  35  34 | 22  16  24  28  20  15  20  20 / 32  50  60  68  75
 3      46  60  38  30  29 \ 17  19  25  15  15  16 / 23  25  37  58  72  72
 4      51  56  31  26  22  23  23  16  13  15 / 22  32  29  42  65  75
 5      35  45  26  18  27  29 \ 16  14  15 / 23  31  34  32  48  73
 6      41  37  20  24  35  22 \ 15  16 / 21  31  32  38  33  50
 7      32  31  24  32  27  21 \ 16 / 26  29  27  35  29  50
```
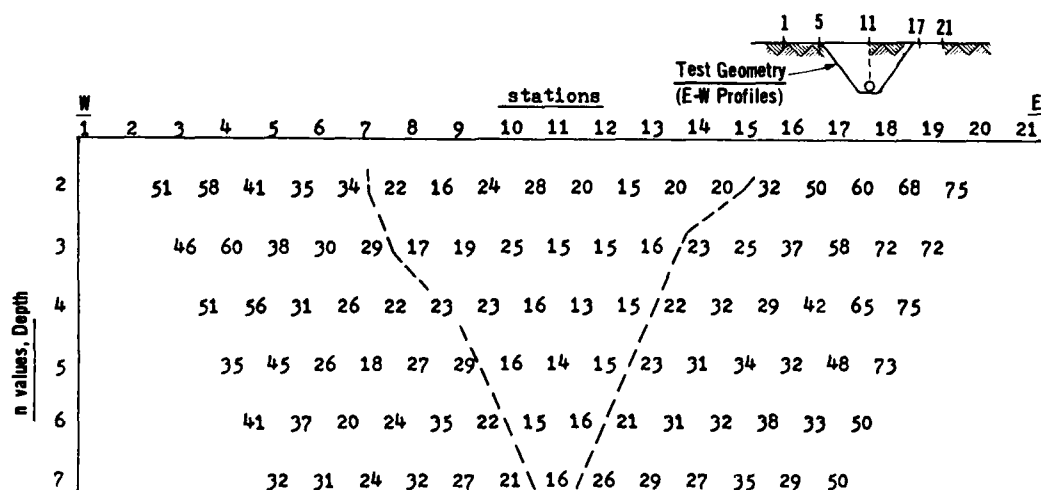
Figure 50. West-east dipole-dipole survey over Cavity Site I; apparent resistivity in ohm-metres. (Dashed lines represent inferred disturbed/undisturbed boundary. Cavity center at Station 11)

N | 1 2 3 4 5 6 7 8 9 10 11 12 13 14 15 16 17 18 19 20 21 | S

```
n values, Depth

 2 |    30  14  20  22  12  32  16  19  21  29  22  28  29  16  42  15  47  28
 3 |      23  15  22  15  16  23  16  15  20  22  22  21  17  24  26  24  39
 4 |        26  20  16  21  18  25  13  17  19  24  20  16  31  23  37  25
 5 |          31  17  23  23  20  30  16  18  22  27  23  36  32  36  45
 6 |            21  22  24  27  18  29  17  23  20  25  27  51  36  40
 7 |              27  24  27  19  29  29  19  26  29  44  40  42  59
```
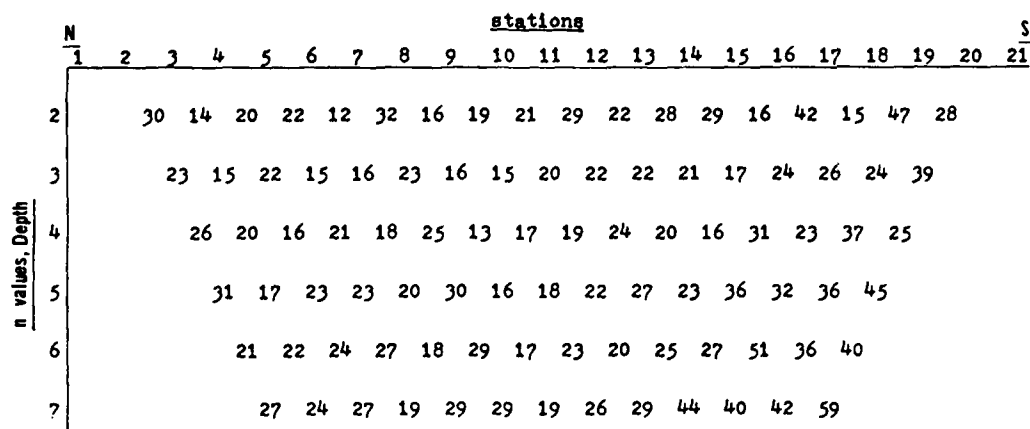
Figure 51. North-south dipole-dipole survey over Cavity Site III; apparent resistivity in ohm-metres; cavity center at Station 11

Test Geometry

W | 1 2 3 4 5 6 7 8 9 10 11 12 13 14 15 16 17 18 19 20 21 | E

```
n values, Depth

 2 |   52  49  65  52  68  69 /21  35  28  29  28 (52) 36 \98  73  66  52  62
 3 |     41  48  54  57  69 /21  23  24  22  21 (43) 25  33 \72  62  54  52
 4 |       41  45  60  66 /23  23  21  25  18 (43) 21  29  26 \79  52  49
 5 |         39  52  71 /23  24  21  21  25 (41) 28  27  23  27 \67  50
 6 |           44  44 /25  25  22  21  20 (63) 21  27  23  25  24 \74
 7 |             50 /23  27  21  21  19 (64  39) 29  23  23  16  26 \
```
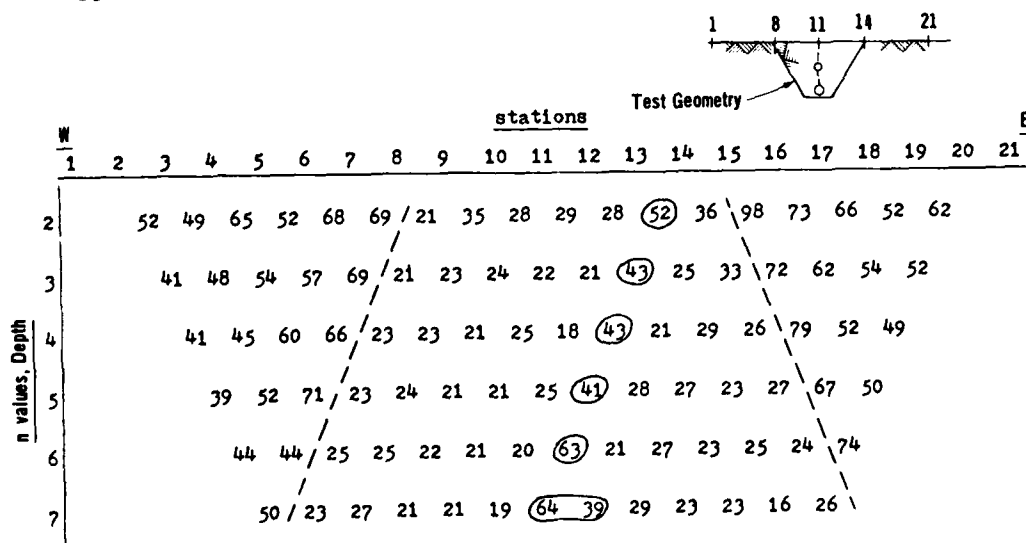
Figure 52. West-east dipole-dipole survey over Cavity Site III; apparent resistivity in ohm-metres. (Circled anomalous values indicate possible effect due to cavity. Dashed lines represent inferred disturbed/undisturbed boundary. Cavity center at Station 11)

E   **stations**   **W**

	1	2	3	4	5	6	7	8	9	10	11	12	13	14	15	16	17	18	19	20	21
2		62	62	68	60	37	23	40	20	25	24	30	32	22	38	65	73	64	64		
3			49	55	55	39	22	27	27	18	18	22	30	22	27	41	59	53	62		
4				48	52	40	26	27	30	25	17	19	30	28	34	31	49	47	55		
5					44	39	25	35	25	29	20	13	25	32	44	42	38	42	52		
6						34	24	32	37	31	28	21	18	25	39	55	39	37	41		
7							19	31	37	37	32	26	29	18	34	63	48	39	44		

n values, Depth
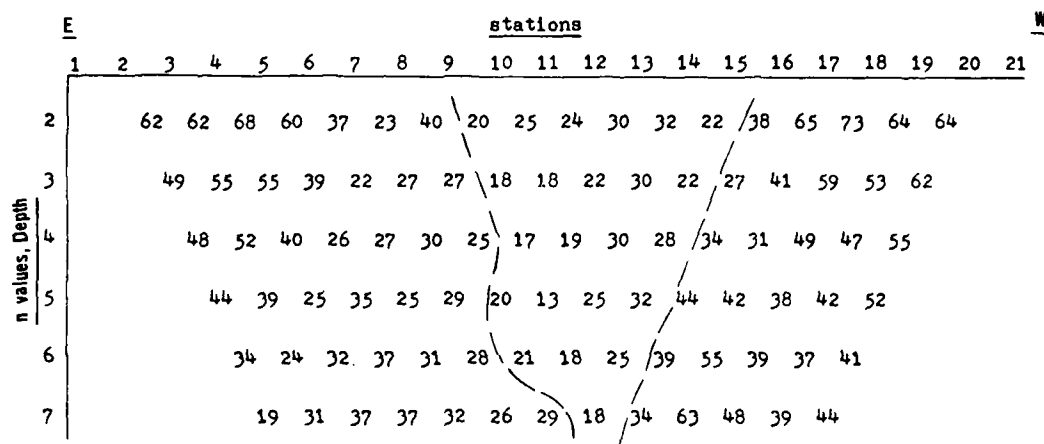
Figure 53. East-west dipole-dipole survey over Cavity Site IV; apparent resistivity in ohm-metres. (Dashed lines represent inferred disturbed/undisturbed boundary. Cavity center at Station 11)
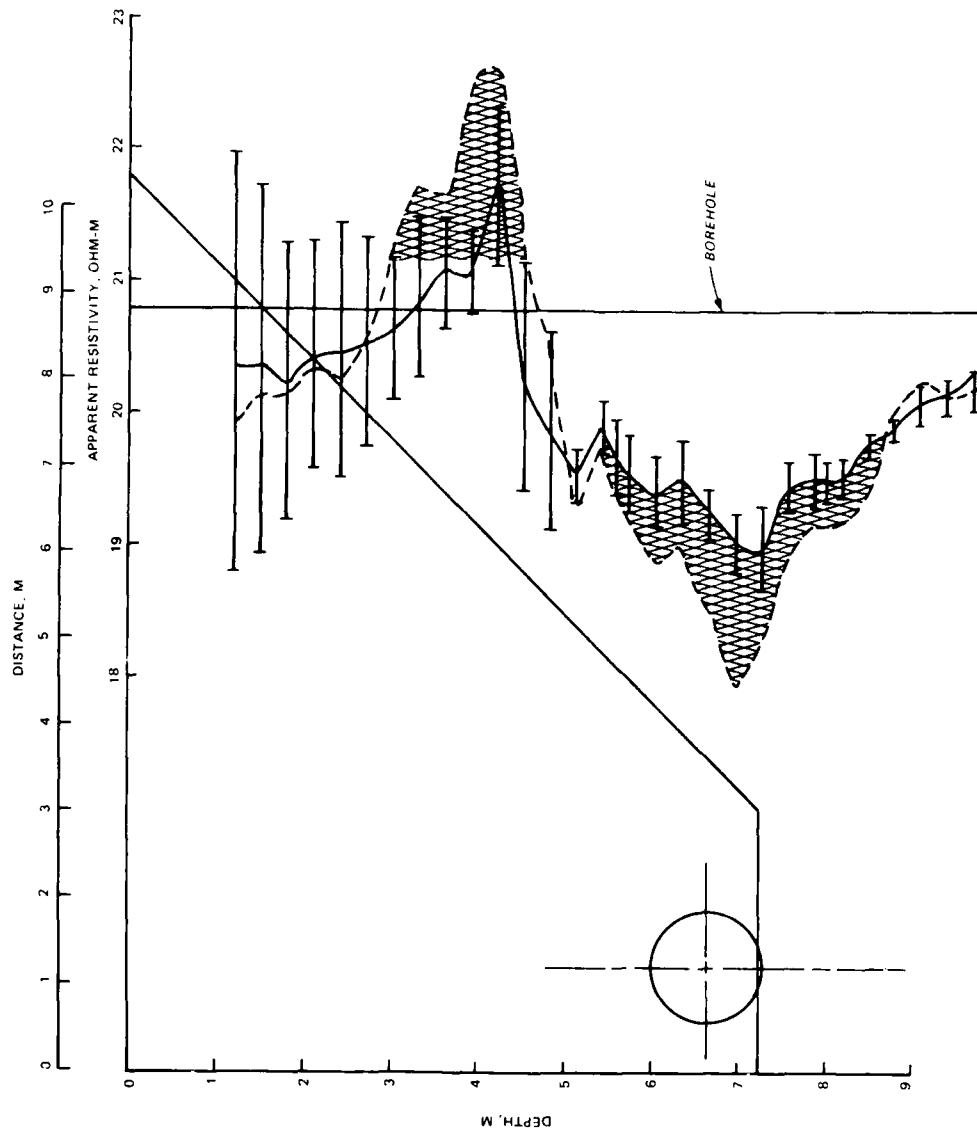
Figure 54. Borehole resistivity surveys. (Solid line indicates mean of single-point surveys in two boreholes. Bars indicate scatter of single-point values. Dashed line indicates crosshole survey. Cross-hatched indicates significant crosshole anomaly)
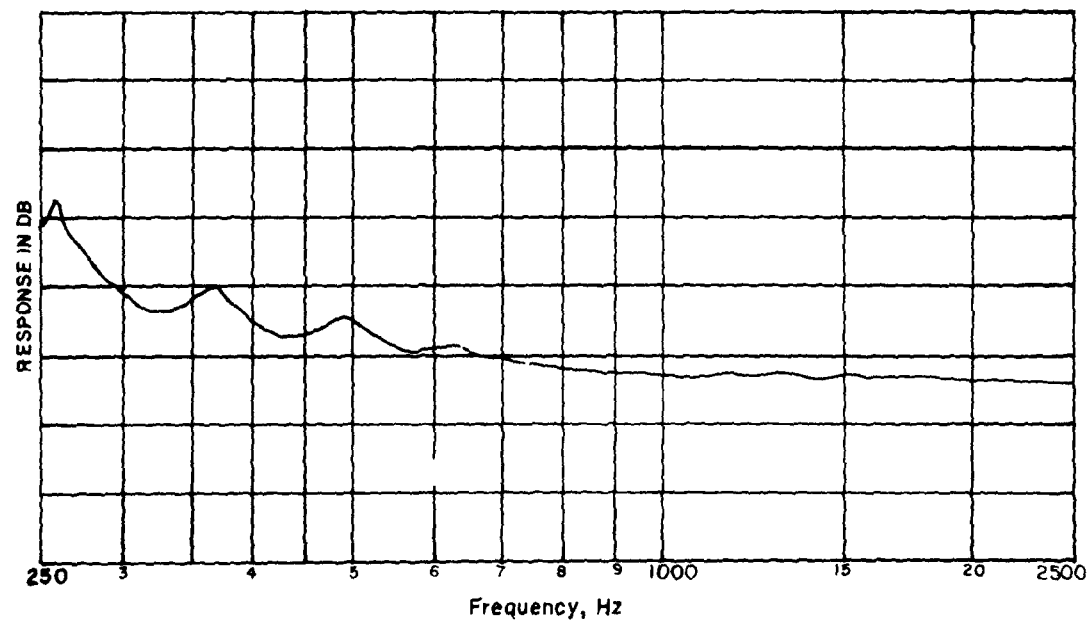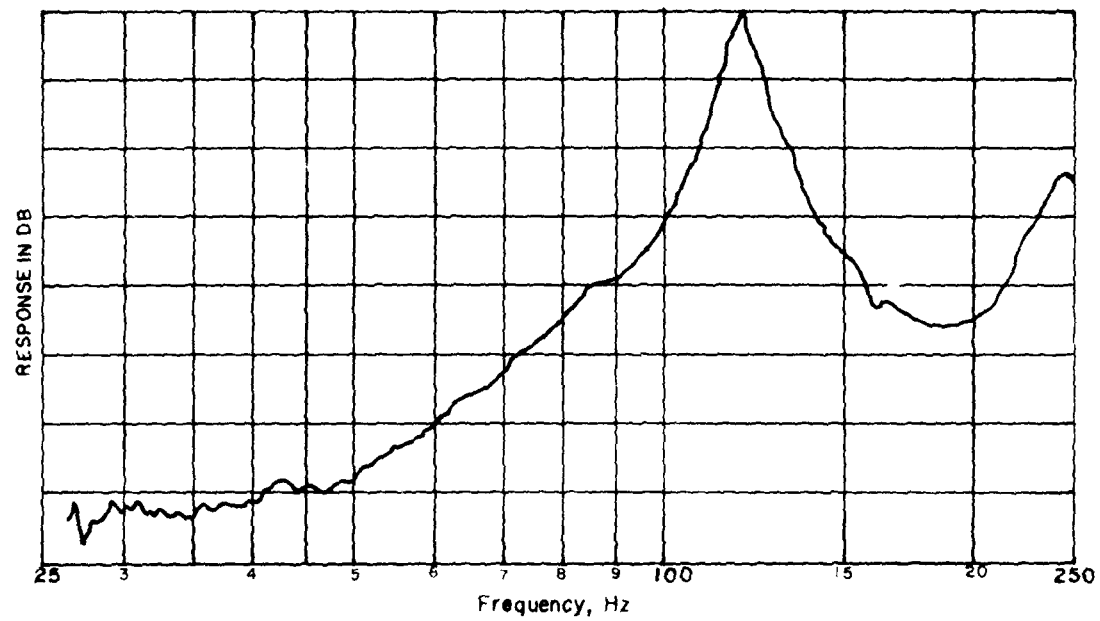
Figure 55. ECHO II recording probing into subsurface at a station directly over Cavity Site I; no reflected signals observed; only harmonics of 120-Hz triangular wave evident
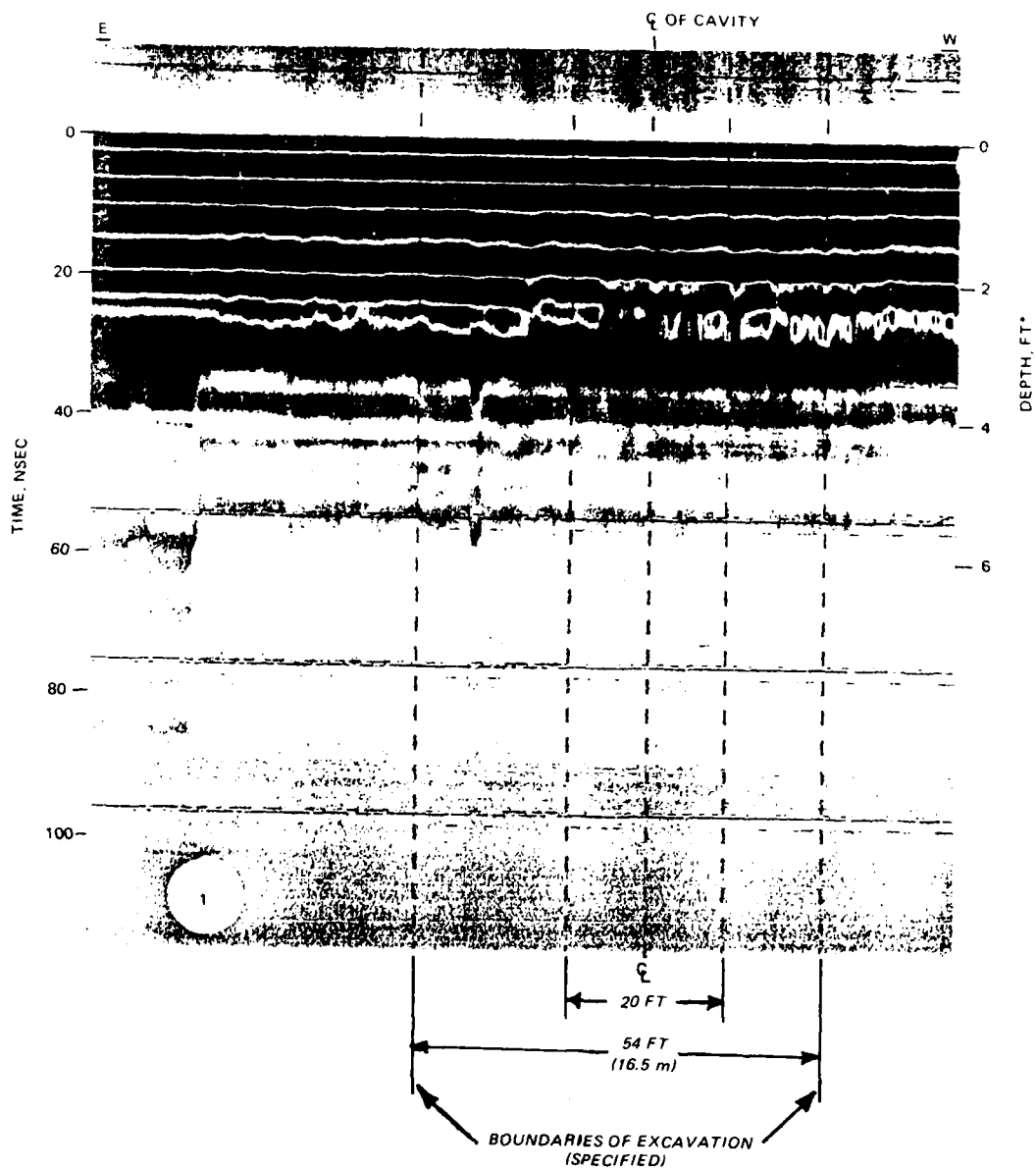
Figure 56. East-west radar profile of Cavity Site III;
100 MHz antennae
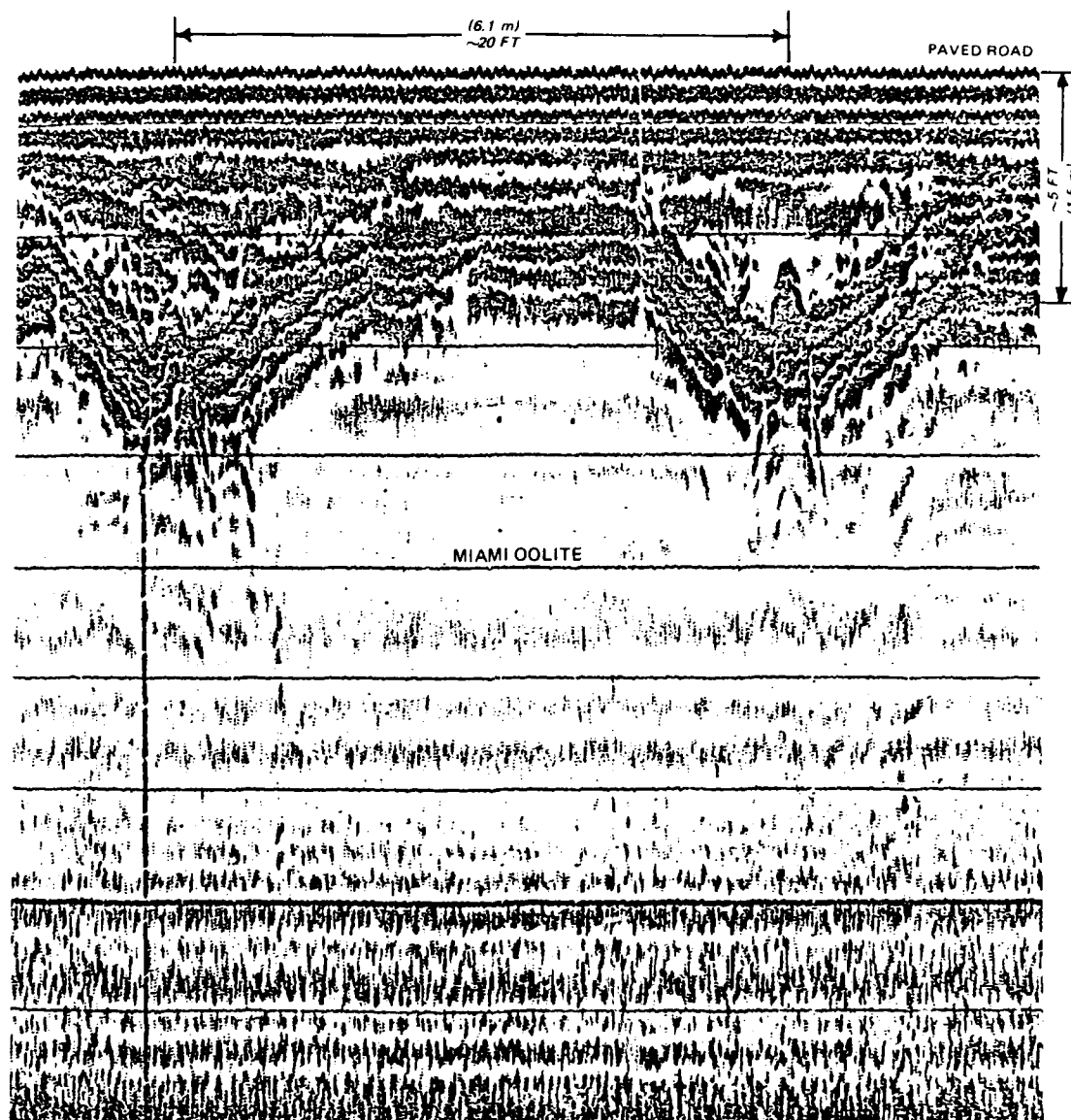
Figure 57. An optimum radar record of pipes in V-shaped trenches. (Trenches were notched in the Miami Oolite and backfilled with the excavated material; record from Miami, Fla.)
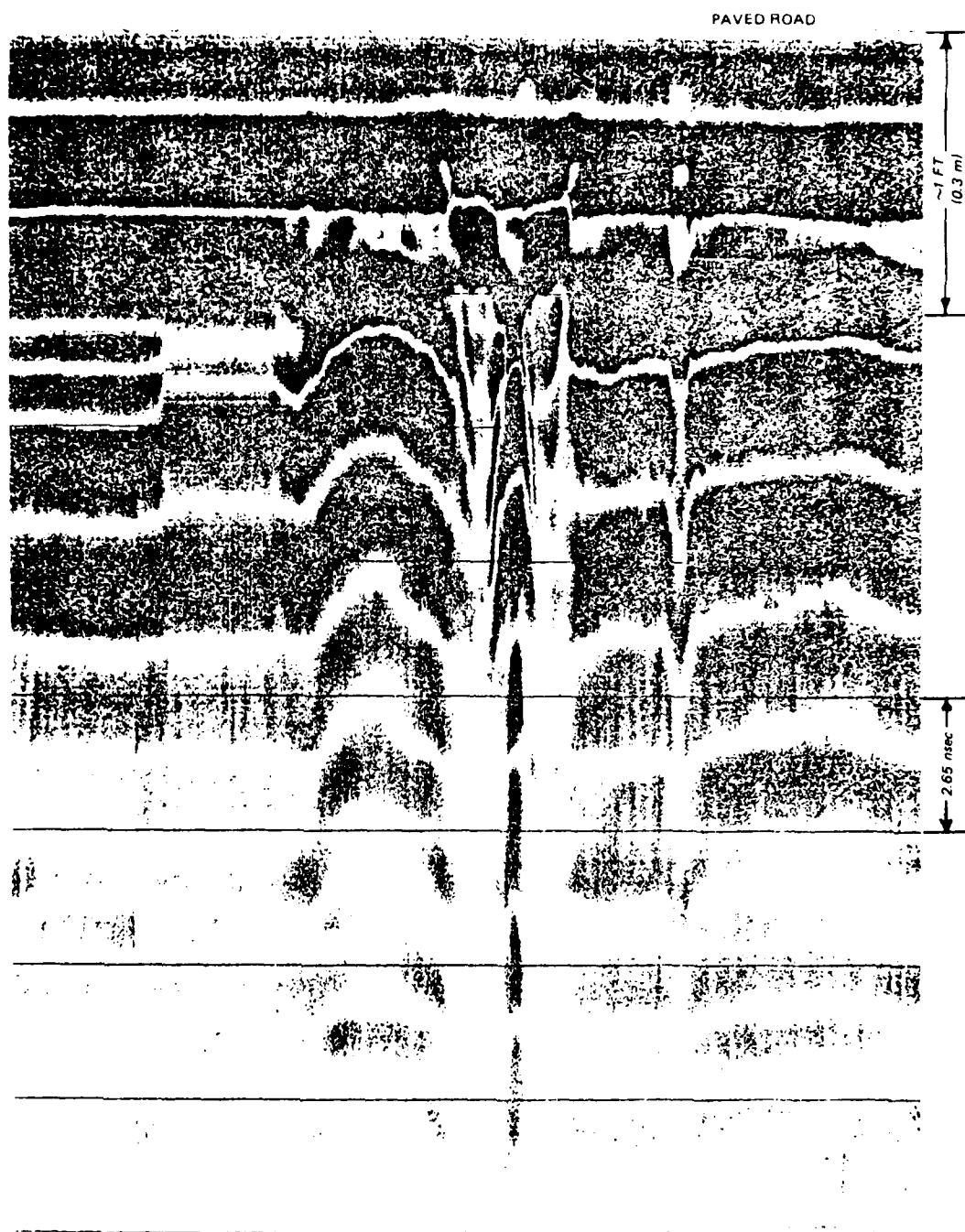
Figure 58. Radar profile of 0.3-m-diam culvert at 0.3-m depth
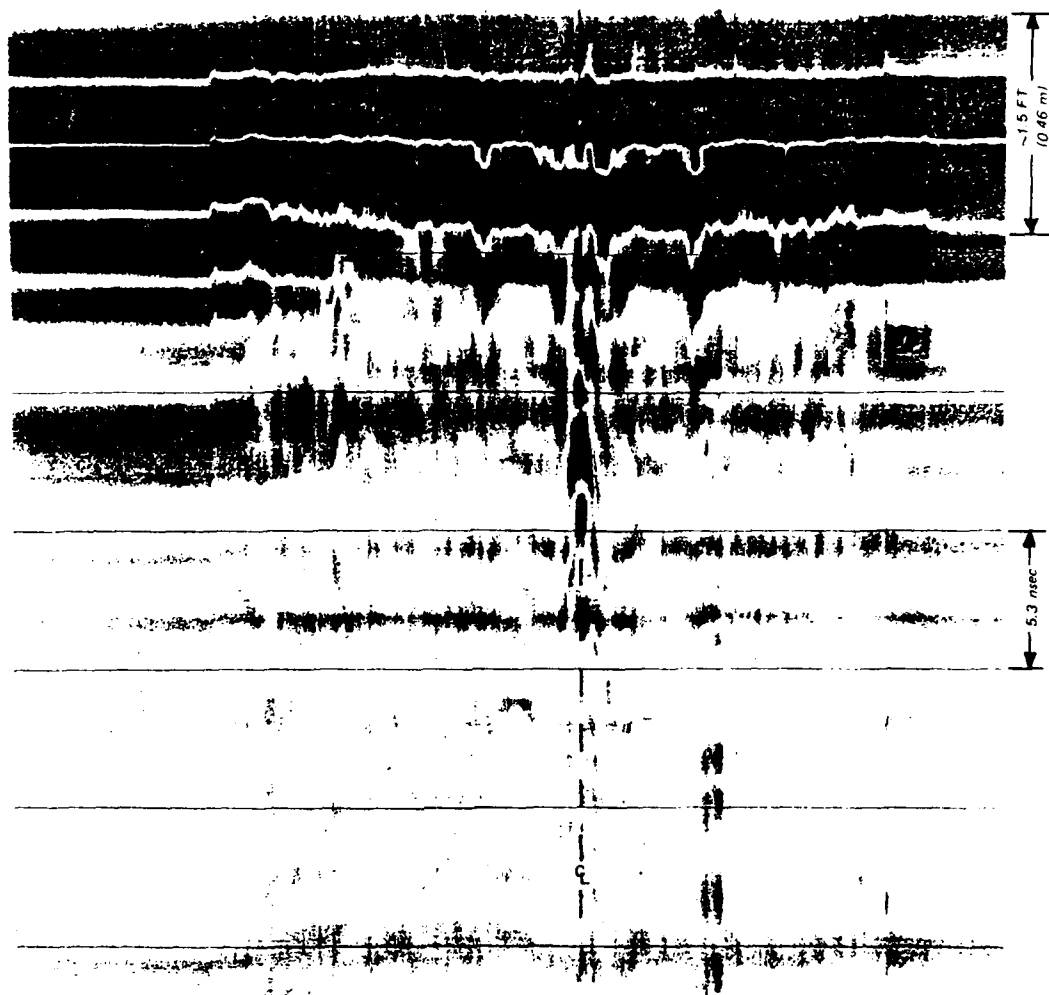
Figure 59. Radar profile of 0.3-m-diam culvert at 0.46-m depth

APPENDIX A: SEISMIC REFLECTION RECORDS

1. Each of the following figures (Al to A8) presents from top to bottom the seismograms obtained from one, two, three, four, and five summed impacts (as illustrated in Figure 26) for reflection Stations 3 through 10 (Figure 25). The dashed line is at 35 msec. Sweep time is 100 msec.
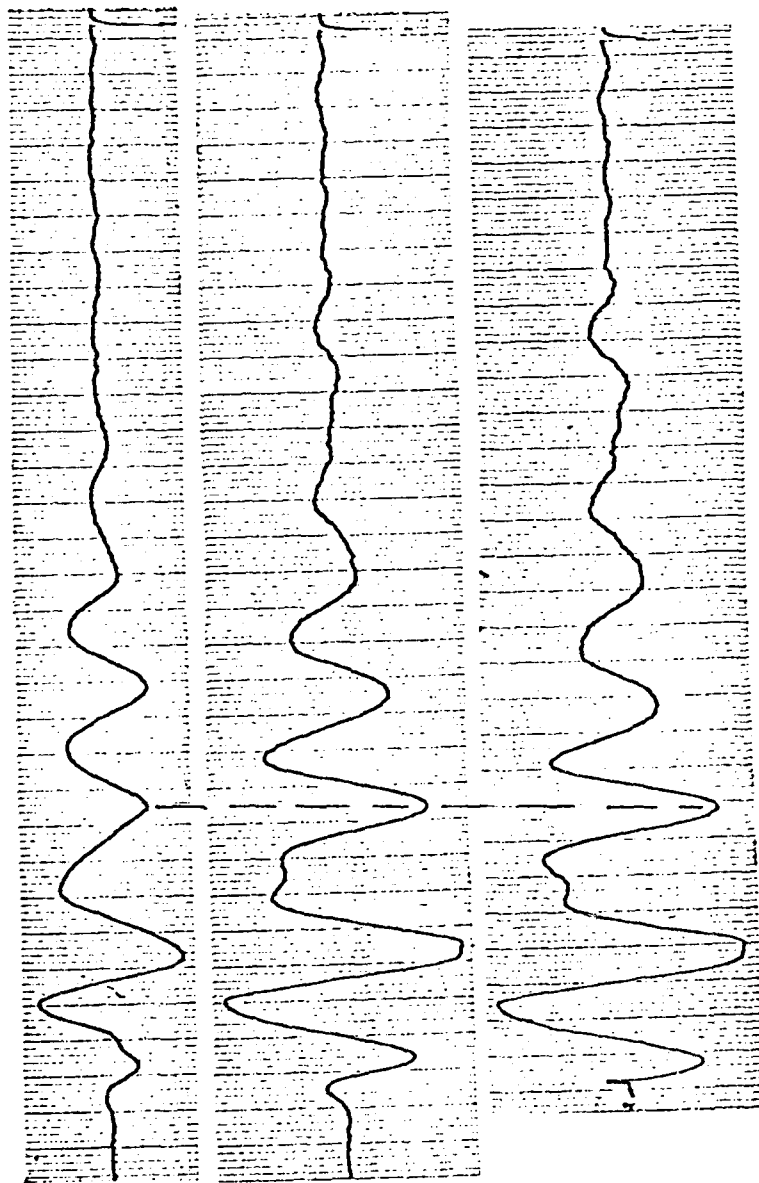
Figure A1. Station 3 (Continued)

A2
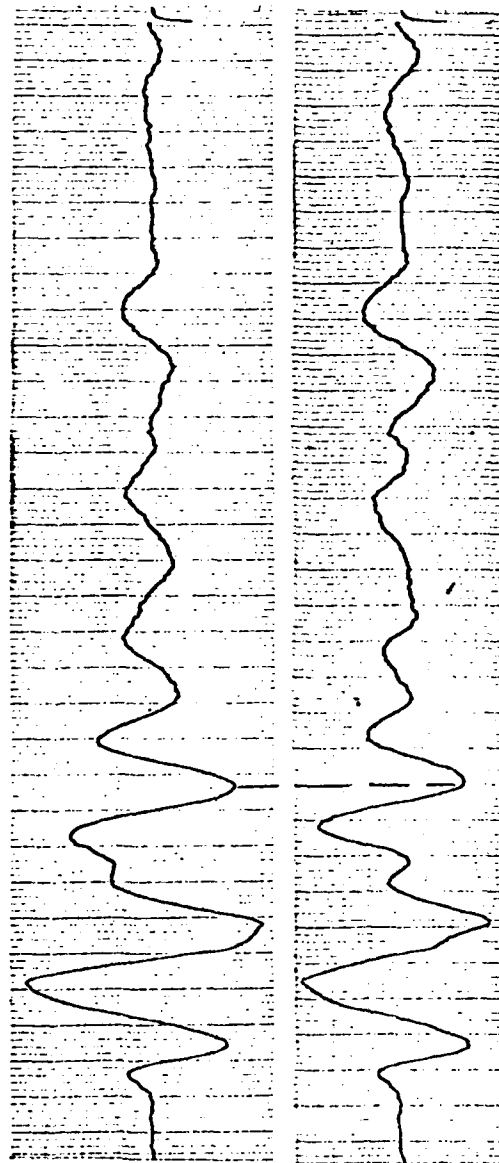
Figure A1. (Concluded)

A3
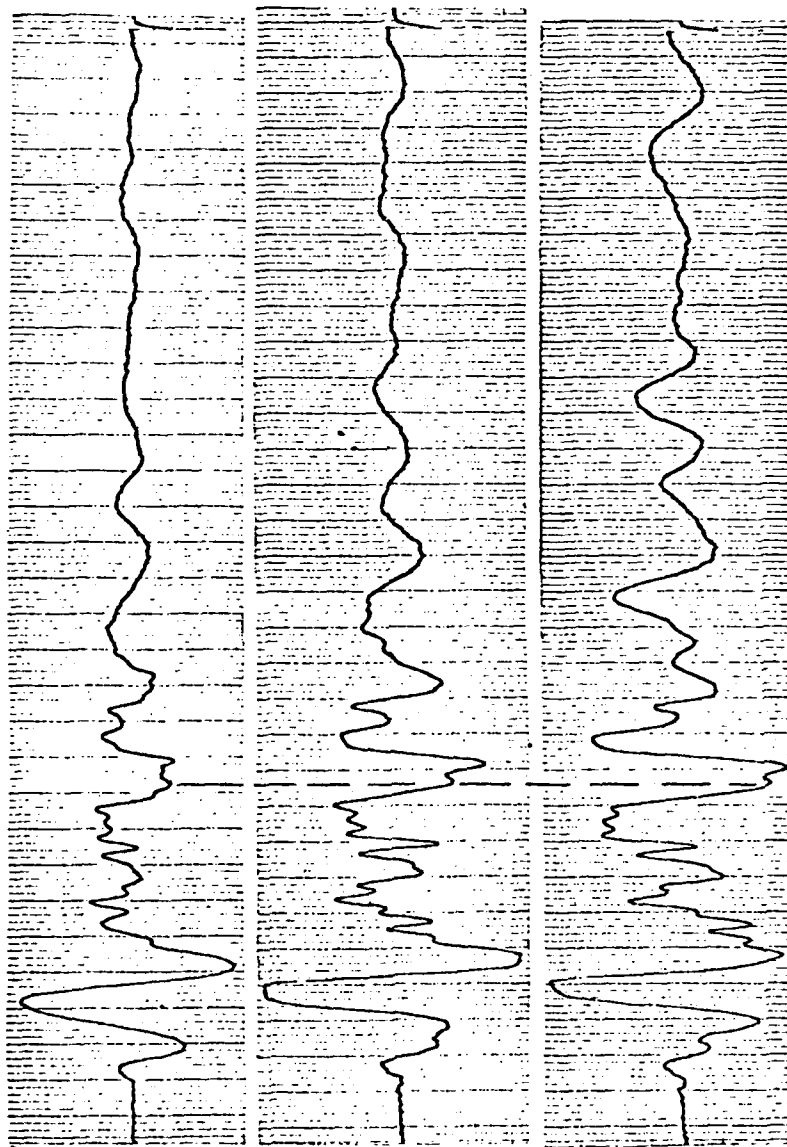
Figure A2. Station 4 (Continued)

A4
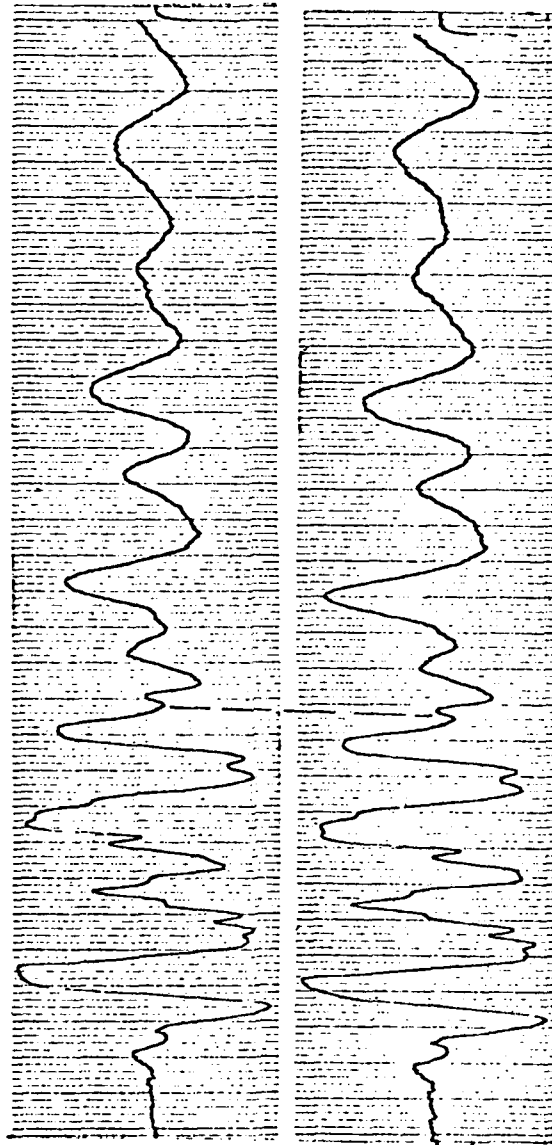
Figure A2. (Concluded)

A5
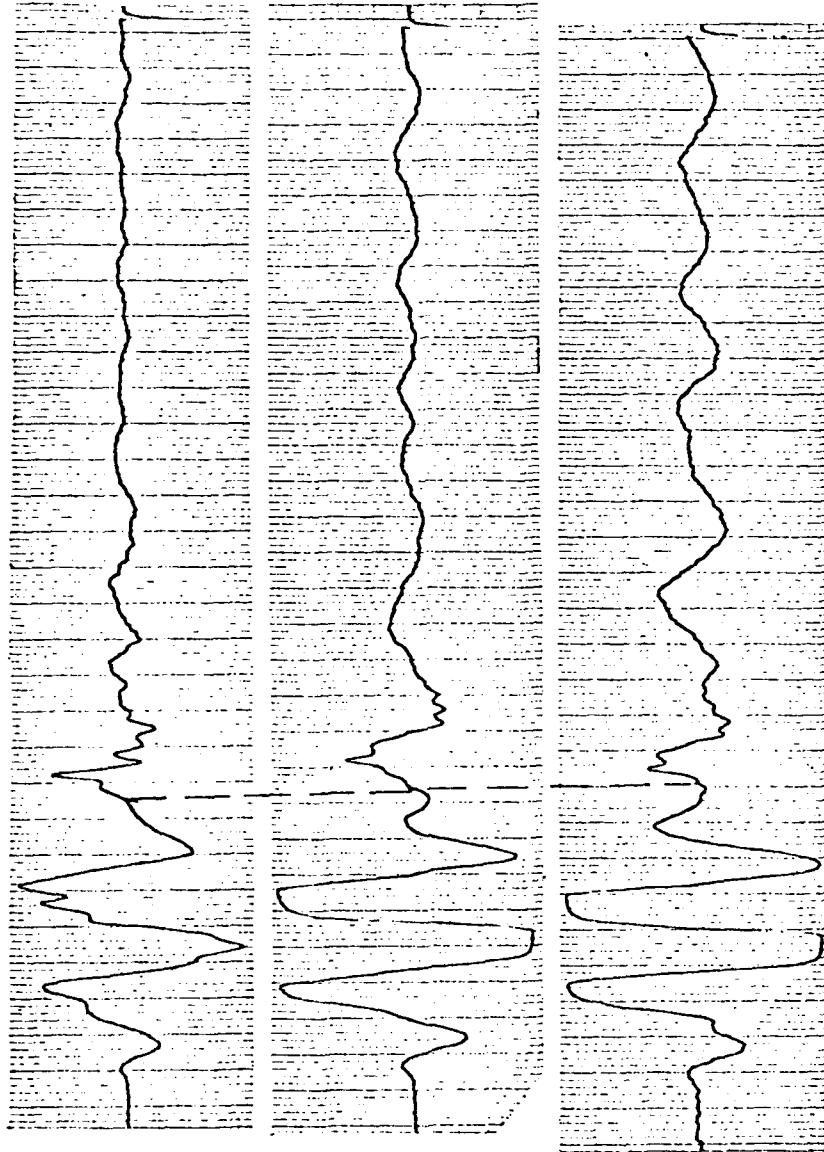
Figure A3. Station 5 (Continued)

A6
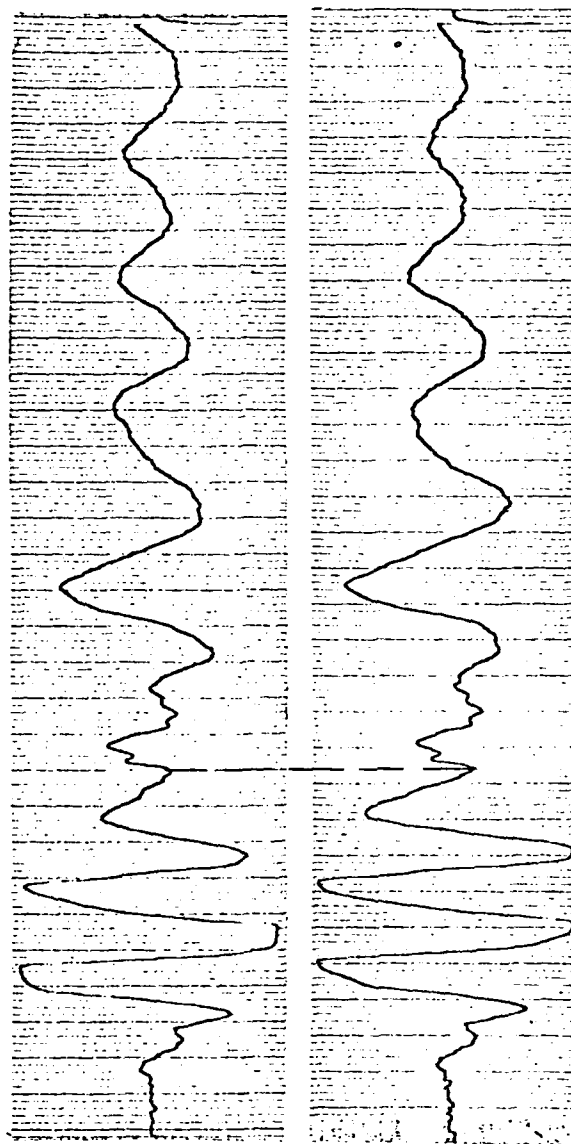
Figure A3. (Concluded)

A7
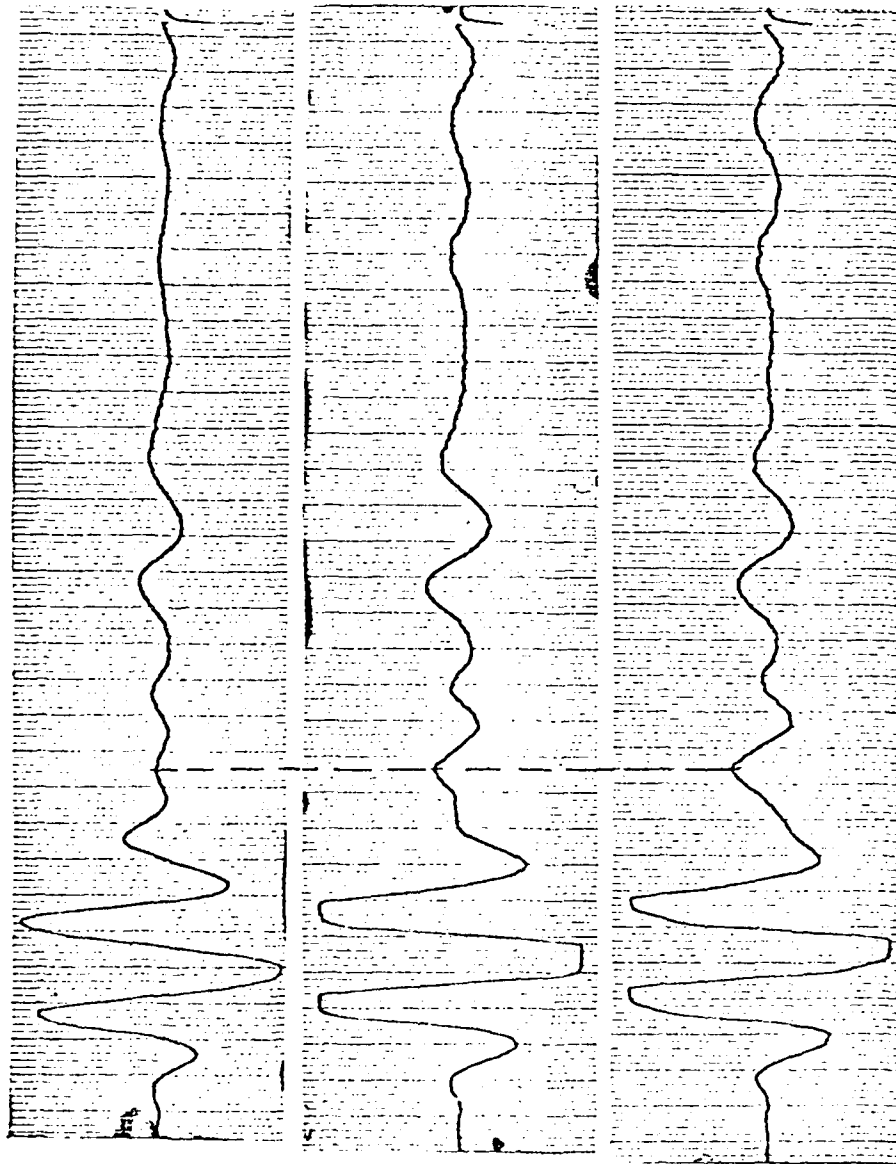
Figure A4. Station 6 (Continued)

A8
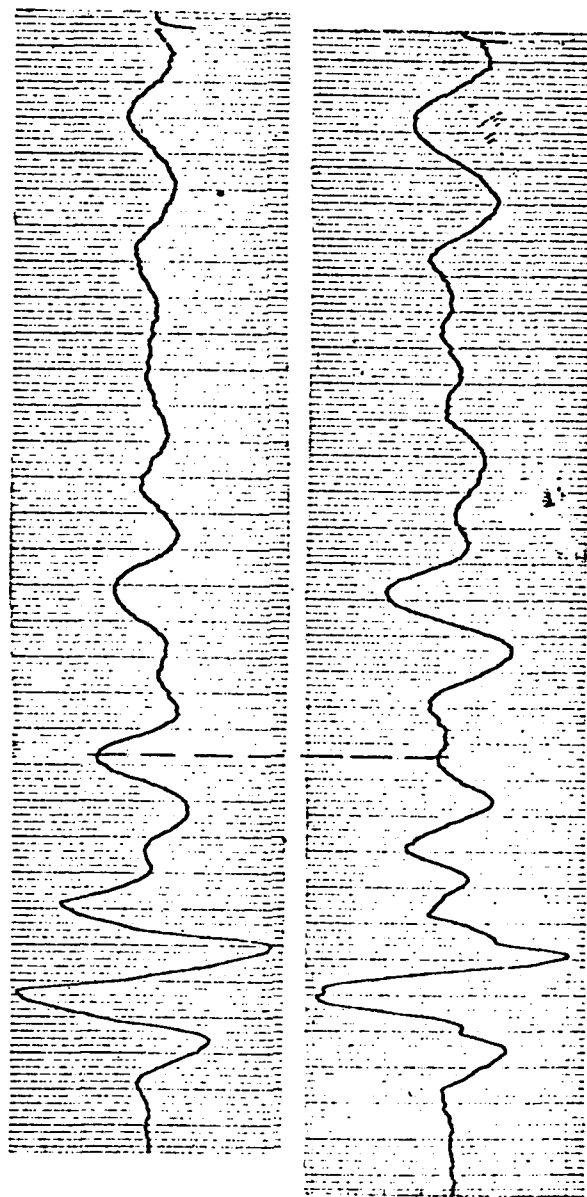
Figure A4. (Concluded)

A9
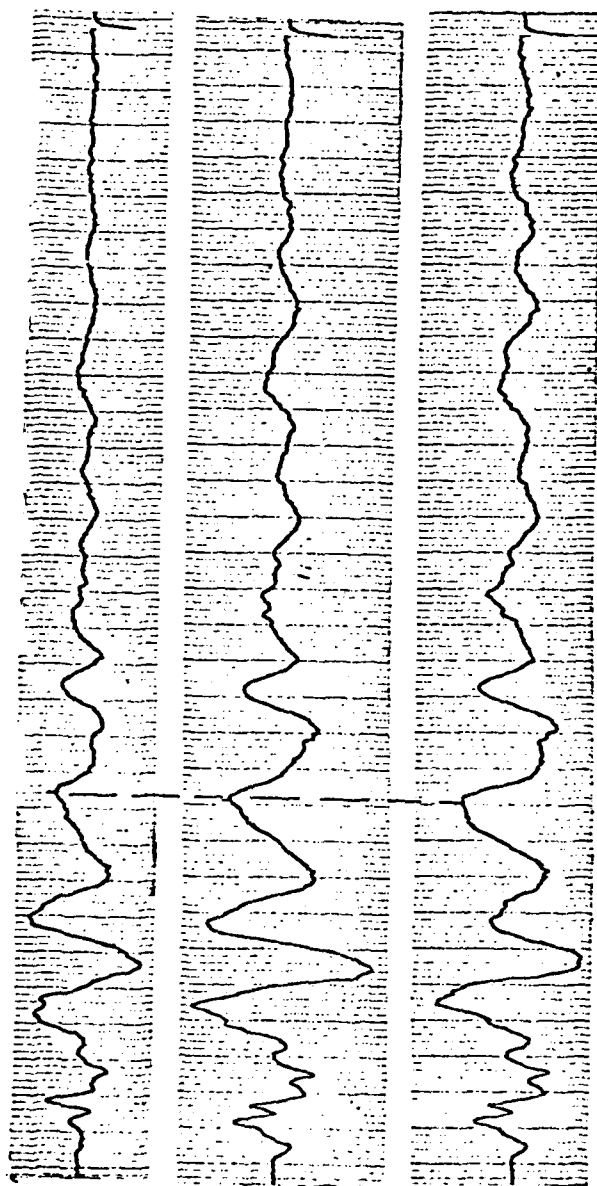
Figure A5. Station 7 (Continued)

A10
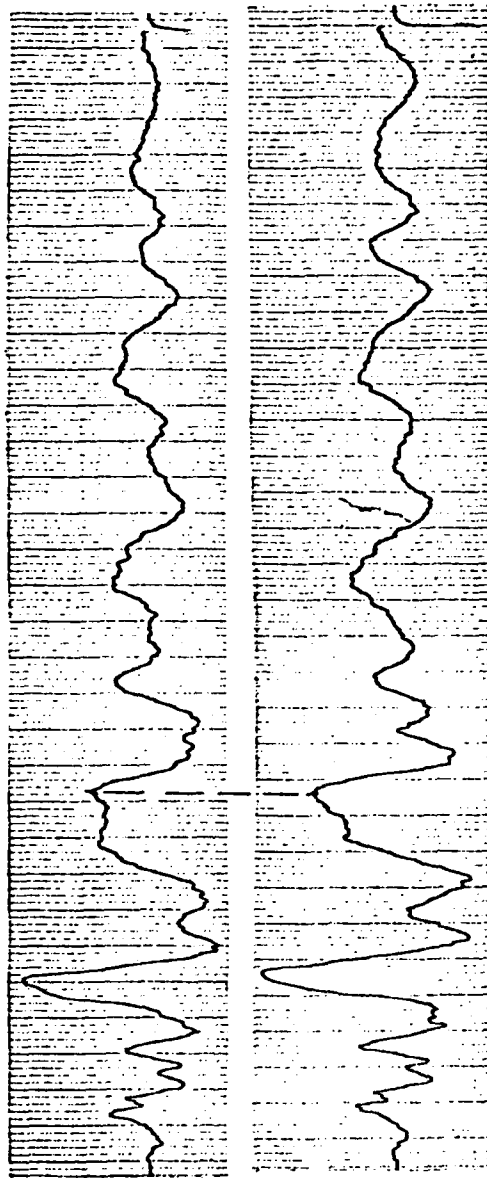
Figure A5. (Concluded)

All
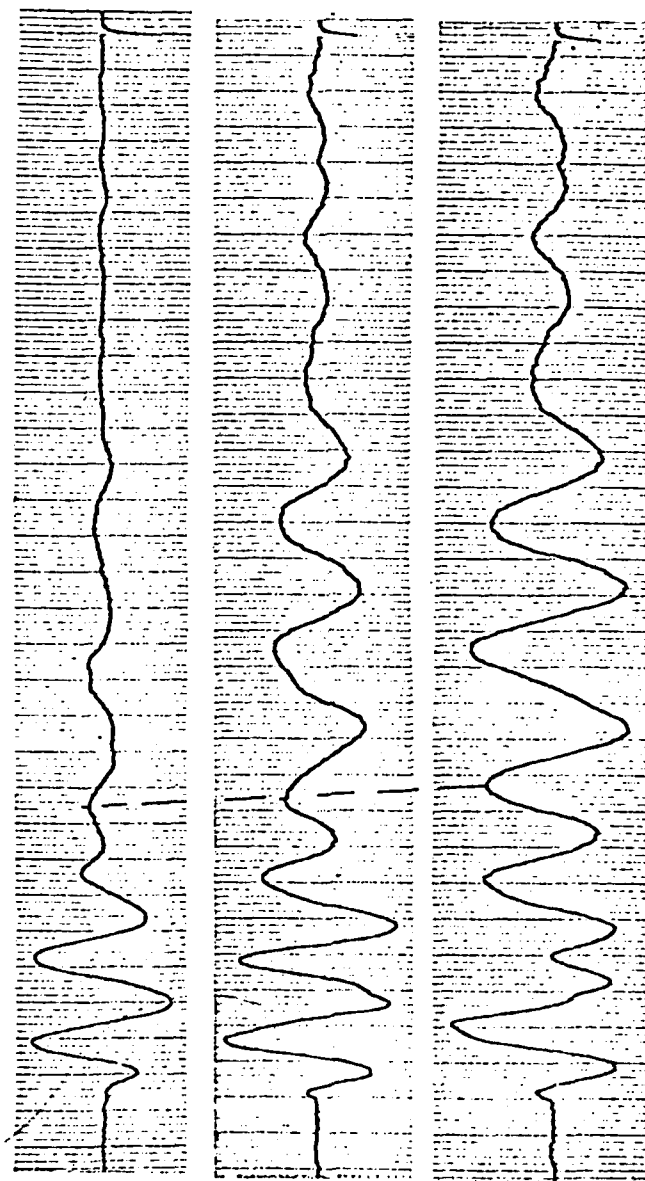
Figure A6. Station 8 (Continued)

A12
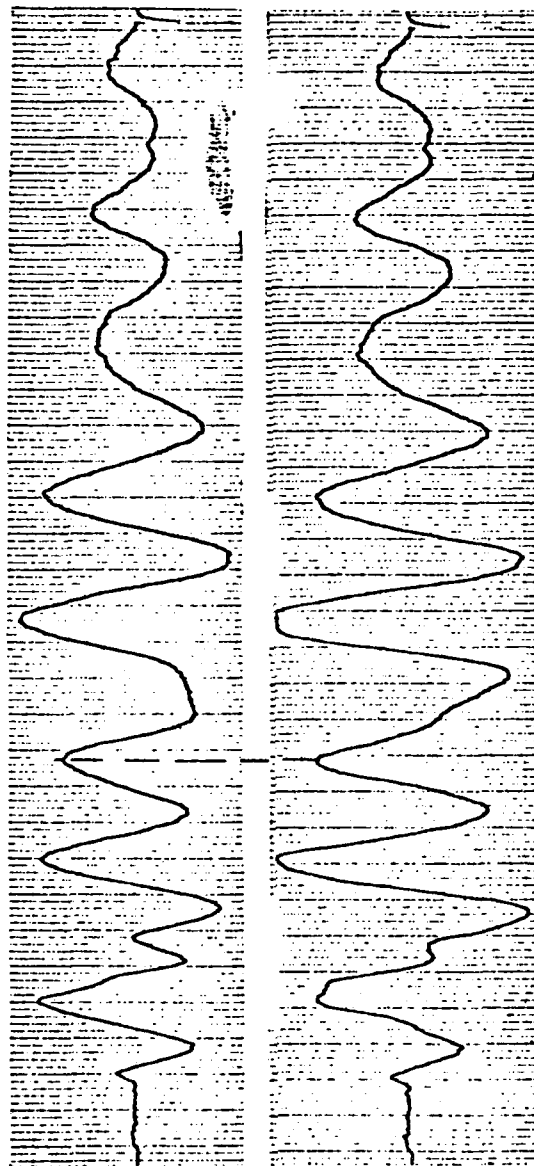
Figure A6. (Concluded)

A13
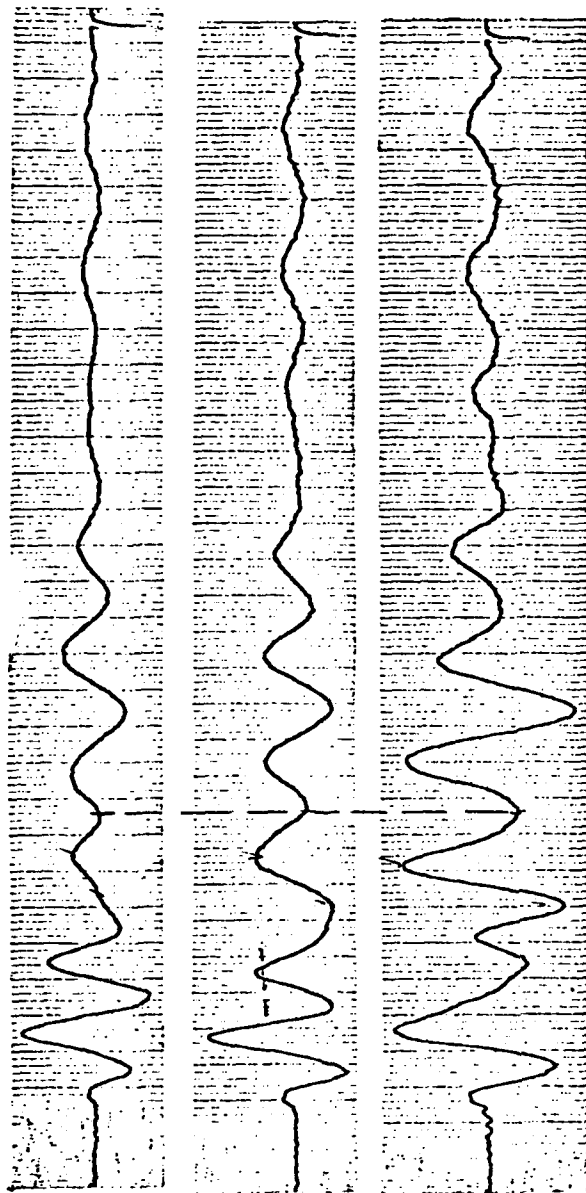
Figure A7. Station 9 (Continued)

A14
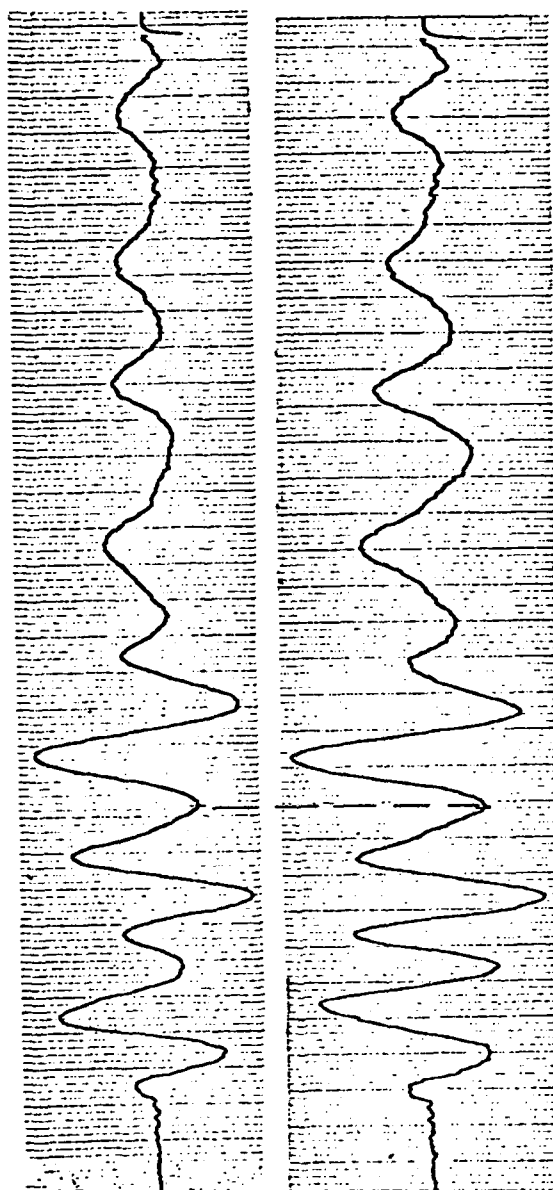
Figure A7. (Concluded)

A15
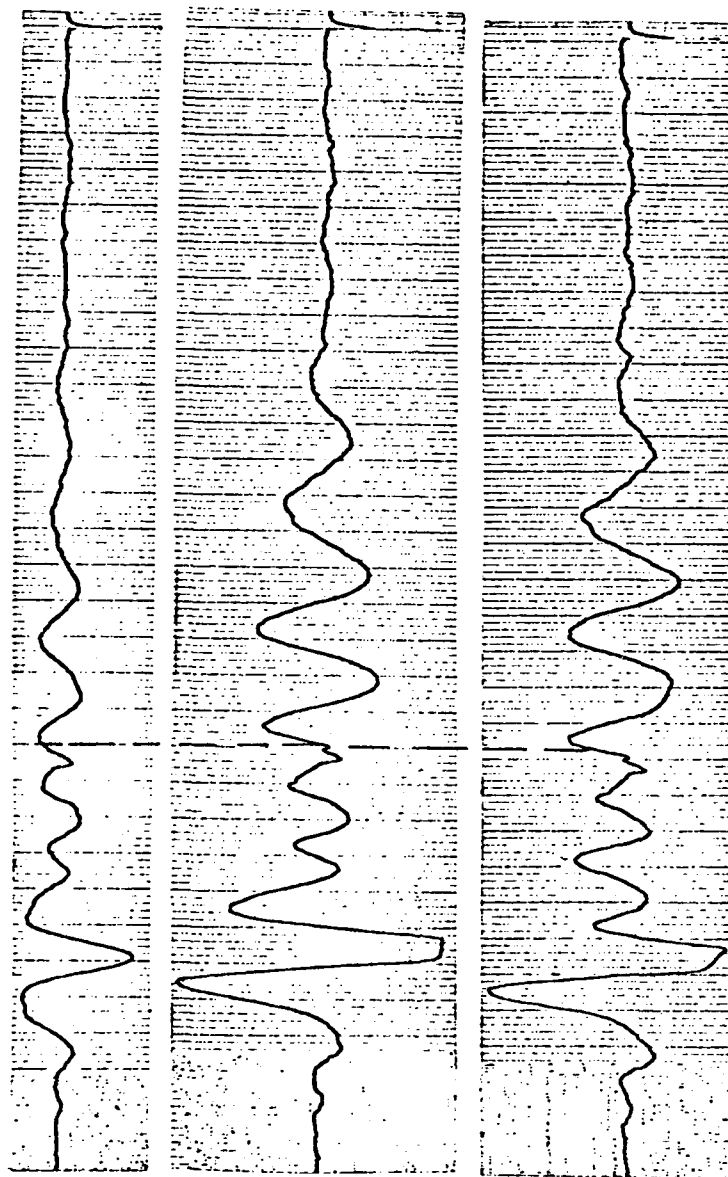
Figure A8. Station 10 (Continued)

A16
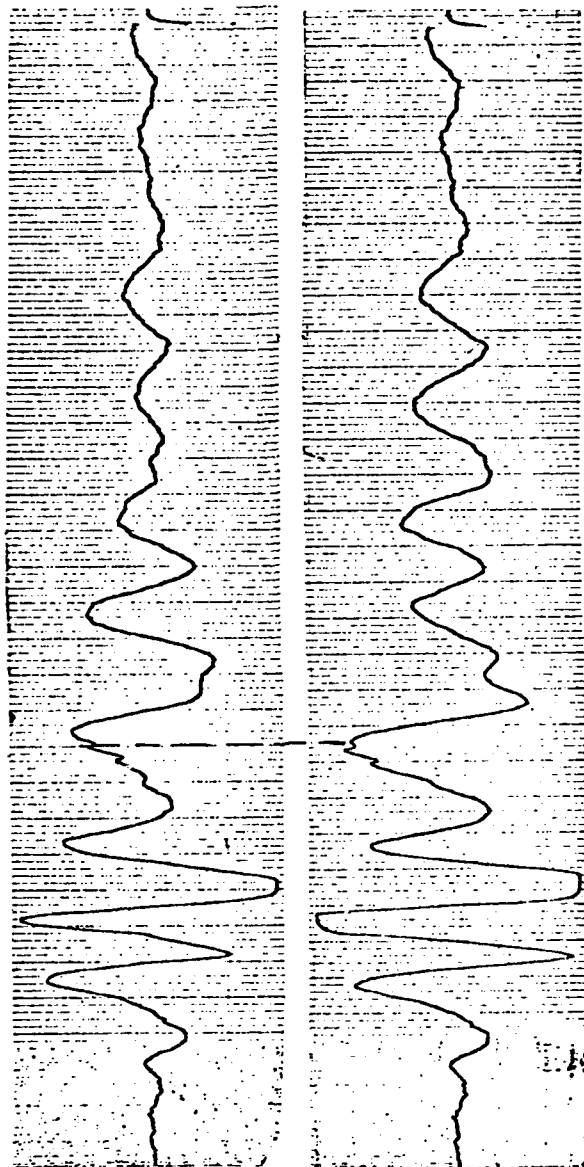
Figure A8. (Concluded)

A17

APPENDIX B

BRISTOW-BATES SURVEYS--DATA SHEETS

BRISTOW RESISTIVITY SURVEY

Project: _____

Test No.: 100 - 200 (C_1 at 100 ft, P_1, P_2 moved outward to 200 ft)

Weather Conditions: _____

Area: WES cavity detection area   2 ft cav

Date: 18 Mar '76

Observer: Murphy

P-P Feet	D Feet	Reading Ohms	Factor 10^3	Resistivity Ohms cm 10^3	Resistivity Ohms cm 10^3	Interpretation
110-120		189/100	3.83	7.2		
120-130		50.5/100	11.5	5.8		
130-140		20.2/150	23.0	3.1		
140-150		10.9/150	38.3	2.6		
150-160		10.5/150	57.5	4.0		
160-170		10.8/150	80.4	5.8		
170-180		5.9/150	107.2	4.2		
180-190		5.8/150	137.9	5.3		
190-200		4/150	172.4	4.6		

5 TO 10 D

PLATE B1

BRISTOW RESISTIVITY SURVEY
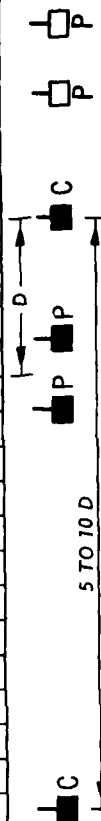
Project: 150-50 (C_1 at 150 ft, P_1, P_2 moved out-ward to 50 ft)

Test No.:

Area: WES Cavity detection area. 2 ft cavity

Date: 18 Mar '76

Observer: Murphy

Weather Conditions: Wet

PLATE B2

P-P Feet	D Feet	Reading Ohms	Factor 10^3	Resistivity Ohms cm 10^3	Resistivity Ohms cm 10^3	Interpretation
140-130	135	118.6/150	3.8	3.0		
130-120	125	51.1/150	11.5	3.9		
120-110	115	38.8/150	23.0	5.9		
110-100	105	22/150	38.3	5.6		
100-90	95	124/150	57.5	4.7		
90-80	85	10.7/150	80.4	5.7		
80-70	75	6/150	107.2	4.3		
70-60	65	5/150	137.9	4.6		
60-50	55	3/150	172.4	3.4		

5 TO 10 D

WES FORM NO. 1941
1 APR 1971

BRISTOW RESISTIVITY SURVEY

Project: _____

Area: _____ WES cavity detection area

Test No.: _____ 200-100

Date: _____ 18 Mar '76

Weather Conditions: _____ Wet

Observer: _____ Murphy

P-P Feet	D Feet	Reading Ohms	Factor 10³	Resistivity Ohms cm 10³
190-180	185	85/100	3.8	3.3
180-170	175	50.8/100	11.5	5.8
170-160	165	25/100	23.0	5.7
160-150	155	11.6/100	38.3	4.4
150-140	145	7/150	57.5	2.7
140-130	135	6/150	80.4	3.2
130-120	125	3.7/150	107.2	2.6
120-110	115	5/150	137.9	4.6
110-100	105	4.6/150	172.4	5.3

Interpretation

Resistivity Ohms cm 10³

5 TO 10 D

WES FORM NO. 1941
1 APR 1971

PLATE B3

BRISTOW RESISTIVITY SURVEY

Project: _____ Area: WES cavity detection test area

Test No.: 100-50 2 ft cavity Date: 19 Mar. '76

Weather Conditions: Cloudy Observer: Murphy

P-P Feet	D Feet	Reading Ohms	Factor 10^3	Resistivity Ohms cm 10^3
95-90		184.5/50	1.915	7.1
90-85		61.7/50	5.745	7.1
85-80		89.1/150	11.491	6.8
80-75		48.3/150	19.151	6.2
75-70		32.3/150	28.727	6.2
70-65		24/175	40.217	5.5
65-60		16.1/175	53.623	5.0
60-55		13/175	68.944	5.1
55-50		13.2/175	86.180	6.5

Resistivity Ohms cm 10^3

5 TO 10 D

WES FORM NO. 1941
1 APR 1971

BRISTOW RESISTIVITY SURVEY

Project: _____

Test No.: __100-200__   __2 ft cav.__

Weather Conditions: _____

Area: __WES cavity detection test area__

Date: __22 Mar. '76__

Observer: __Murphy__

P-P Feet C_1 @ 100	D Feet	Reading Ohms	Factor 10^3	Resistivity Ohms cm 10^3	Resistivity Ohms cm 10^3	Interpretation
105-110		276/75	1.92	7.1		
110-115		122.1/100	5.75	7.0		
115-120		60.6/100	11.5	7.0		
120-125		36.8/100	19.2	7.1		
125-130		28.6/200	28.7	4.1		
130-135		17.1/200	40.2	3.4		
135-140		15.2/300	53.6	2.7		
140-145		12.9/300	68.9	3.0		
145-150		7.5/300	86.2	2.2		
150-155		6.5/300	105.3	2.3		
155-160		11.8/300	126.4	5.0		
160-165		11/300	149.4	5.5		
165-170		7.5/300	174.3	4.4		
170-175		6/300	201.1	4.0		
175-180		4.6/300	229.8	3.5		
180-185		3.5/300	260.5	3.0		
185-190		3/300	293.0	2.9		
190-195		3/300	327.5	3.3		

5 TO 10 D

BRISTOW RESISTIVITY SURVEY

Project: _____

Test No.: ___150-50___   2 ft. cav.

Weather Conditions: _____

Area: ___WES cavity detection test area___

Date: ___19 Mar. '76___

Observer: ___Murphy___

P-P Feet	D Feet	Reading Ohms	Factor 10^3	Resistivity Ohms cm 10^3		Resistivity Ohms cm 10^3		Interpretation
145-140		325.4/200	1.92	3.1				
140-135		99/200	5.75	2.8				
135-130		50/200	11.5	2.9				
130-125		29.3/200	19.2	2.8				
125-120		35.9/200	28.7	5.2				
120-115		27.4/200	40.2	5.5				
115-110		20.2/200	53.6	5.4				
110-105		20.7/300	68.9	4.8				
105-100		19.1/300	86.2	5.5				
100-95		11.6/300	105.3	4.1				
95-90		10.6/300	126.4	4.5				
90-85		8.1/300	149.4	4.0				
85-80		8.4/300	174.3	4.9				
80-75		6.1/300	201.1	4.1				
75-70		3.6/300	229.8	2.8				
70-65		5.3/300	260.5	4.6				
65-60		4.1/300	293.0	4.0				
60-55		3.6/300	327.5	3.9				

WES FORM NO. 1941
1 APR 1971

PLATE B6

5 TO 10 D
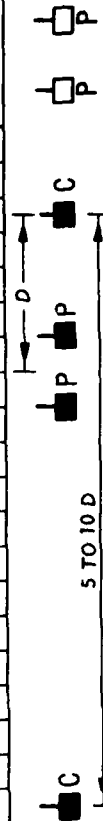
BRISTOW RESISTIVITY SURVEY

Project: _____

Test No.: 150-200   2 ft cav.

Weather Conditions: _____

Area: WES cavity detection test area

Date: 19 Mar. '76

Observer: Murphy

P-P Feet	D Feet	Reading Ohms	Factor 10^3	Resistivity Ohms cm 10^3		Resistivity Ohms cm 10^3		Interpretation
155-160		703/350	1.92	3.9				
160-165		315.2/350	5.75	5.2				
165-170		138.6/350	11.5	4.6				
170-175		76.1/350	19.2	4.2				
175-180		50/350	28.7	4.1				
180-185		34/350	40.2	3.9				
185-190		24.9/350	53.6	3.8				
190-195		21/350	68.9	4.1				
195-200		14.6/350	86.2	3.6				

5 TO 10 D

WES FORM NO. 1941
1 APR 1971

PLATE B7

BRISTOW RESISTIVITY SURVEY

Project: _____

Test No.: __200-100__ 2 ft cav.

Weather Conditions: _____

Area: __WES cavity detection test area__

Date: __19 Mar. '76__

Observer: __Murphy__

P-P Feet	D Feet	Reading Ohms	Factor 10³	Resistivity Ohms cm 10³	Resistivity Ohms cm 10³	Interpretation
195-190			1.92			
190-185		95.4/350	5.75	1.6		
185-180		55.3/350	11.5	1.8		
180-175		32.9/350	19.2	1.8		
175-170		23.6/350	28.7	1.9		
170-165		19.9/350	40.2	2.3		
165-160		13/350	53.6	2.0		
160-155		4.2/200	68.9	1.4		
155-150		4.1/200	86.2	1.8		
150-145		3.7/200	105.3	1.9		
145-140		3.6/200	126.4	2.3		
140-135		1.5/200	149.4	1.1		
135-130		4.1/200	174.3	3.6		
130-125		3.2/200	201.1	3.2		
125-120		2.9/200	229.8	3.3		
120-115		3.6/200	260.5	4.7		
115-110		2.2/200	293.0	3.2		
110-105		2/200	327.5	3.3		
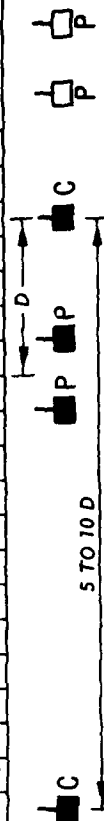
5 TO 10 D

D

WES FORM NO. 1 APR 1971   1941

PLATE B8

BRISTOW RESISTIVITY SURVEY

Project: _____

Test No.: __110-150__   __2 ft cav.__

Weather Conditions: _____

Area: __WES cavity detection test area__

Date: __2 Apr '76__

Observer: __Murphy__

P-P Feet	D Feet	Reading Ohms	Factor 10³	Resistivity Ohms cm 10³	Resistivity Ohms cm 10³	Interpretation
112–114		5.5	0.766	4.2		
114–116		2.5	2.30	5.8		
116–118		1.2	4.60	5.5		
118–120		0.8	7.66	6.1		
120–122		0.57	11.49	6.5		
122–124		0.36	16.09	5.8		
124–126		0.25	21.45	5.4		
126–128		0.13	27.6	3.6		
128–130		0.10	34.5	3.5		
130–132		0.09	42.1	3.8		
132–134		0.056	50.6	2.8		
134–136		0.050	59.8	3.0		
136–138		0.047	69.7	3.3		
138–140		0.036	80.4	2.9		
140–142		0.026	91.9	2.4		
142–144		0.033	104.2	3.4		
144–146		0.019	117.2	2.2		
196–148		0.019	31.0	2.5		
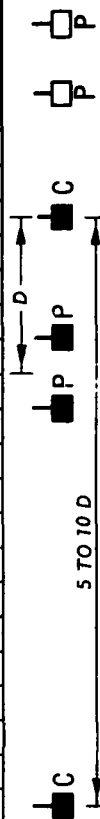
5 TO 10 D

WES FORM NO. 1941
1 APR 1971

PLATE B9

BRISTOW RESISTIVITY SURVEY

Project: _____

Test No.: 130-110   2 ft cav.

Weather Conditions: _____

Area: _____

Date: 2 Apr. '76

Observer: Murphy

P-P Feet	D Feet	Reading Ohms	Factor 10^3	Resistivity Ohms cm 10^3	Resistivity Ohms cm 10^3	Interpretation
128-126		2.7	0.766	2.1		
126-124		1.1	2.30	2.5		
124-122		0.7	4.60	3.2		
122-120		0.58	7.66	4.4		
120-118		0.40	11.49	4.6		
118-116		0.26	16.09	4.2		
116-114		0.20	21.45	4.3		
114-112		0.14	27.6	3.9		
112-110		0.11	34.5	3.8		

C   P   P   D   P   C

5 TO 10 D

P   P

PLATE B10
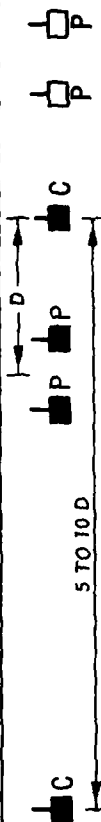
BRISTOW RESISTIVITY SURVEY

Project: _____ Area: _____

Test No.: 130-170   2 ft cav. Date: April 2 '76

Weather Conditions: _____ Observer: Murphy

P-P Feet	D Feet	Reading Ohms	Factor 10³	Resistivity Ohms cm 10³	Resistivity Ohms cm 10³	Interpretation
132-134		02.6	0.766	2.0		
134-136		01.1	2.30	2.5		
136-138		0.62	4.60	2.9		
138-140		0.32	7.66	2.5		
140-142		0.18	11.49	2.1		
142-144		0.19	16.09	3.1		
144-146		0.10	21.45	2.1		
146-148		.086	27.6	2.4		
148-150		.061	34.5	2.1		
150-152		0.048	42.1	2.0		
152-154		0.038	50.6	1.9		
154-156		0.048	59.8	2.9		
156-158		0.067	69.7	4.7		
158-160		0.074	80.4	5.9		
160-162		0.063	91.9	5.8		
162-164		0.053	104.2	5.5		
166-168		0.036	131.0	4.7		

5 TO 10 D

WES FORM NO. 1941
1 APR 1971

PLATE B11

BRISTOW RESISTIVITY SURVEY

Project: _____   Area: _____

Test No.: __150-110__   __2 ft cav.__   Date: __2 Apr '76__

Weather Conditions: _____   Observer: __Murphy__

PLATE B12

P-P Feet	D Feet	Reading Ohms	Factor 10^3	Resistivity Ohms cm 10^3	Interpretation / Resistivity Ohms cm 10^3
148-146		2.8	0.766	2.1	
146-144		00.9	2.30	2.1	
144-142		0.63	4.60	2.9	
142-140		0.30	7.66	2.3	
140-138		0.24	11.49	2.8	
138-136		0.18	16.09	2.9	
136-134		0.11	21.45	2.4	
134-132		.078	27.6	2.2	
132-130		.082	34.5	2.8	
130-128		0.050	42.1	2.1	
128-126		0.047	50.6	2.4	
126-124		0.058	59.8	3.5	
124-122		0.058	69.7	4.0	
122-120		0.067	80.4	5.4	
120-118		0.057	91.9	5.2	
118-116		0.050	104.2	5.2	
114-112		0.035	131.0	4.6	

5 TO 10 D   D

C   P   P   P   C
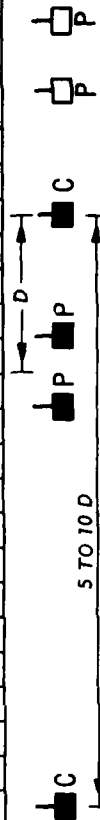
WES FORM NO.   1941
1 APR 1971

BRISTOW RESISTIVITY SURVEY

Project:

Test No.: 150-190   2 ft cav.

Area:

Date: 2 Apr 76

Observer: Murphy

Weather Conditions:

P-P Feet	D Feet	Reading Ohms	Factor 10³	Resistivity Ohms cm 10³	Resistivity Ohms cm 10³	Interpretation
152-154		02.2	0.766	1.7		
154-156		0.92	2.30	2.1		
156-158		0.69	4.60	3.2		
158-160		0.58	7.66	4.4		
160-162		0.40	11.49	4.6		
162-164		0.26	16.09	4.2		
164-166		0.20	21.45	4.3		
166-168		0.14	27.6	3.9		
168-170		0.11	34.5	3.8		
170-172		0.086	42.1	3.6		
172-174		0.063	50.6	3.2		
174-176		0.060	59.8	3.6		
176-178		0.049	69.7	3.4		
178-180		0.042	80.4	3.4		
180-182		0.035	91.9	3.2		
182-184		0.032	104.2	3.3		
184-186		0.028	117.2	3.3		
186-188		0.027	131.0	3.5		

5 TO 10 D

WES FORM NO. 1941
1 APR 1971

PLATE B13

BRISTOW RESISTIVITY SURVEY

Project:

Test No.: 170-130   2 ft cav.

Weather Conditions:

Area:

Date: 2 Apr 76

Observer: Murphy

P-P Feet	D Feet	Reading Ohms	Factor 10^3	Resistivity Ohms cm 10^3	Resistivity Ohms cm 10^3	Interpretation
168-166		07.8	0.766	6.0		
166-164		03.4	2.30	7.8		
164-162		01.6	4.60	7.4		
162-160		01.0	7.66	7.7		
160-158		0.66	11.49	7.6		
158-156		0.41	16.09	6.6		
156-154		0.20	21.45	4.3		
154-152		0.11	27.6	3.0		
152-150		.080	34.5	2.8		
150-148		.062	42.1	2.6		
148-146		.056	50.6	2.8		
146-144		0.042	59.8	2.5		
144-142		0.050	69.7	3.5		
142-140		0.030	80.4	2.1		
140-138		0.030	91.9	2.8		
138-136		0.030	104.2	3.1		
136-134		0.022	117.2	2.6		
134-132		0.018	131.0	2.4		

5 TO 10 D

WES FORM NO. 1941
1 APR 1971

BRISTOW RESISTIVITY SURVEY
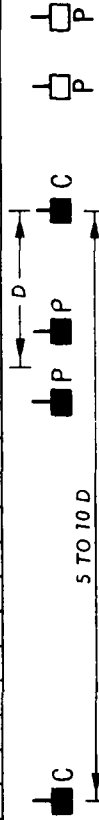
Project: _____

Test No.: 170-200   2 ft cav.

Weather Conditions: _____

Area: _____

Date: 2 Apr 76

Observer: Murphy

P-P Feet	D Feet	Reading Ohms	Factor 10^3	Resistivity Ohms cm 10^3	Resistivity Ohms cm 10^3	Interpretation
172-174		06.5	0.766	5.0		
174-176		02.9	2.30	6.7		
176-178		01.4	4.60	6.4		
178-180		0.83	7.66	6.4		
180-182		0.51	11.49	5.9		
182-184		0.37	16.09	6.0		
184-186		0.27	21.45	5.8		
186-188		0.22	27.6	6.1		
188-190		0.17	39.5	5.9		
190-192		0.146	42.1	6.1		
192-194		0.107	50.6	5.4		
194-196		0.081	59.8	4.8		
196-198		0.073	69.7	5.1		
198-200		.065	80.4	5.2		

5 TO 10 D

BRISTOW RESISTIVITY SURVEY

Project:

Area: Cavity detection test area

Test No.: 50 – 240   Center line of cavity @ 140' on line

Date: 2 June '76

Weather Conditions: Hot, partly cldy, grnd moist

Observer: Murphy

PLATE B16

P-P Feet	D Feet	Reading Ohms	Factor 10^3 ($\frac{cm}{}$)	Resistivity Ohms cm 10^3
60-70		1.5	3.83	5.7
70-80		0.5	11.5	5.8
80-90		0.2	23.0	4.6
90-100		0.11	38.3	4.2
100-110		0.066	57.5	3.8
110-120		0.051	80.4	4.1
120-130	*	0.021	107	2.2
130-140		0.014	138	1.9
140-150		0.011	172	1.9
150-160		0.009	211	1.9
160-170		0.015	253	3.8
170-180		0.012	299	3.6
180-190		0.010	349	3.5
190-200		0.009	402	3.6
200-210		0.005	460	2.30
210-220		0.004	521	2.1
220-230		0.004	586	2.3
230-240		0.003	655	2.0

Resistivity Ohms cm 10^3

Interpretation

WES FORM NO. 1941
1 APR 1971

*Note – boring two ft south of line at 130 ft point.

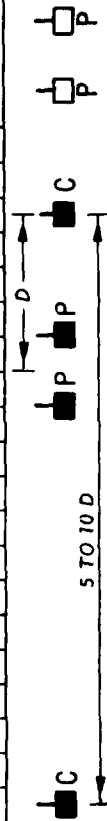5 TO 10 D

BRISTOW RESISTIVITY SURVEY

Project: _____

Area: _____

Test No.: 100 - 240   4 ft cav.

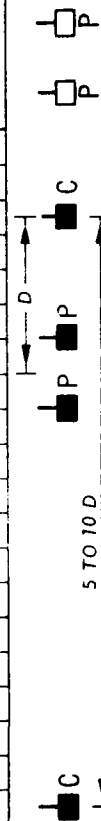Date: 2 Apr 76

Weather Conditions: _____

Observer: Murphy

P-P Feet	D Feet	Reading Ohms	Factor 10^3	Resistivity Ohms cm 10^3
110-120		01.5	3.83	5.7
120-130		0.30	11.5	3.5
130-140		0.118	23.0	2.7
140-150		0.078	38.3	3.0
150-160		0.045	57.5	2.6
160-170		0.067	80.4	5.4
170-180		0.046	107	4.9
180-190		0.035	138	4.8
190-200		0.023	172	4.0
200-210		0.016	211	3.4
210-220		0.012	253	3.0
220-230		0.009	2.99	2.7
230-240		0.010	349	3.5

Resistivity Ohms cm 10^3

Interpretation

P   P   D   P   C

5 TO 10 D

C

PLATE B17

BRISTOW RESISTIVITY SURVEY
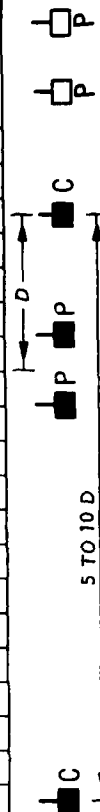
Project: _____ Area: _____

Test No.: _____ 150-0 _____ 4 ft cav. _____ Date: _____ 2 Apr 76 _____

Weather Conditions: _____ Observer: _____ Murphy _____

PLATE B18

P-P Feet	D Feet	Reading Ohms	Factor 10^3	Resistivity Ohms cm 10^3
140-130		0.56	3.83	2.1
130-120		0.22	11.5	2.5
120-110		0.21	23.0	4.8
110-100		0.112	38.3	4.3
100-90		0.082	57.5	4.7
90-80		0.051	80.4	4.1
80-70		0.039	107	4.2
70-60		0.026	138	3.6
60-50		0.018	172	3.1
50-40		0.016	211	3.4
40-30		0.012	253	3.0
30-20		0.011	299	2.7
20-10		0.008	349	2.8
10.0		0.007	402	2.8

Resistivity Ohms cm 10^3

Interpretation

5 TO 10 D

WES FORM NO. 1941
1 APR 1971

BRISTOW RESISTIVITY SURVEY

Project: _____

Test No.: __150-240__   __4 ft cav.__

Date: __2 Apr 76__

Observer: __Murphy__

Weather Conditions: _____

P-P Feet	D Feet	Reading Ohms	Factor 10^3	Resistivity Ohms cm 10^3		Resistivity Ohms cm 10^3		Interpretation
160-170		0.81	3.83	3.1				
170-180		0.34	11.5	3.9				
180-190		0.18	23.0	4.1				
190-200		0.09	38.3	3.4				
200-210		0.060	57.5	3.5				
210-220		0.037	80.4	3.0				
220-230		0.026	107	2.8				
230-240		0.024	138	3.3				
240-250			172					

5 ꓴ 10 D

WES FORM NO.   1941
1 APR 1971

PLATE B19

BRISTOW RESISTIVITY SURVEY

Project: _____

Test No.: ___200-10___

Weather Conditions: _____

Area: _____

Date: ___2 Apr 76___   4 ft cav.

Observer: ___Murphy___

P-P Feet	D Feet	Reading Ohms	Factor 10^3	Resistivity Ohms cm 10^3	Resistivity Ohms cm 10^3	Interpretation
190-180		1.7	3.83	6.5		
180-170		0.48	11.5	5.5		
170-160		0.24	23.0	5.5		
160-150		0.064	38.3	2.5		
150-140		0.042	57.5	2.4		
140-130		0.028	80.4	2.3		
130-120		0.023	107	2.5		
120-110		0.028	138	3.9		
110-100		0.020	172	3.4		
100-90		0.017	211	3.6		
90-80		0.013	253	3.3		
80-70		0.010	299	3.0		
70-60		0.008	349	2.8		
60-50		0.007	402	2.8		
50-40		0.006	460	2.8		
40-30		0.005	521	2.6		
30-20		0.005	586	2.9		
20-10		0.003	655	2.0		
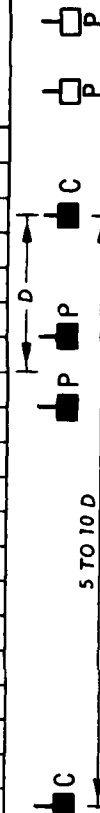
5 TO 10 D

BRISTOW RESISTIVITY SURVEY

Project: _____ **Area:** WES cavity test – 4x4x20 cavity

Test No.: 50-145 C_1 @ 50   4 ft   **Date:** 3 June '76

Weather Conditions: Prtly cldy, hot, grnd moist to wet   **Observer:** Murphy
Water table @ 30' ± depth

P-P Feet	D Feet	Reading Ohms	Factor 10^3	Resistivity Ohms cm 10^3	Resistivity Ohms cm 10^3	Interpretation
55-60		2.5	1.92	4.8		
60-65		0.91	5.75	5.2		
65-70		0.55	11.5	6.3		
70-75		0.30	19.2	5.8		
75-80		0.20	28.7	5.7		
80-85		0.12	40.2	4.8		
85-90		0.086	53.6	4.6		
90-95		0.062	68.9	4.3		
95-100		0.052	86.2	4.5		
100-105		0.038	105	4.0		
105-110		0.027	126	3.4		
110-105		0.027	149	4.0		
115-120		0.021	174	3.7		
120-125		0.012	201	2.4		
125-130		0.008	230	1.8		
130-135		0.007	261	1.8		
135-140		0.006	293	1.8		
140-145		0.006	328			
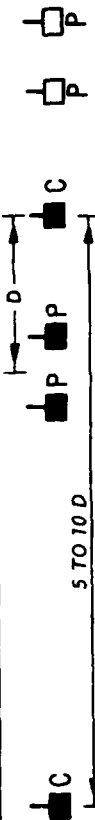
5 TO 10 D

WES FORM NO. 1941
1 APR 1971

PLATE B21

BRISTOW RESISTIVITY SURVEY

Project: _____ Area: _____

Test No.: __100-05__ __C_1 @ 100__ __4 ft cav.__ Date: __2 Apr 76__

Weather Conditions: _____ Observer: __Murphy__

PLATE B22

P-P Feet	D Feet	Reading Ohms	Factor 10^3	Resistivity Ohms cm 10^3	Interpretation
95-90		2.6	1.92	5.0	
90-85		0.95	5.75	5.5	
85-80		0.43	11.5	4.9	
80-75		0.28	19.2	5.4	
75-70		0.17	28/7	4.9	
70-65		0.111	40.2	4.5	
65-60		0.069	53.6	3.7	
60-55		0.050	68.9	3.4	
55-50		0.039	86.2	3.4	
50-45		0.036	105	3.8	
45-40		0.032	126	4.0	
40-35		0.025	149	3.7	
35-30		0.020	174	3.5	
30-25		0.017	201	3.4	
25-20		0.016	230	3.7	
20-15		0.015	261	3.9	
15-10		0.012	293	3.5	
10-05		0.008	328	2.6	

5 TO 10 D
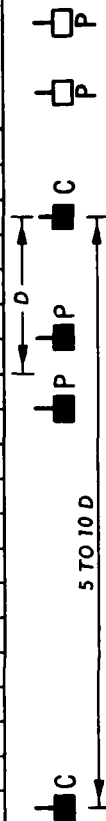
BRISTOW RESISTIVITY SURVEY

Project: _____ Area: _____

Test No.: 100-195 4 ft cav. Date: 2 Apr 76

Weather Conditions: _____ Observer: Murphy

P-P Feet	D Feet	Reading Ohms	Factor 10³	Resistivity Ohms cm 10³	Resistivity Ohms cm 10³	Interpretation
105-110		2.6	1.92	5.0		
110-115		0.95	5.75	5.5		
115-120		0.48	11.5	5.5		
120-125		0.20	19.2	3.8		
125-130		0.10	28.7	2.9		
130-135		0.070	40.2	2.8		
135-140		0.052	53.6	2.8		
140-145		0.043	68.9	3.0		
145-150		0.031	86.2	2.7		
150-155		0.023	105	2.4		
155-160		0.020	126	2.5		
160-165		0.031	149	4.6		
165-170		0.035	174	6.1		
170-175		0.026	201	5.2		
175-180		0.020	230	4.6		
180-185		0.021	261	5.5		
185-190		0.015	293	4.4		
190-195		0.014	328	4.6		

WES FORM NO. 1941
1 APR 1971

5 TO 10 D

BRISTOW RESISTIVITY SURVEY

Project: _____

Test No.: 150-55

Weather Conditions:

Area: _____

Date: 2 Apr 76

Observer: Murphy

4 ft cav.

PLATE B24

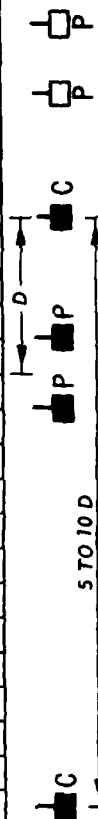| P-P Feet	D Feet	Reading Ohms	Factor 10³	Resistivity Ohms cm 10³	Resistivity Ohms cm 10³	Interpretation
145-140		1.07	1.92	2.1		
140-135		0.40	5.75	2.3		
135-130		0.21	11.5	2.4		
130-125		0.12	19.2	2.3		
125-120		0.098	28.7	2.8		
120-115		0.109	40.2	4.4		
115-110		0.094	53.6	5.0		
110-105		0.060	68.9	4.1		
105-100		0.050	86.2	4.3		
100-95		0.048	105	5.0		
95-90		0.035	126	4.4		
90-85		0.029	149	4.3		
85-80		0.023	174	4.0		
80-75		0.022	201	4.4		
75-70		0.018	230	4.1		
70-65		0.015	261	3.9		
65-60		0.011	293	3.2		
60-55		0.009	328	3.0		

5 TO 10 D

WES FORM NO. 1941
1 APR 1971

BRISTOW RESISTIVITY SURVEY

Project: _____

Area: _____

Test No.: 150-230   4 ft cav.

Date: 2 Apr 76

Weather Conditions: Immediately after 30 min. rain shower.

Observer: Murphy

P-P Feet	D Feet	Reading Ohms	Factor 10³	Resistivity Ohms cm 10³
155-160		0.93	1.92	1.8
160-165		0.45	5.75	2.6
165-170		0.36	11.5	4.1
170-175		0.20	19.2	3.8
175-180		0.130	28.7	3.7
180-185		0.113	40.2	4.5
185-190		0.069	53.6	3.7
190-195		0.060	68.9	4.1
195-200		0.035	86.2	3.0
200-205		0.031	105	3.3
205-210		0.029	126	3.7
210-215		0.022	149	3.3
215-220		0.015	174	2.6
220-225		0.013	201	2.6
225-230		0.013	230	3.0

Resistivity Ohms cm 10³

Interpretation

5 TO 10 D

WES FORM NO. 1941
1 APR 1971

PLATE B25

BRISTOW RESISTIVITY SURVEY

Project: _____

Test No.: 200-105   C₁ @ 200   4 ft cav.

Area: _____

Date: 2 Apr 76

Observer: Murphy

Weather Conditions: _____

PLATE B26

P-P Feet	D Feet	Reading Ohms	Factor 10^3	Resistivity Ohms cm 10^3	Resistivity Ohms cm 10^3	Interpretation
195-190		3.8	1.92	7.3		
190-185		1.07	5.75	6.2		
185-180		0.62	11.5	7.1		
180-175		0.29	19.2	5.6		
175-170		0.20	28.7	5.7		
170-165		0.148	40.2	5.9		
165-160		0.087	53.6	4.7		
160-155		0.037	68.9	2.5		
155-150		0.026	86.2	2.2		
150-145		0.021	105	2.2		
145-140		0.019	126	2.4		
140-135		0.016	149	2.4		
135-130		0.013	174	2.3		
130-125		0.011	201	2.2		
125-120		0.011	230	2.5		
120-115		0.015	261	3.9		
115-110		0.015	293	4.4		
110-105		0.011	328	3.6		

5 TO 10 D

WES FORM NO. 1941
1 APR 1971

BRISTOW RESISTIVITY SURVEY

Project: _____ Area: _____

Test No.: 110-148 Date: 3 Jun '76
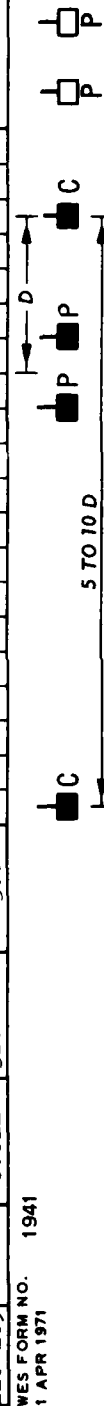
Weather Conditions: Hot, prtly cldy, ground moist Observer: Murphy

water table 30 ft. ± ½ ft

P-P Feet	D Feet	Reading Ohms (cm)	Factor 10^3	Resistivity Ohms cm 10^3	Resistivity Ohms cm 10^3	Interpretation
112-114		5.4	0.766	4.1		
114-116		2.0	2.30	4.6		
116-118		0.83	4.60	3.8		
118-120		0.44	7.66	3.4		
120-122		0.32	11.5	3.7		
122-124		0.23	16.1	3.7		
124-126		0.13	21.4	2.8		
126-128		0.10	27.6	2.8		
128-130		0.076	34.5	2.6		
130-132		0.060	42.1	2.5		
132-134		0.054	50.6	2.7		
134-136		0.046	59.8	2.8		
136-138		0.034	69.7	2.4		
138-140		0.042	80.4	3.4		
140-142		0.041	91.9	3.8		
142-144		0.023	104	2.4		
144-146		0.026	117	2.4		
146-148		0.021	131	3.0		

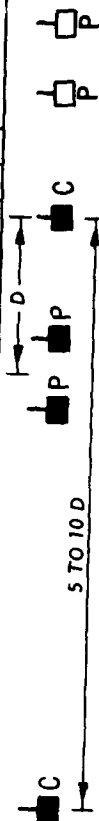5 TO 10 D

WES FORM NO. 1941
1 APR 1971

BRISTOW RESISTIVITY SURVEY

Project: _____

Test No.: 130-90   4 ft cav.

Weather Conditions: _____
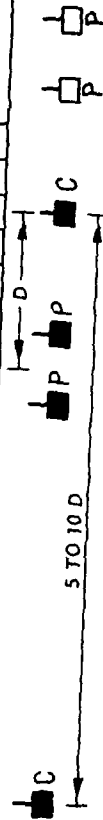
Area: _____

Date: 2 Apr 76

Observer: Murphy

PLATE B28

P-P Feet	D Feet	Reading Ohms	Factor 10^3	Resistivity Ohms cm 10^3	Resistivity Ohms cm 10^3	Interpretation
128-126		2.6	0.766	2.0		
126-124		0.91	2.30	2.1		
124-122		0.49	4.60	2.3		
122-120		0.26	7.66	2.0		
120-118		0.17	11.5	2.0		
118-116		0.17	16.1	2.7		
116-114		0.19	21.5	4.1		
114-112		0.15	27.6	4.1		
112-110		0.10	34.5	3.5		
110-108		0.079	42.1	3.3		
108-106		0.055	50.6	2.8		
106-104		0.050	59.8	3.0		
104-102		0.047	69.7	3.3		
102-100		0.047	80.4	3.8		
100-98		0.042	91.9	3.9		
98-96		0.039	104.2	4.1		
96-94		0.034	117.2	4.0		
94-92		0.025	131	3.3		

5 TO 10 D

BRISTOW RESISTIVITY SURVEY

Project:

Area:

Test No.150-190 4 ft cav.

Date: 2 Apr 76

Weather Conditions:

Observer: Murphy

P-P Feet	D Feet	Reading Ohms	Factor 10^3	Resistivity Ohms cm 10^3
152-154		2.1	0.766	1.6
154-156		0.79	2.30	1.8
156-158		0.38	4.60	1.7
158-160		0.22	7.66	1.7
160-162		0.18	11.5	2.1
162-164		0.20	16.1	3.2
164-166		0.18	21.5	3.9
166-168		0.14	27.6	3.9
168-170		0.117	34.5	4.0
170-172		0.085	42.1	3.6
172-174		0.084	50.6	4.3
174-176		0.072	59.8	4.3
176-178		0.054	69.7	3.8
178-180		0.051	80.4	4.1
180-182		0.044	91.9	4.0
182-184		0.044	104	4.6
184-186		0.033	117	3.9
186-188		0.033	131	4.3

Resistivity Ohms cm 10^3

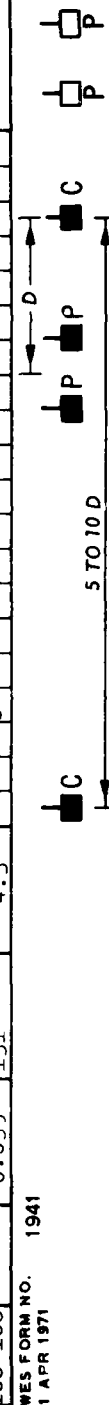Interpretation

5 TO 10 D

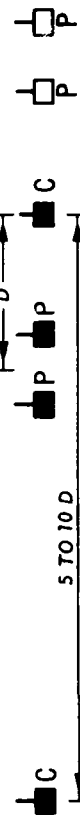WES FORM NO. 1941
1 APR 1971

PLATE B29

BRISTOW RESISTIVITY SURVEY

Project: _____ Area: _____

Test No.: 130-170 4 ft cav. Date: 2 Apr 76

Weather Conditions: _____ Observer: Murphy

P-P Feet	D Feet	Reading Ohms	Factor 10³	Resistivity Ohms cm 10³	Resistivity Ohms cm 10³	Interpretation
132-134		3.1	0.766	2.4		
134-136		1.05	2.3	2.4		
136-138		0.42	4.60	1.9		
138-140		0.35	7.66	2.7		
140-142		0.26	11.5	3.0		
142-144		0.12	16.1	1.9		
144-146		0.106	21.5	2.3		
146-148		0.080	27.6	2.2		
148-150		0.065	34.5	2.2		
150-152		0.048	42.1	2.0		
152-154		0.042	50.6	2.1		
154-156		0.040	59.8	2.4		
156-158		0.033	69.7	2.3		
158-160		0.030	80.4	2.4		
160-162		0.035	91.9	3.2		
162-164		0.049	104	5.1		
164-166		0.047	117	5.5		
166-168		0.042	131	5.5		
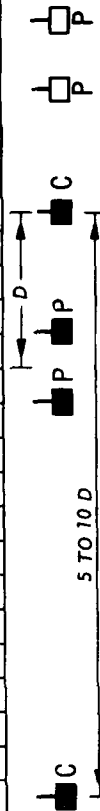
5 TO 10 D

C   P   P   P   C

WES FORM NO. 1941
1 APR 1971

BRISTOW RESISTIVITY SURVEY

Project: _____

Test No.: __150-110__

Weather Conditions: _____

Area: _____

Date: __2 Apr 76__

Observer: __Murphy__

4 ft cav.

P-P Feet	D Feet	Reading Ohms	Factor 10³	Resistivity Ohms cm 10³	Resistivity Ohms cm 10³	Interpretation
148-146		2.3	0.766	1.8		
146-144		0.94	2.30	2.2		
144-142		0.39	4.60	1.8		
142-140		0.33	7.66	2.5		
140-138		0.21	11.5	2.4		
138-136		0.12	16.1	1.9		
136-134		0.10	21.5	2.2		
134-132		0.085	27.6	2.3		
132-130		0.065	34.5	2.2		
130-128		0.054	42.1	2.3		
128-126		0.044	50.6	2.2		
126-124		0.041	59.8	2.5		
124-122		0.043	69.7	3.0		
122-120		0.039	80.4	3.1		
120-118		0.033	91.9	3.0		
118-116		0.042	104	4.4		
116-114		0.050	117	5.9		
114-112		0.044	131	5.8		

WES FORM NO. 1941
1 APR 1971

PLATE B31

BRISTOW RESISTIVITY SURVEY

Project:

Test No.: 170-130   4 ft cav.

Weather Conditions:

Area:

Date: 2 Apr 76

Observer: Murphy

P-P Feet	D Feet	Reading Ohms	Factor 10^3	Resistivity Ohms cm 10^3	Resistivity Ohms cm 10^3													Interpretation
168-166		6.7	0.766	5.1													
166-164		3.0	2.30	6.90													
164-162		1.7	4.60	7.8													
162-160		0.64	7.66	4.9													
160-158		0.35	11.5	4.0													
158-156		0.22	16.1	3.5													
156-154		0.16	21.5	3.4													
154-152		0.110	27.6	3.0													
152-150		0.080	34.5	2.8													
150-148		0.071	42.1	3.0													
148-146		0.060	50.6	3.0													
146-144		0.054	59.8	3.2													
144-142		0.043	69.7	3.0													
142-140		0.051	80.4	4.1													
140-138		0.042	91.9	3.9													
138-136		0.026	104	2.7													
136-134		0.027	117	3.2													
134-132		0.024	131	3.1													

WES FORM NO. 1941
1 APR 1971

5 TO 10 D

PLATE B32
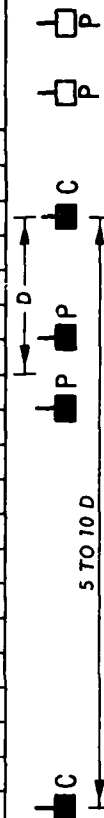
In accordance with letter from DAEN-RDC, DAEN-ASI dated
22 July 1977, Subject: Facsimile Catalog Cards for
Laboratory Technical Publications, a facsimile catalog
card in Library of Congress MARC format is reproduced
below.